



Synthesis of data products for ocean carbonate chemistry

2

- Li-Qing Jiang^{1, 2}, Amanda Fay³, Jens Daniel Müller⁴, Lydia Keppler⁵, Dustin Carroll^{6,7}, Siv K. 3
- Lauvset⁸, Tim DeVries⁹, Judith Hauck^{10,11}, Christian Rödenbeck¹², Luke Gregor^{4,13}, Nicolas 4
- Metzl¹⁴, Andrea J. Fassbender¹⁵, Jean-Pierre Gattuso^{16, 17}, Peter Landschützer¹⁸, Rik
- Wanninkhof¹⁹, Christopher Sabine²⁰, Simone R. Alin¹⁵, Mario Hoppema²¹, Are Olsen²², Matthew
- P. Humphreys²³, Kumiko Azetsu-Scott²⁴, Dorothee C. E. Bakker²⁵, Leticia Barbero^{19, 26},
- 8
- Nicholas R. Bates^{27, 28}, Nicole Besemer¹⁹, Henry C. Bittig²⁹, Albert E. Boyd^{19, 26}, Daniel Broullón³⁰, Wei-Jun Cai³¹, Brendan R. Carter³², Thi-Tuyet-Trang Chau^{33, 34}, Chen-Tung Arthur
- Chen³⁵, Frédéric Cyr^{36,37}, John E. Dore³⁸, Ian Enochs¹⁹, Richard A. Feely¹⁵, Hernan E. Garcia², 10
- Marion Gehlen³³, Lucas Gloege³, Melchor González-Dávila³⁹, Nicolas Gruber⁴, Yosuke Iida⁴⁰, 11
- Masao Ishii⁴¹, Esther Kennedy⁴², Alex Kozyr^{1,2}, Nico Lange⁸, Claire Lo Monaco¹⁴, Derek P. 12
- Manzello⁴³, Galen A. McKinley³, Natalie M. Monacci⁴⁴, Xose A. Padin³⁰, Ana M. Palacio-13
- Castro^{19, 26}, Fiz F. Pérez³⁰, Alizée Roobaert⁴⁵, J. Magdalena Santana-Casiano³⁹, Jonathan Sharp¹⁵, 14
- ⁴⁶, Adrienne Sutton¹⁵, Jim Swift⁴⁷, Toste Tanhua⁴⁸, Maciej Telszewski⁴⁹, Jens Terhaar^{50, 51}, 15
- Ruben van Hooidonk⁵², Anton Velo³⁰, Andrew J. Watson⁵³, Angelicque E. White²⁰, Zelun Wu³¹, 16
- Hyelim Yoo^{1, 2}, Jiye Zeng⁵⁴. 17

- ¹Cooperative Institute for Satellite Earth System Studies, Earth System Science Interdisciplinary Center, University 19
- 20 of Maryland, College Park, Maryland 20740, United States.
- 21 ²NOAA/NESDIS National Centers for Environmental Information, Silver Spring, Maryland 20910, United States.
- 22 ³Lamont-Doherty Earth Observatory, Columbia University, Palisades, New York 10964, United States.
- 23 ⁴Environmental Physics, Institute of Biogeochemistry and Pollutant Dynamics, ETH Zürich, Zürich, Switzerland.
- 24 ⁵Vycarb Inc., Brooklyn, New York, United States.
- 25 ⁶Moss Landing Marine Laboratories, San José State University, Moss Landing, California, United States.
- 26 ⁷Jet Propulsion Laboratory, California Institute of Technology, Pasadena, California, United States.
- 27 ⁸NORCE Norwegian Research Centre, Bjerknes Centre for Climate Research, Bergen, Norway.
- 28 ⁹Department of Geography and Earth Research Institute, University of California, Santa Barbara, California, United
- 29
- 30 ¹⁰Alfred Wegener Institute Helmholtz Centre for Polar and Marine Research, Bremerhaven, Germany
- 31 ¹¹University of Bremen, Bremen, Germany.
- 32 ¹²Max Planck Institute for Biogeochemistry, Jena, Germany.
- 33 ¹³Swiss Data Science Center, ETH Zurich and EPFL, Zurich, Switzerland
- 34 ¹⁴Laboratoire LOCEAN/IPSL, Sorbonne Université-CNRS-IRD-MNHN, 75005 Paris, France.
- 35 ¹⁵NOAA/OAR Pacific Marine Environmental Laboratory, Seattle, Washington 98115, United States.
- 36 ¹⁶Sorbonne Université, CNRS, Laboratoire d'Océanographie de Villefranche, 06230 Villefranche-sur-Mer, France.
- 37 ¹⁷Institute for Sustainable Development and International Relations, Paris, France.
- 38 ¹⁸Flanders Marine Institute (VLIZ), Jacobsenstraat 1, 8400 Ostend, Belgium.
- 39 ¹⁹NOAA/OAR Atlantic Oceanographic and Meteorological Laboratory, Miami, Florida 33149, United States.
- 40 ²⁰Department of Oceanography, University of Hawai'i at Mānoa, 1000 Pope Rd., Honolulu, Hawaii 96822, United
- 41
- 42 ²¹Alfred Wegener Institute Helmholtz Centre for Polar and Marine Research, Bremerhaven, Germany.
- 43 ²²Geophysical Institute, University of Bergen and Bjerknes Centre for Climate Research, Bergen, Norway.
- 44 ²³Department of Ocean Systems, NIOZ Royal Netherlands Institute for Sea Research, Texel, the Netherlands.





- 45 ²⁴Fisheries and Oceans, Canada, Bedford Institute of Oceanography, Dartmouth, Nov Scotia, Canada.
- 46 ²⁵Centre for Ocean and Atmospheric Sciences, School of Environmental Sciences, University of East Anglia,
- 47 Norwich NR4 7TJ, United Kingdom.
- 48 ²⁶Cooperative Institute for Marine and Atmospheric Studies, Rosenstiel School of Marine and Atmospheric Science,
- 49 University of Miami, Miami, Florida 33149, United States.
- 50 ²⁷Bermuda Institute of Ocean Sciences, ASU-BIOS, 17 Biological Lane, St. Georges, GEO1, Bermuda.
- 51 ²⁸School of Ocean Futures, Arizona State University, Tempe, Arizona 85281, United States.
- 52 ²⁹Leibniz Institute for Baltic Sea Research Warnemünde (IOW), Rostock, Germany.
- 53 ³⁰Instituto de Investigacions Mariñas, IIM CSIC, Vigo, Spain.
- 54 31School of Marine Science and Policy, University of Delaware, Newark, Delaware 19716, United States.
- 55 ³²Independent Researcher.
- 56 33Laboratoire des Sciences du Climat et de l'Environnement, LSCE-IPSL, CEA-CNRS-UVSQ, Université Paris-
- 57 Saclay, 91191 Gif-sur-Yvette, France.
- 58 ³⁴Laboratoire Interdisciplinaire des Sciences du Numérique (LISN), Centre de recherches INRIA, Université Paris—
- 59 Saclay, René Thom, F–91190, Gif–sur–Yvette, France.
- 60 ³⁵Department of Oceanography, National Sun Yat-Sen University, Kaohsiung, Taiwan.
- 61 ³⁶Northwest Atlantic Fisheries Centre, Fisheries and Oceans Canada, St. John's, Newfoundland and Labrador,
- 62 Canada
- 63 37Current affiliation: Centre for Fisheries Ecosystems Research, Fisheries and Marine Institute of Memorial
- 64 University of Newfoundland, St. John's, Canada.
- 65 38Department of Land Resources and Environmental Sciences, Montana State University, Bozeman, Montana,
- 66 United States.
- 67 ³⁹Instituto de Oceanografía y Cambio Global, IOCAG, Universidad de Las Palmas de Gran Canaria, 35017 Las
- 68 Palmas de Gran Canaria, Spain.
- 69 ⁴⁰Atmosphere and Ocean Department, Japan Meteorological Agency, 3-6-9 Toranomon, Minato City, Tokyo, Japan.
- 70 ⁴¹Meteorological Research Institute, Japan Meteorological Agency, Tsukuba, Japan.
- 71 ⁴²University of California Davis, Bodea Marine Laboratory, Davis, California, United States.
- 72 ⁴³Coral Reef Watch, U.S. National Oceanic and Atmospheric Administration, College Park, Maryland, United
- 73 States.
- 74 ⁴⁴College of Fisheries and Ocean Sciences, University of Alaska Fairbanks, Fairbanks, Alaska, United States.
- 75 ⁴⁵Flanders Marine Institute (VLIZ), Jacobsenstraat 1, 8400 Ostend, Belgium.
- 76 46Cooperative Institute for Climate, Ocean, and Ecosystem Studies, University of Washington, Seattle, Washington,
- 77 United States.
- 78 ⁴⁷Scripps Institution of Oceanography, La Jolla, California, United States.
- 79 ⁴⁸GEOMAR Helmholtz Centre for Ocean Research Kiel, Kiel, Germany.
- 80 ⁴⁹International Ocean Carbon Coordination Project, Institute of Oceanology of Polish Academy of Sciences, Sopot,
- 81 Poland.
- 82 ⁵⁰Climate and Environmental Physics, Physics Institute, University of Bern, Bern, Switzerland.
- 83 ⁵¹Oeschger Centre for Climate Change Research, University of Bern, Bern, Switzerland.
- 84 ⁵²Science for Climate Change Resilience, Boulder, Colorado 80302, United States.
- 85 ⁵³Global Systems Institute, University of Exeter, Exeter, United Kingdom.
- 86 ⁵⁴National Institute for Environmental Studies, Tsukuba, Japan.
- 87 Correspondence to: Li-Qing Jiang (liqing.jiang@noaa.gov)





88 Abstract. As the largest active carbon reservoir on Earth, the ocean is a cornerstone of the global carbon cycle, 89 playing a pivotal role in modulating ocean health and regulating climate. Understanding these crucial roles requires 90 access to a broad array of data products documenting the changing chemistry of the global ocean as a vast and 91 interconnected system. This review article provides a comprehensive overview of 60 existing ocean carbonate 92 chemistry data products, encompassing compilations of cruise datasets, derived gap-filled data products, model 93 simulations, and compilations thereof. It is intended to help researchers identify and access data products that best 94 align with their research objectives, thereby advancing our understanding of the ocean's evolving carbonate 95 chemistry.





1 Introduction

Since the onset of the Industrial Revolution in 1750, human activities, such as the burning of fossil fuels, cement production, and land-use change, have emitted ~2600 Gt carbon dioxide (CO₂) into the atmosphere, causing the atmospheric CO₂ levels to increase by ~50% (DeVries, 2022; Friedlingstein et al., 2025; Tans and Keeling, 2025). The global carbon cycle, encompassing the exchange of CO₂ among the atmosphere, oceans, terrestrial ecosystems, and geosphere, plays a critical role in regulating atmospheric CO₂ levels (Archer, 2010; DeVries, 2022; Holzer and DeVries, 2022). As the largest dynamic CO₂ reservoir, the ocean holds approximately 45 times the amount of carbon found in the atmosphere currently and actively exchanges it with the air above and sediments below. On timescales from decades to millennia, the ocean imposes a dominant control over atmospheric CO₂ levels (Revelle and Suess, 1957; Broecker, 1982; Archer et al., 2009; DeVries, 2022).

The ocean currently absorbs about a quarter of human-caused CO₂ emissions (Sabine et al., 2004; Gruber et al., 2019a; Carroll et al., 2022; Crisp et al., 2022; Terhaar et al., 2022a; Gruber et al., 2023; DeVries et al., 2023; Müller et al., 2023; Schimel and Carroll, 2024). The chemistry of the ocean has been shifting as a result of atmospheric CO₂ uptake (Feely et al., 2023; Ma et al., 2023; Müller et al., 2023; Fassbender et al., 2023; Keppler et al., 2023; Jiang et al., 2023; Müller and Gruber, 2024). Since the beginning of the Industrial Revolution, the dissolved inorganic carbon (DIC) content in the surface ocean has risen from 1690 to 1730 Gt of Carbon, and in the subsurface ocean from 35,400 to 35,560 Gt C (Sabine et al., 2004; Müller et al, 2023). This seemingly small increase of 0.5% belies a significant depletion of the oceans' buffer capacity (DeVries, 2022).

As CO₂ enters seawater, a portion of it reacts with water to form carbonic acid. This is the first in a series of rapid acid-base reactions that release protons and decrease the availability of carbonate ions, which are building materials that many marine organisms, such as mollusks, crustaceans, and corals, use to construct their shells and skeletons (Gattuso and Hansson, 2011). This process, termed as "ocean acidification (OA)", has already decreased surface ocean pH by roughly 0.11 (~30% increase in acidity) since 1750 (Orr et al., 2005; Jiang et al., 2019; Kwiatkowski et al., 2020; Jiang et al., 2023; IPCC, 2023). In the subsurface ocean, the trends of some acidification parameters, e.g., pH and hydrogen ion content ([H⁺]), can be even greater due to the increasing sensitivity of [H⁺] to changes in DIC with depth (Chen et al., 2017; Fassbender et al., 2023; Müller and Gruber, 2024). This ongoing acidification threatens critical ocean ecosystem services, including food security, fisheries, aquaculture, and the broader Blue Economy, for billions of people globally (Cooley and Doney, 2009; Doney et al., 2020).

In some parts of the ocean, OA is driven not only by the uptake of carbon but also by other processes (Delaigue et al., 2024), for example via alkalinity changes driven by freshening of the Arctic Ocean (Terhaar et al., 2021a) or changes in the carbon and alkalinity export from Arctic rivers (Terhaar et al., 2019; Qi et al., 2022; Bertin et al. 2023). Local anthropogenic inputs through rivers or from air pollution also lead to OA (e.g. Sarma et al, 2015; Sridvi and Sarma, 2021). In addition, coastal eutrophication and hypoxia could cause enhanced OA in oxygendepleted bottom water due to weakened seawater buffer capacity by biologically induced CO₂ (Cai et al. 2011). If anthropogenic CO₂ emissions continue without mitigation, as per the shared socioeconomic pathway (SSP5-8.5)



136

137

138

139

140

141142

143

144

145

146

147

148

149

150

151

152

153

154

155

156157



scenario, surface ocean pH could decrease by a further 0.3 to 0.4 by 2100, equivalent to a 100–150% increase in acidity (Kwiatkowski et al., 2020; Jiang et al., 2023). If society, however, succeeds at reducing emissions, the future acidity level becomes highly uncertain as it sensitively depends on the transient response of the Earth system and the amount of reductions of non-CO₂ radiative agents (Terhaar et al., 2023).

In summary, monitoring ocean carbonate chemistry is essential for (a) tracking the evolving ocean carbon sink, and (b) understanding ocean acidification and its ecological impacts. Additionally, monitoring ocean carbonate chemistry is crucial when considering marine carbon dioxide removal (mCDR) strategies such as ocean alkalinity enhancement (OAE), artificial upwelling, ocean fertilization and electrochemical ocean CO₂ removal (Kheshgi, 1995; Bach et al., 2019; Schimel and Carroll, 2024; Oschlies et al., 2025). The ocean's vast and interconnected nature necessitates that data from individual oceanographic cruises be meticulously preserved, subject to rigorous quality control, and uniformly formatted to promote their usability (Brett et al., 2020; Schoderer et al., 2024). Following the methodology established by Lange et al. (2023), we have curated an exhaustive catalogue of synthesis products pertaining to ocean carbonate chemistry, including cruise data compilations, gridded gap-filled data products, and other derived data products. This compilation spans both global and regional scales, providing a holistic view of the current state of ocean biogeochemistry data aggregation.

2 Methods

In this paper, data products are defined as outputs that aggregate, quality-control, and transform individual datasets from multiple sources into a unified, structured format to support research, decision-making, or operational needs for specific end users. The data products included in this study were identified through a literature review and discussions with researchers via the Ocean Acidification Information Exchange.

3 Results and Discussion

3.1 Data products for ocean carbonate chemistry

The aim of establishing this catalog of ocean carbonate chemistry data synthesis products is to enhance user access and raise awareness of available resources. The list will be regularly updated to include the latest data synthesis products. Contributors are encouraged to submit new data products through the Ocean Acidification Information Exchange (OAIE) interface: https://www.oainfoexchange.org/members/updates/71585. If preferred, submissions can also be directed via email to noaa.ocads@noaa.gov.

- 158 These products are organized based on end-user needs:
- 1. Cruise data compilations (no interpolation or extrapolation).
- 2. Time-series data products (no interpolation or extrapolation).
- 3. Derived gap-filled (interpolated) products for the surface ocean, starting with products offering a



164

165

166167

168

169170

171

172

173

174

175

176

177

178179

180

181

182 183

184

185

186 187

188

189

190

191

192

193

194



- climatological snapshot of the ocean, followed by those showing temporal changes.
 - 4. Derived gap-filled (interpolated) products for the interior ocean, also starting with products offering a climatological snapshot of the ocean, followed by those showing temporal changes.
 - 5. Multi-product analyses of 3 and 4. These compilations also include hindcast model simulations of the ocean carbon cycle and biogeochemistry.
 - 6. Model and hybrid data products projecting ocean carbon variables into the future [Note: Here the term "model" refers to ocean biogeochemical models (Fennel et al., 2022). If a statistical model or machine learning model is used for gap filling, the product is not categorized as a model output product in this compilation.]

Each section includes numbered descriptions of each data product in that class, as well as a summary table of the data products with corresponding IDs so the user can easily jump to the associated product description. Although some data products, such as Surface Ocean CO2 Atlas (SOCAT) and Lamont-Doherty Earth Observatory (LDEO) surface partial pressure of carbon dioxide (pCO₂) Database report only one ocean carbonate variable, i.e., fugacity of carbon dioxide (fCO₂), they provide a foundation from which additional variables can be derived using empirical algorithms. For instance, total alkalinity content (TA) can be estimated from salinity and temperature and other factors (Lee et al., 2006) and by neural network approaches such as those developed by Velo et al. (2013) and Broullón et al. (2019). Beyond TA, neural network algorithms have been extended to estimate dissolved inorganic carbon (DIC) as demonstrated by Broullón et al. (2020), and even the full marine carbonate system (MCS) through frameworks like CANYON-B/CONTENT (Bittig et al., 2018) and Empirical Seawater Property Estimation Routines (ESPERs) (Carter et al., 2021). While these methods primarily employ neural networks, both Velo et al. (2013) and Carter et al. (2021) provide alternative estimation approaches based on local interpolation, through their 3dimensional moving window multilinear regression algorithm (3DwMLR) and locally interpolated regression (LIR) methods, respectively. Utilizing such derived data, the complete suite of ocean carbonate parameters can then be calculated using computer software, such as CO2SYS (Lewis and Wallace, 1998; van Heuven et al., 2011; Orr et al., 2018; Sharp et al., 2023) or its Python implementation PyCO2SYS (Humphreys et al., 2022). An in-depth explanation of the methods employed for these calculations can be found in the Supplementary material of Jiang et al. (2022a).

3.1.1 Cruise data compilations (no interpolation or extrapolation):

The data compilations described in this section standardize datasets collected from individual research vessels, ships of opportunity (SOOP), and unmanned platforms, presenting them in a uniform format for easy access. These datasets typically undergo both primary QC (identifying outliers and obvious errors within an individual cruise dataset) and secondary QC (objectively comparing data from one cruise against another or a previously synthesized dataset to quantify systematic differences in reported values).





- 1) SOCAT: The Surface Ocean CO₂ Atlas (SOCAT) represents the most extensive collection of observational ocean CO₂ data for the global surface ocean (Bakker et al., 2016). It features fugacity of carbon dioxide (fCO₂) measurements from both the open ocean and the coastal ocean, predominantly sourced from research vessels, SOOP, and autonomous platforms including fixed moorings and autonomous surface vehicles (ASVs). Since 2013, SOCAT has been updated annually, and assigned dataset flags indicating uncertainty and completeness of metadata. SOCAT is also available as a gridded product. To access the latest version of the SOCAT data product (with 40 million data points), visit https://socat.info/.
- 2) LDEO Surface pCO₂ Database: Dr. Taro Takahashi [Lamont Doherty Earth Observatory (LDEO), Palisades, New York] started synthesizing global surface ocean CO₂ data in 1997, compiling three decades of observations (~250,000 measurements) to create inaugural monthly global surface pCO₂ maps (Takahashi et al., 1997; Takahashi et al., 2002). The most recent version (V2019) expanded this dataset to approximately 14.2 million surface water pCO_2 measurements spanning from 1957–2019. Distinct from the SOCAT database, the LDEO database reports pCO₂, instead of fCO₂, exclusively from equilibrator-CO₂ analyzer systems, with an average estimated uncertainty of ± 2.5 μ atm. The database is also interpolated onto a global surface ocean 4° x 5° grid for a reference year 2000 (Takahashi et al., 2009) and 2010 (Fay et al. 2024). Access to the LDEO surface pCO₂ database (Version 2019) is provided by the Ocean Carbon and Acidification Data System (OCADS) with the DOI: "10.3334/CDIAC/otg.ndp088(v2015)", accessible at: https://www.ncei.noaa.gov/data/oceans/ncei/ocads/metadata/0160492.html. Additionally, there is a dedicated webpage at OCADS for the LDEO Database: https://www.ncei.noaa.gov/access/ocean-carbonacidification-data-system/oceans/LDEO Underway Database/.
 - 3) GLODAPv2: The Global Ocean Data Analysis Project Version 2 (GLODAPv2) aggregates biogeochemical data collected from discrete bottle samples, offering extensive global coverage from the surface to depths (Key et al., 2015; Olsen et al., 2016; Lauvset et al., 2024). While GLODAP is primarily a product for basin-scale repeat hydrography data, it also includes coastal datasets and observations from a few time-series. The GLODAPv2 data product provides rigorously quality-controlled measurements for 14 essential oceanographic variables: temperature, salinity, dissolved oxygen, nitrate, silicate, phosphate, dissolved inorganic carbon (DIC), total alkalinity (TA), pH, chlorofluorocarbons (CFC-11, CFC-12, CFC-113), carbon tetrachloride (CCl₄), and sulfur hexafluoride (SF₆). These variables, excluding temperature, undergo both primary and secondary quality control procedures to detect outliers and adjust for significant measurement biases. GLODAPv2 was first published in 2016 and has been updated annually through a living data process in Earth System Science Data since 2019. For these updates, new data (including historical data not previously included in the data product) are quality controlled and adjusted to the 2016 version (Olsen et al., 2019; Olsen et al., 2020; Lauvset et al., 2021; Lauvset et al., 2022; Lauvset et al., 2024). Since the global repeat hydrography programs operate with decadal repetitions, the aim is to produce a completely new version of GLODAP, where all cruise datasets will be reevaluated, every





- decade. Release of the GLODAPv3 data product is planned for 2026. For more information on the
 secondary quality control process, refer to Tanhua et al. (2010) and Lauvset and Tanhua (2015).

 GLODAPv2 offers two kind of products: the collection of quality controlled data from discrete bottle
 samples taken at sampling location (Key et al., 2015; Olsen et al., 2016; Olsen et al., 2019; Olsen et al.,
 2020; Lauvset et al., 2021; Lauvset et al., 2022; Lauvset et al., 2024), and a gridded product, interpolated to
 a 1°x1° grid and the 33 standard depth levels of WOA (World Ocean Atlas) (Lauvset et al., 2016). All
 versions of the GLODAPv2 data product can be accessed at https://glodap.info/.
 - 4) JOA Suite: The Java OceanAtlas (JOA) Suite offers both a user-friendly application and a library of ocean profile data curated by Jim Swift (Scripps Institution of Oceanography, La Jolla, California, USA). Similar to GLODAPv2, this data product serves as a comprehensive repository of quality-controlled discrete bottle based measurements (and limited CTD), spanning from the surface to the depths of the global ocean. Unlike GLODAPv2, no offset corrections were applied to the JOA data product. The JOA data product encompasses a range of oceanographic variables including temperature, salinity, dissolved oxygen, DIC, TA, silicate, phosphate, nitrate, nitrite, CFC-11, CFC-12, SF₆, and CTD parameters associated with the water sample data. To access the JOA application and data, visit: https://joa.ucsd.edu/. Currently, there is not a peer-reviewed paper or public-accessible report for this data product. Cite the data product itself as: "Swift, J. (2022), Java OceanAtlas Data, https://joa.ucsd.edu/Data_homepage", or cite the entire JOA Suite as: "Swift, J. and Osborne, J. (2022), The Java OceanAtlas Suite, https://joa.ucsd.edu".
 - 5) WOD: In addition to the GLODAPv2 and JOA Suite, users can also access historical and recent original biogeochemical data collected from discrete bottle samples in a uniform format and units, along with their originator quality control (QC) flags, through the World Ocean Database (WOD) (Mishonov et al., 2024). Like the JOA Suite, these measured data remain unaltered. The WOD allows users to filter and subset data with specific variables, platforms, institutions, projects, regions, or time periods (Garcia et al., 2024). Users can visualize sampling locations on a "distribution plot" and access a cruise list for all selected data and variables. Users also have the option of exporting data in NetCDF or Comma-Separated Values (CSV) formats. Additionally, all data in the WOD are reproducible and traceable to their original sources archived at NOAA's National Centers for Environmental Information (NCEI) for long-term preservation. The WOD is accessible at https://www.ncei.noaa.gov/products/world-ocean-database.
 - 6) SNAPO-CO₂: Metzl et al. (2024) aggregated over 44,400 measurements of DIC and TA from a series of research cruises and ships of opportunity (SOOP) across various oceanic regions in 1993-2022, under the aegis of several French research programs, to create a product called "Service National d'Analyse des Paramètres Océaniques du CO₂ (SNAPO-CO₂)". The majority of the samples were analyzed by the Service National d'Analyse des Paramètres Océaniques du CO₂ (SNAPO-CO₂) at the LOCEAN laboratory in Paris, France. Sampling was performed either from CTD-rosette casts (Niskin bottles) or collected from the ship's flow-through system (intake at roughly 5m depth). DIC and TA determinations were conducted





- simultaneously through potentiometric titration in a closed-cell setup, calibrated with certified reference material to achieve an accuracy of \pm 4 μ mol kg⁻¹ for both parameters, as per Edmond (1970). This methodology was also applied for real-time measurements during OISO cruises, with data from the South Indian Ocean for 1998–2018 included in this compilation. The data is split into two sets one for the global ocean and coastal zones, and another for the Mediterranean Sea both accessible in the same format: https://doi.org/10.17882/95414. Additionally, this data product is available at OCADS (DOI: "10.25921/ptyh-0y90"): https://www.ncei.noaa.gov/data/oceans/ncei/ocads/metadata/0285681.html (Metzlet al., 2023)
- 7) Arctic Ocean anthropogenic carbon estimates: This dataset includes anthropogenic carbon estimates in the Arctic Ocean based on measurements of transient tracers, such as CFC-12 and SF₆ (Terhaar et al., 2020; Tanhua et al., 2009). Using the transient time distribution (TTD) method, anthropogenic carbon estimates were estimated at measurement locations across all basins of the Arctic Ocean between 1983 and 2005. In addition to these estimates, adjusted estimates of anthropogenic carbon at these locations are provided that account for differences in the saturation of transient tracers and anthropogenic carbon in Arctic Ocean surface waters that caused anthropogenic carbon estimates to be biased low (Terhaar et al., 2020). It is recommended to use the adjusted estimates. This dataset can be accessed at https://doi.org/10.17882/103920 (Terhaar et al., 2024).
- 8) CODAP-NA: Jiang et al. (2021) curated and synthesized two decades of discrete measurements of carbonate system variables, dissolved oxygen, and nutrient chemistry data from the North American continental shelves to generate the first version of Coastal Ocean Data Analysis Data Product in North America (CODAP-NA). The 2021 release encompasses 3,391 oceanographic profiles from 61 research cruises spanning the North American continental shelves from Alaska to Mexico in the west and from Canada to the Caribbean in the east. It includes 14 key variables, including temperature, salinity, DO, DIC, TA, pH, carbonate ion, fCO₂, silicate, phosphate, nitrate, all of which have undergone rigorous quality control. Note that certain datasets meeting the GLODAPv2 QC standards are also included in the GLODAPv2 since its 2022 release. CODAP-NA is available at OCADS (DOI: "10.25921/531n-c230"): https://www.ncei.noaa.gov/data/oceans/ncei/ocads/metadata/0219960.html (Jiang et al., 2020).
- 9) AZMP Carbon: Gibb et al. (2023) compiled carbonate parameters data from the Canadian Atlantic Zone Monitoring Program (AZMP Carbon) since 2014. More than 100 seagoing missions are represented in this dataset. The sample strategy corresponds generally to full-depth water samples mostly collected along standardised hydrographic sections. The majority of these data were collected as part of the Atlantic Zone Monitoring Program (AZMP) of Fisheries and Oceans Canada (DFO). Implemented in 1998, the AZMP aims to characterize and understand the causes of oceanic variability at the seasonal, inter-annual and decadal scales in support of, among other things, fisheries management in the Atlantic Zone (including the Gulf of St. Lawrence, the Scotian shelf and the Newfoundland and Labrador shelf). Since 2014, a minimum





301

302

303

304

305

306

307

308

309

310

311

312

313

314

315

316

317

318

319320

321

322

323

324

325

326

327328

329

330

331

332

333

334

of two of the three following carbonate parameters, TA, DIC and pH, are also acquired by the program at standardised hydrographic stations across the zone (sampled up to three times a year). Each measurement is completed with corresponding temperature, salinity and, when available, nutrients and dissolved oxygen concentration data. This dataset also includes samples collected as part of ships of opportunity, fishing and other scientific trips. The entire dataset comprises 19,531 discrete samples [last updated 21 August 2024]. Among this number, 18,085 have at least two of the three carbonate system parameters (e.g., TA, DIC and pH), allowing the derivation of other parameters such as the saturation state relative to aragonite and calcite (Ω_{arg} and Ω_{cal}) and partial pressure of CO_2 (pCO_2 , in μ atm) using the CO2SYS program modified for Python (https://github.com/mvdh7/PyCO2SYS/tree/v1.2.1, last access: 8 January 2023; Humphreys et al., 2020). The full dataset of measured and derived parameters is available from the Federated Research Data Repository: https://doi.org/10.20383/102.0673 (Cyr et al., 2022) and is updated annually.

- 10) MOCHA: Kennedy et al. (2023) curated a comprehensive coastal ocean data product called "Multistressor Observations of Coastal Hypoxia and Acidification (MOCHA)", encompassing temperature, salinity, dissolved oxygen, ocean carbonate variables (TA, DIC, pH, pCO₂, fCO₂), nutrients, and chlorophyll measurements from the full water column along the U.S. west coast. The synthesis integrates observations from 71 different sources, including high-resolution autonomous sensors, synoptic oceanographic cruises, and shoreline samples. The MOCHA synthesis spans from the shoreline to well-beyond the continental shelf and incorporates observations from CODAP-NA, CalCOFI, and other large-scale oceanographic cruises to facilitate linking nearshore, high-resolution observations to broader oceanographic conditions. It boasts 15.9 million temperature readings, 5.0 million salinity measurements, 3.9 million dissolved oxygen records, and 2.3 million pH measurements, along with 8,368 dissolved inorganic carbon, 10,144 total alkalinity, and 505,000 pCO₂/fCO₂ measurements, with limited additional chlorophyll and nutrient observations. To reduce the computational load from high-resolution sensors, the synthesis is also available as a "daily aggregated" dataset, with all data sources averaged by day, location, and depth. All data in the MOCHA synthesis product has been quality controlled to a "plausible and reasonable" standard, but researchers requiring high-precision coastal data may need to apply additional QC tests. The data product is available at OCADS (DOI: "10.25921/2vve-fh39"): https://www.ncei.noaa.gov/data/oceans/ncei/ocads/metadata/0277984.html, while the methods and product are described in Kennedy et al. (2024).
- 11) ARIOS: The Acidification in the Rias and the Iberian Continental Shelf (ARIOS) project involved compiling and analyzing the historical record of carbon system measurements and associated parameters conducted by the Instituto de Investigaciones Mariñas (IIM-CSIC) in Vigo, Spain. This dataset comprises 3,343 oceanographic stations and 17,653 discrete samples, combining measurements of pH, alkalinity, and other physical (pressure, temperature and salinity) and biogeochemical parameters (dissolved oxygen, nitrate, phosphate, and silicate) off the northwestern Iberian Peninsula from June 1976 to September 2018





(Padin et al., 2020). The oceanography cruises funded by 24 projects were primarily carried out in the Ría de Vigo coastal inlet, but also in an area ranging from the Bay of Biscay to the Portuguese coast. Robust seasonal cycles and long-term trends were calculated along a longitudinal section, gathering data from the coastal and oceanic zone of the Iberian upwelling system. The pH in the surface waters of these separated regions, which were highly variable due to intense photosynthesis and the remineralization of organic matter, showed an interannual acidification ranging from 0.0012 to 0.0039 yr⁻¹ that increased towards the coastline and interior embayments. A synthesis paper is available at https://doi.org/10.5194/essd-12-2647-2020 (Padin et al., 2020), and the data product is available at https://doi.org/10.20350/digitalCSIC/12498 (Pérez et al., 2020).

- (2023) compiled a data product of discrete seawater samples collected each May and September over a 10-year period from 2008 to 2017 along the long-term hydrographic line in the Gulf of Alaska (GAK Line). Samples were collected from a sampling rosette on a profiling CTD. Data variables include profiled seawater temperature, salinity, and dissolved oxygen. Discrete sample variables include dissolved oxygen (i.e., Winkler titrations), macronutrients (nitrate, nitrite, phosphate, silicic acid), dissolved inorganic carbon (DIC), and total alkalinity (TA). The repeat hydrographic cruises were funded by the Alaska Ocean Observing System (AOOS), the Exxon Valdez Oil Spill Trustee Council (EVOS), Gulf Watch Alaska, and the North Pacific Research Board (NPRB) and were mostly conducted aboard the United States Fish and Wildlife Service (USFWS) R/V Tiĝlax̂. All carbonate parameters were analysed at the Ocean Acidification Research Center (OARC) at the University of Alaska Fairbanks (UAF). This data product is available at OCADS (DOI: 10.25921/x9sg-9b08):

 https://www.ncei.noaa.gov/data/oceans/ncei/ocads/metadata/0277034.html (Monacci et al., 2023), and the synthesis paper can be accessed at https://doi.org/10.5194/essd-16-647-2024 (Monacci et al., 2024).
- 13) Coral Reef Carbonate Chemistry Off the Florida Keys: Palacio-Castro et al. (2023) compiled discrete seawater samples from 38 permanent stations located along 10 inshore-offshore transects at the Florida Coral Reef. These samples were collected as part of NOAA's National Coral Reef Monitoring Program (NCRMP) and the South Florida Ecosystem Restoration Research (SFER) cruises. Sampling efforts commenced in 2010, with every two months collections initiated in 2015, resulting in a total of 47 sampling cruises and 1,538 discrete seawater samples. For all samples, a minimum of two of the carbonate equilibrium parameters (TA, DIC) were measured, in addition to salinity and temperature. The aragonite saturation state (Ω_{Ar}), partial pressure of CO₂ (pCO₂) and pH were derived from the measured parameters using the R package seacarb (Gattuso et al., 2021a). The time series analysis provides insight into the dynamic carbonate conditions spanning the inshore to offshore gradients, encompassing four distinct regions of the Florida Coral Reef: Biscayne Bay, the Upper Keys, Middle Keys, and Lower Keys. The findings underscore significant variability in the seasonality and interannual trends of surface carbonate



370 chemistry across different regions and reef zones. Data is available at NCEI (DOI: "10.25921/vfz0-dg77"): 371 https://www.ncei.noaa.gov/access/metadata/landing-page/bin/iso?id=gov.noaa.nodc:NCRMP-CO3-Atlantic 372 (Manzello et al., 2018). 373 14) Salish cruise data package and multi-stressor data product: Alin et al. (2021) compiled data from 35 374 individual cruise data sets that sampled marine waters of the southern Salish Sea and northern Washington 375 coast (USA) during 2008-2018. These data sets were collected in support of research and monitoring efforts 376 of the University of Washington Puget Sound Regional Synthesis Model (2008-2013), Washington Ocean 377 Acidification Center (WOAC, 2014-present), NOAA Ocean Acidification Observing Network, Northwest 378 Association of Networked Ocean Observing Systems, and NOAA Pacific Marine Environmental 379 Laboratory. Ongoing seasonal sampling occurred during April, July, and September for Puget Sound cruises 380 has occurred under WOAC support since 2014 and most frequently during May and October for Sound-to-381 Sea cruises, which sample from Puget Sound through the Strait of Juan de Fuca to the northern Washington 382 coast. The Salish cruise data package contains observations from a total of 715 oceanographic profiles, 383 with > 7490 sensor measurements of temperature, salinity, and oxygen; ≥ 6070 measurements of discrete 384 oxygen and nutrient (nitrate, phosphate, silicate, ammonium, nitrite) samples; and ≥ 4462 measurements of 385 inorganic carbon variables (DIC and TA). Alin et al. (2023) published a follow-on data product based on the 386 Salish cruise data package, which only included the 3971 samples with complete information for 387 temperature, salinity, oxygen, nutrients, DIC, and TA. To facilitate applications of this data product to 388 understanding multi-stressor ocean conditions in Pacific Northwest marine waters by various end users, Alin et al. (2023) also included the most commonly used calculated carbonate system parameters in this 389 390 data product (pH_{total}, fCO₂, pCO₂, Ω _{Ar}, Ω _{Ca}). The data package is available at OCADS (DOI: 391 "10.25921/zgk5-ep63"): https://www.ncei.noaa.gov/access/ocean-carbon-acidification-data-392 system/oceans/SalishCruise DataPackage.html. The multi-stressor data product is available at: 393 https://www.ncei.noaa.gov/access/ocean-carbon-acidification-data-394 system/oceans/SalishCruises DataProduct.html. Two synthesis papers describing the data package and 395 interpreting the data product can be found at: https://essd.copernicus.org/articles/16/837/2024/ (Alin et al. 2024a) and https://bg.copernicus.org/articles/21/1639/2024/ (Alin et al. 2024b). 396

Table 1. Ocean carbonate chemistry data products out of cruise data compilations (no gridding or gap filling).

No.	Name	Open or coastal ocean	Surface or water column	Discrete bottle or continuous	Highlights	Reference
1	SOCAT	Open + Coastal	Surface	Continuous	The largest collection of surface ocean carbon observations	Bakker et al. (2016)
2	LDFO Surface pCO ₂ Onen +		Surface	Continuous	The LDEO database reports pCO ₂ exclusively from equilibrator-CO ₂ analyzer systems	Takahashi et al. 2017





400

401

402403

					Adjustments are applied by	
3	GLODAPv2	Open ocean	Water column	Discrete bottle	comparing data in the deep ocean (>2000 m) using a crossover and inversion method as described by Johnson et al (2001).	Lauvset et al. (2024)
4	JOA Suite	Open ocean	Water column	Discrete bottle	Similar to GLODAPv2, with no adjustments	Swift (2022)
5	WOD	Open ocean	Water column	Discrete bottle	Similar to GLODAPv2, with no adjustments	Mishonov et al. (2024)
6	SNAPO-CO ₂	Open + Coastal	Water column	Discrete bottle and semi- continuous	A compilation of cruises from multiple French initiatives	Metzl et al. (2024)
7	Arctic Ocean anthropogenic carbon estimates	Open ocean	water column	Discrete bottle (normalized to year 2005)	Observation-based estimates of anthropogenic carbon in the Arctic Ocean	Tanhua et al. (2009); Terhaar et al. (2020)
8	CODAP-NA	Coastal ocean	Water column	Discrete bottle	Similar to GLODAPv2, but for the coastal ocean	Jiang et al. (2021)
9	AZMP Carbon	Continental Shelf and slope	Water column	Discrete bottle	A compilation of cruises from the Atlantic Zone Monitoring Program (AZMP) since 2014	Gibb et al. (2023)
10	МОСНА	Coastal ocean	Water column	Discrete bottle + Continuous	U.S. West Coast	Kennedy et al. (2024)
11	ARIOS	Coastal ocean	Water column	Discrete bottle	An OA Database for the Galician Upwelling Ecosystem off the NW Iberian Peninsula from 1976 to 2018	Padin et al., (2020)
12	Marine inorganic carbon chemistry observations in the northern Gulf of Alaska	Coastal ocean	Water Discrete bottle A synthesis of twenty 2008 to 2017 on the G		A synthesis of twenty cruises from 2008 to 2017 on the Gulf of Alaska (GAK) Line	Monacci et al. (2023)
13	Coral Reef Carbonate Chemistry Off the Florida Keys	emistry Off the $\begin{bmatrix} \text{Coastal} / \\ \text{regional} \end{bmatrix}$ water Discrete bottle pH, Ω_{arag} , in different areas of		Temporal trends of DIC, TA, p CO ₂ , pH, Ω_{arag} , in different areas of the Florida Keys	Palacio-Castro et al. (2023)	
14	Salish cruise data package and multi- stressor data product	Coastal / estuarine	Water column	Discrete bottle	A data compilation and multi- stressor (ocean acidification, hypoxia, temperature) data product based on cruises from 2002 to 2018 in the southern Salish Sea and Washington coast	Alin et al. (2021, 2023)

398 3.1.2 Time-series data products (no interpolation or extrapolation):

The time-series data products described in this section include observations collected at regular time intervals, over a sustained period, and at fixed locations. The data often represent changes in a particular oceanographic variable over time, such as temperature, salinity, TA and DIC. The list below includes both climate-quality time-series data products compiled at selected stations, and data products compiling time-series measurements at multiple locations. Additionally, some hydrographic sections are measured regularly enough to warrant being called a time



405

406

407

408

409

410

411

412

413

414

415

416

417

418

419

420

421

422

423

424 425

426 427

428

429 430

431

432433

434

435

436

437

438



series, e.g., Line P (Freeland, 2007), sections in the northwest Pacific (Ishii et al., 2011a), the OVIDE lines (Mercier et al., 2024). Measurements from these sections are typically included in cruise data compilations (3.1.1) and are not listed separately here.

- 15) BATS: The Bermuda Atlantic Time-series Study (BATS) observations and data products extend to forty years of observations of DIC and TA and ocean acidification indicators, and constitute the longest continuous record of warming, salinification, ocean deoxygenation, and ocean acidification in the open ocean (Bates and Johnson, 2023). The sustained observations at the BATS site began in October 1988, approximately 80 km to the south-east of Bermuda (https://bios.asu.edu/bats). The program comprises monthly cruises with CTD, water-column biogeochemical sampling and rate measurements (e.g., primary and export production) plus additional cruises in the spring period and annual transects between the Gulf Stream and Puerto Rico. CO2-carbonate chemistry sampling includes full-depth bottle DIC and alkalinity data (including additional surface measurements going back to 1983 collected at the Hydrostation S site). Hydrostation S is located ~25 km south-east of Bermuda (https://bios.asu.edu/research/projects/hydrostation-s) and began in 1954 with biweekly cruises each year. Underway fCO₂/pCO₂ data collected from the R/V Atlantic Explorer that supports the BATS and Hydrostation S sites constitutes part of the annual data submission to SOCAT. The BATS project page at the Biological and Chemical Oceanography Data Management Office (BCO-DMO) includes metadata and data streams (https://demo.bco-dmo.org/project/2124). Hydrostation S data and DOIs are also available at BCO-DMO (https://www.bco-dmo.org/project/859583).
- 16) HOT: The Hawaii Ocean Time-series (HOT) CO₂ measurement program documents 35+ years of inorganic carbon dynamics in the open waters of the central North Pacific. Since October 1988, full ocean depth profiles of DIC and TA have been analyzed, and direct measurements of pH have been made over most of this longest-running Pacific Ocean time-series study. The overall scientific mission of HOT has been to sustain observations of the variability of hydrological and ecological properties, elemental cycling, heat fluxes, and circulation of the North Pacific Subtropical Gyre (NPSG). The program is based on shipboard observations and experiments conducted on ~10 expeditions per annum to Station ALOHA (22.75°N, 158°W). HOT program background information and details of sampling strategy may be found in Karl and Lukas (1996) and Karl et al. (2001). Results from the HOT CO2 measurement program may be found in Winn et al. (1994, 1998), Dore et al. (2003, 2009, 2014), and Knor et al. (2023). The HOT project page, metadata, data streams and data identifiers are listed at https://www.bco-dmo.org/project/2101. A surface ocean data product that includes CO2SYS-calculated values of pCO₂, carbonate mineral saturation states and other derived quantities may be found at https://hahana.soest.hawaii.edu/hot/hotco2/hotco2.html and https://doi.org/10.5281/zenodo.15060930. A MAPCO2 system on the Woods Hole Oceanographic Institution Hawaii Ocean Time-series Site mooring (WHOTS; https://www.soest.hawaii.edu/whots/) has provided a near-continuous record of surface pCO₂ since 2004, and is anchored by the longer high-accuracy





440

441

442

443

444

445

446

447

448

449

450

451

452

453

454

455

456

457

458 459

460

461

462463

464

465

466

467

468 469

470

471

- HOT ship-based program (see Sutton et al. 2019 and Knor et al. 2023). These synergistic measurements have contributed to global ocean carbon observation networks (e.g., the newly released SOCATv22), which have improved our ability to characterize natural and anthropogenic drivers of ocean carbon uptake and acidification.
 - 17) ESTOC: The European Station for Time Series in the Ocean (ESTOC) began carbon dioxide monitoring in October 1995, providing a 30-year record on total alkalinity (TA), pH, and dissolved inorganic carbon (DIC). This dataset represents the longest continuous monthly record of warming, rising carbon dioxide levels, and acidification in the eastern North Atlantic (González-Dávila and Santana-Casiano, 2023). ESTOC is located 100 km north of the Canary Islands archipelago (https://plocan.eu/en/installations/oceanobservatory). The program includes a ship-based observation system, measuring physical, chemical, and biological parameters throughout the 3,670-meter water column. It also features a moored platform for surface meteorological and oceanic observations as well as subsurface measurements, maintained by the Canary Island Oceanic Platform (PLOCAN, https://plocan.eu/en) and the University of Las Palmas de Gran Canaria (https://iocag.ulpgc.es/research/research-units/quima). Carbon dioxide system measurements include full-depth bottle sampling for photometric pH, total alkalinity, and DIC, conducted monthly from 1995 to 2008, every two months until 2018, and semiannually in recent years due to limited ship time, timed to coincide with moored structure maintenance. ESTOC is also visited every two weeks by a volunteer observing ship, ES-SOOP-CanOA (https://meta.icos-cp.eu/resources/stations/OS 687B), part of the European Research Infrastructure ICOS (https://www.icos-cp.eu/observations/ocean/stations), which provides real-time surface data on carbon dioxide fluxes and ocean acidification. The program also includes the CO₂-ESTOC oceanographic buoy (https://meta.icos-cp.eu/labeling/). The full dataset with DOIs is accessible on Pangaea (González-Dávila and Santana-Casiano, 2023).
 - 18) Point B Time-series: The Point B time series documents the carbonate chemistry at a coastal site of the Bay of Villefranche (43.686200N 7.314800E) in Villefranche-sur-mer, France, northwestern Mediterranean Sea. Since January 2007, seawater is sampled weekly at 1 and 50 m, and analyzed for total dissolved inorganic carbon and total alkalinity (Kapsenberg et al., 2017). Salinity and temperature are extracted from CTD profiles. Parameters of the carbonate system such as pH (total hydrogen ion scale) are calculated using the R package seacarb. Data are available at Pangaea: https://doi.org/10.1594/PANGAEA.727120 (Gattuso et al., 2021b).
 - 19) Ny-Ålesund Time-series: The Ny-Ålesund time series documents the carbonate chemistry at a coastal site of Kongsfjorden, Spitsbergen (78.930660N 11.920030E) during the period 2015-2021. It is the first high-frequency (1 hour), multi-year (6 years) dataset of salinity, temperature, dissolved inorganic carbon, total alkalinity, pCO₂, and pH in the High-Arctic Ocean (Gattuso et al., 2023a). Data are available at Pangaea: https://doi.org//10.1594/PANGAEA.957028 (Gattuso et al., 2023b).





- 20) SPOTS: The Synthesis Product for Ocean Time-Series (SPOTS) is a ship-based biogeochemical pilot, aiming at regularly providing high quality data from fixed time-series stations with consistent format and semantics (Lange et al., 2024a). The pilot includes data from 12 fixed ship-based time-series programs with a focus on the Global Ocean Observing System's biogeochemical essential ocean variables. These stations represent unique marine environments across a variety of spatiotemporal resolutions and ranges, with data from 1983 to 2021. While implementing the FAIR Principles (Wilkinson et al., 2016) and open data, Lange et al. also improved the metadata of the time-series stations to interoperate with the IOC-UNESCO Ocean Data and Information System (ODIS). Additionally, an extensive quality assessment resulted in enhanced intra- and inter-station comparability. Altogether, SPOTS' pilot increased the readiness of biogeochemical time-series (Lange et al., 2023) and facilitates a variety of applications that benefit from the collective value of biogeochemical time-series observations. Data are available at https://www.bco-dmo.org/dataset/896862 with the DOI "10.26008/1912/bco-dmo.896862.2" (Lange et al., 2024b).
- 21) Autonomous pCO₂ and pH time series from 40 surface buoys: Sutton et al. (2019) established a living dataset comprising 40 individual autonomous moored surface ocean pCO2 time series established between 2004 and 2013, 17 of them also include autonomous pH measurements. These time series characterize a wide range of surface-ocean carbonate conditions, across a variety of environments, including 17 oceanic and 13 coastal locations, as well as 10 coral reefs. The dataset serves as a significant resource for assessing the natural variability of surface ocean carbonate chemistry across diverse regions. Data are available at OCADS (DOI "10.7289/v5db8043"): https://www.ncei.noaa.gov/data/oceans/ncei/ocads/metadata/0173932.html (Sutton et al., 2018). Additionally, there is a dedicated webpage at OCADS for this project: https://www.ncei.noaa.gov/access/ocean-carbon-acidification-data-system/oceans/Moorings/ndp097.html.

Table 2. Time-series based ocean carbonate chemistry data synthesis products.

No.	Name	Open or coastal ocean	Surface or water column	Discrete bottle or autonomous	Highlights	Reference
15	BATS	Open	Top 4600 m	CTD profiles, discrete bottle data from hydrocast, rate measurements (primary, export and bacterial production), biomass and other biological measurements, underway measurements	One of the longest continuous record of warming, salinification, ocean deoxygenation, and ocean acidification in the open ocean	Bates and Johnson (2020, 2023)
16	НОТ	Open	Top 4500 m	Discrete Bottle for shipboard measurements; sensor measurements on WHOTS mooring	35+ years of inorganic carbon dynamics in the open waters of the central North Pacific	Dore et al. (2009)





17	ESTOC	Open	Top 3570m	Discrete Bottle for shipboard measurements; sensor measurements on ESTOC mooring	The longest continuous monthly record of warming, rising carbon dioxide levels, and OA in the eastern North Atlantic	González- Davila and Santana- Casiano (2023)
18	Point B Time- series	Coastal	5 and 50 m	CTD profiles, discrete bottle data	Carbonate chemistry at a coastal site of the Bay of Villefranche, France	Kapsenberg et al. (2017)
19	Ny-Ålesund Time- series	Coastal	12 m	CTD, discrete bottle data, sensor measurements at the COSYNA/MOSES-AWIPEV underwater observatory	Carbonate chemistry at a coastal site of Kongsfjorden, Spitsbergen	Gattuso et al. (2023)
20	SPOTS	Open + Coastal	Water column	Discrete	The pilot includes biogeochemical data from 12 fixed ship-based time series programs	Lange et al. (2024a), Lange et al. (2024b)
21	Autonomous pCO ₂ and pH time series from 40 surface buoys	Open + Coastal	Surface	Autonomous	Based on 40 moored surface pCO ₂ time series, with 17 of them containing pH	Sutton et al. (2019)

3.1.3 Gridded and derived data products - Surface:

This section describes gridded data products that have been derived from observations through interpolation and gap-filling procedures, and depict the surface ocean. Note that this compilation focuses primarily on data products with global coverage, acknowledging that many regional gap-filled products became available in recent years and shall be include in future updates:

22) Updated Takahashi delta fCO₂ and flux climatology: Following on previous climatologies published by the late Taro Takahashi in 1997 and 2009, Fay et al. (2024) created a legacy climatology using his methodology and the updated SOCAT database of observations. This product provides 12 months of delta fCO₂values and corresponding fluxes for a base year of 2010 at 4° x 5° resolution subsequently subgridded to 1° x 1° resolution and near-global coverage. This climatology represents the mean of ocean conditions over the last four decades and is distinctive relative to many other mechanistic machine learning approaches in that it interpolates in time and space using only the available fCO₂ data and a surface water advection scheme rather than using proxy variables for gap filling. It uses the median of observations to determine a reference year of 2010 and fluxes are provided using air-sea partial pressure differences and inputs from the SeaFlux product (Fay et al., 2021). The climatology product is available at OCADS (DOI: "10.25921/295g-sn13"): https://www.ncei.noaa.gov/data/oceans/ncei/ocads/metadata/0282251.html. The related manuscript is available at ESSD: https://doi.org/10.5194/essd-16-2123-2024 (Fay et al., 2024).





- and coastal oceans. It is a monthly climatological gridded global surface ocean pCO2 data product without adjusting for a specific reference year. Developed on a higher-resolution 0.25° × 0.25° global surface-ocean grid, this product is the result of combining two neural network-based pCO2 products: the open ocean product described below (i.e., Landschützer et al. 2016) and the coastal product created by Laruelle et al (2017). Consequently, it represents coastal zones better. Data collected between 1998 and 2015 from the SOCAT database (Version 5) were used to create this data product. The merged climatology is available at OCADS (DOI: "10.25921/qb25-f418"): https://www.ncei.noaa.gov/data/oceans/ncei/ocads/metadata/0209633.html. Additionally, there is a dedicated web page at OCADS for this project: https://www.ncei.noaa.gov/access/ocean-carbonacidification-data-system/oceans/MPI-ULB-SOM_FFN_clim.html.
- 24) VLIZ-SOM-FFN: Landschützer et al. (2016) employed the Self-Organizing Map-Feed-Forward Network (SOM-FFN) neural network method designed by Landschützer et al. (2013) to map the sea surface pCO₂ from the Surface Ocean CO₂ Atlas (SOCAT; see above No. 1) (Bakker et al., 2014) to generate monthly pCO₂ fields on a 1° x 1° global surface ocean grid, covering the period from 1982 to near present. It is based on the gridded pCO₂ measurements from SOCAT and is updated regularly. The creation of the pCO₂ fields involve a two-step neural network approach, which has been extensively detailed and validated in previous works by Landschützer et al. (2013, 2014, 2016). In the initial step, the global ocean is clustered into biogeochemical provinces, and subsequently, the non-linear relationship between CO2 driver variables and gridded data from SOCAT (Bakker et al. 2016) is reconstructed. Air-sea CO2 fluxes are also computed based on the air-sea pCO₂ difference, utilizing a bulk gas transfer formulation as described by Landschützer et al. (2013, 2014, 2016). The product is available at OCADS (DOI: "10.7289/v5z899n6"): https://www.ncei.noaa.gov/data/oceans/ ncei/ocads/metadata/0160558.html. Additionally, there is a dedicated page at OCADS for this project: https://www.ncei.noaa.gov/access/ocean-carbon-acidification-data-system/oceans/SPCO2 1982 present ETH SOM FFN.html.
 - 25) JMA-MLR: Iida et al. (2021) developed a monthly data product for inorganic carbon variables on a 1° × 1° global surface ocean grid for the period 1993–2018. Variables include dissolved inorganic carbon (DIC), total alkalinity (TA), CO₂ partial pressure (*p*CO₂), sea-air CO₂ flux, pH, and aragonite saturation state (Ω_{arag}). They leveraged data products such as SOCAT.v2019 (Bakker et al., 2016) and GLODAPv2.2019 (Olsen et al., 2019), as well as satellite-based variables, including sea-surface dynamic height (SSDH), mixed layer depth (MLD), and chlorophyll-a. The product is updated annually using the latest SOCAT and GLODAPv2 data. The data product can be accessed at: https://www.data.jma.go.jp/kaiyou/english/co2_flux/co2_flux_data_en.html.



26) OceanSODA-ETHZ:

(a) OceanSODA-ETHZv1 is a monthly gridded global surface ocean data product for multiple ocean carbon variables, including dissolved inorganic carbon (DIC), total alkalinity (TA), partial pressure of carbon dioxide (pCO₂), pH on total scale, and saturation states of aragonite and calcite (Ω_{arag} and Ω_{calc}) (Gregor and Gruber, 2020; Gregor and Gruber, 2021; Gregor and Gruber, 2023; Ma et al., 2023). This dataset is structured on a 1°×1° global surface ocean grid with monthly resolution from 1982–2022, facilitating research on OA over seasonal to decadal scales. The OceanSODA-ETHZ data product was created by extrapolating in time and space the surface ocean observations of fCO₂ from SOCATv2022 (Bakker et al., 2016) and TA from GLODAPv2.2022 using the newly developed Geospatial Random Cluster Ensemble Regression (GRaCER) method (Gregor, 2021). TA and pCO₂ were then used to calculate the remaining parameters of the marine carbonate system with the PyCO2SYS software (Humphreys et al., 2022). Phosphate and silicate from the World Ocean Atlas (2018) product were used (Boyer et al., 2018; Garcia et al., 2018a). The OceanSODA-ETHZ data product is available at OCADS (DOI: "10.25921/m5wx-ja34"): https://www.ncei.noaa.gov/data/oceans/ncei/ocads/ metadata/0220059.html.

temporal resolution, providing estimates starting from 1982 (Gregor et al., 2024a; Gregor et al., 2024b). The high-resolution outputs are suitable for investigating the shorter- and finer-scale dynamics of surface fCO_2 . Despite sharing a name with its predecessor, OceanSODA-ETHZv2 does not provide TA estimates and employs a different methodology, as described in the following steps: 1) The atmospheric trend of CO_2 is removed by subtracting marine boundary layer CO_2 concentrations from SOCAT fCO_2 producing a new target Δ^*CO_2 to reduce the biases at the start and end of the time series. 2) An 8-day seasonal climatology of Δ^*CO_2 is estimated using Gradient Boosted Decision Trees (GBDT), which is later used as a predictor. 3) The non-seasonal thermal component is removed from Δ^*CO_2 , resulting in a new target, $\Delta^*CO_2^{\text{nonT}}$. 4)

(b) OceanSODA-ETHZv2 is a surface fCO_2 product with a $0.25^{\circ} \times 0.25^{\circ}$ spatial resolution and an 8-day

The new target is estimated using a feed-forward neural network, with the GBDT as one of the forcing variables. 5) Steps 4 through to 1 are inverted to arrive at fCO_2 . 6) Air-sea CO_2 fluxes are computed using ERA5 winds. Data are available at https://doi.org/10.5281/zenodo.11206365 and are updated annually.

27) LDEO-HPD fCO₂ product: The LDEO Hybrid Physics Data (LDEO-HPD) estimates the temporal evolution of surface ocean fCO₂ and air-sea CO₂ exchange, utilizing the strengths of observations and global ocean biogeochemical models (GOBMs) (Gloege et al., 2022). GOBMs are internally consistent, mechanistic representations of the ocean circulation and carbon cycle, and have long been the standard for making spatiotemporally resolved estimates of air-sea CO₂ fluxes. However, there is often a bias between the modelled fCO₂ and available surface ocean measurements (Fay and McKinley 2021). The LDEO-HPD approach trains an eXtreme Gradient Boosting (XGB) algorithm to learn a non-linear relationship between model-data fCO₂ mismatch and observed predictor variables: SST, SSS, chlorophyll concentration, mixed layer depth). The GOBM fCO₂ is then corrected with the predicted model-data misfit to estimate real-world fCO₂ for the observation period (Gloege et al. 2022). The results in reconstructed monthly surface ocean





583 fCO_2 and air-sea CO_2 fluxes on a $1^{\circ} \times 1^{\circ}$ grid in the open ocean beginning in 1982. Additional information 584 can be found at oceancarbon.ldeo.columbia.edu. The data product is available at: 585 https://zenodo.org/records/4760205. 586 28) LDEO HPD product with extended temporal coverage: Building on the work of Gloege et al. (2022), 587 the LDEO-HPD product as mentioned above (nr. 25) can be extended back in time to predict fCO2 for all 588 available model years. Bennington et al (2022a) find that the largest component of the GOBM corrections 589 is climatological. The smaller corrections at other timescales suggest either that these are well captured by 590 the GOBMs or the data are insufficient. The dominance of climatological corrections supports the 591 extension of the LDEO-HPD fCO2 product backwards in time. A climatology of model-observation misfits 592 for the best-observed period (2000-present) is applied to the GOBMs for 1959-1981, while an inter-593 annually varying correction is used for 1982 onward. (Bennington et al 2022a). This results in 594 reconstructed monthly surface ocean fCO2 and air-sea CO2 fluxes on a 1° × 1° grid covering the open 595 ocean, beginning in 1959. Since 2022, the LDEO-HPD Back in Time product has been included in the 596 annual release of the Global Carbon Budget. Additional information can be found at 597 oceancarbon.ldeo.columbia.edu. The data product can be accessed via Zenodo at 598 https://zenodo.org/records/13891722. 599 29) LDEO fCO₂ - Residual Method: A frequently used approach for estimating full-coverage fCO₂ is to train 600 a machine learning algorithm on sparse in situ fCO2 data and associated physical and biogeochemical 601 observations. While these associated variables have well-known relationships to fCO2, it is often unclear 602 how they mechanistically drive fCO2 around the world. The LDEO fCO2-Residual method takes the basic 603 approach and enhances connections between physical understanding and reconstructed fCO2. The novel 604 approach used here includes applying pre-processing to the fCO2 data to remove the direct effect of temperature - a relationship well-documented in literature and lab experiments (Takahashi et al. 2002). 605 606 This enhances the biogeochemical/physical component of fCO₂ in the target variable (now fCO₂-Residual) 607 and reduces the complexity that the machine learning must disentangle. The resulting algorithm has 608 physically understandable connections between input data and the output biogeochemical/physical 609 component of fCO₂ (Bennington et al. 2022b). This results in reconstructed monthly surface ocean fCO₂ 610 and air-sea CO₂ fluxes on a 1° × 1° grid covering the open ocean, beginning in 1982 and extended to the 611 most recent year of available data. Additional information can be found at oceancarbon.ldeo.columbia.edu. 612 The data product can be accessed via Zenodo at https://zenodo.org/records/13941548. 613 30) CMEMS-LSCE surface ocean carbon data products: 614 (a) CMEMS-LSCEv1: Monthly surface ocean pCO2 and air-sea CO2 fluxes on a 1° × 1° grid in both the 615 open ocean and coastal seas from 1985-2019 were reconstructed by Chau et al., (2022). CMEMS-LSCE is 616 short for Copernicus Marine Environment Monitoring Service - Laboratoire des Sciences du Climat et de

l'Environnement. This product is generated from an ensemble-based reconstruction of pCO₂ maps trained



619

620

621

622

623

624

625

626 627

628

629

630

631

632

633

634

635

636

637638

639

640

641

642

643

644

645

646

647

648

649 650



with gridded data from SOCATv2020 (Bakker et al., 2016). Sea-surface pCO₂ values (converted from the original fCO₂ values in SOCATv2020) were regressed against a set of predictors with non-linear functions, i.e., feed-forward neural network (FFNN) models. The predictors include: sea-surface height (SSH), SST, SSS, MLD, chlorophyll a (Chl-a), atmospheric CO₂ mole fraction (xCO₂), and geographical coordinates (longitudes and latitudes). This data product is accessible at: https://data.ipsl.fr/catalog/srv/eng/catalog.search#/metadata/a2f0891b-763a-49e9-af1b-78ed78b16982. (b) CMEMS-LSCEv2: CMEMS-LSCEv2 corresponds to the latest version of the CMEMS-LSCE FFNN. It uses the same ensemble-based reconstruction method for pCO₂ maps as CMEMS-LSCEv1. Improvements include downscaling the spatial resolution to 0.25° × 0.25° and reproducing additional surface ocean carbonate system variables on a global grid from 1985 onwards (Chau et al., 2024a). The additional surface ocean carbonate system variables are: pCO₂, DIC, TA, pH, and saturation states with respect to aragonite (Ω_{ar}) and calcite (Ω_{ca}) . Surface ocean pCO_2 is reconstructed based on an ensemble of neural network models mapping gridded observation-based data provided by SOCATv2022 (Bakker et al., 2016). Surface ocean TA is estimated with a multiple linear regression approach (Carter et al., 2016, 2017). The remaining carbonate variables are calculated from pCO₂ and TA using a MATLAB version of CO2SYS (Lewis and Wallace, 1998; Van Heuven et al., 2011). The CMEMS-LSCE product is updated yearly for surface ocean pCO_2 , air-sea fluxes, and the carbonate system variables. Updates are phased with release of the SOCAT database. For surface ocean pCO2 and air-sea fluxes the temporal coverage is extended to the present date with a latency of 1 month (Chau et al., 2024b). Both the multi-year reconstruction and the near-real time prediction can be accessed through the CMEMS portal: https://doi.org/10.48670/moi-00047.

31) CarboScope (Jena-MLS): The Jena Mixed-Layer Scheme (within the CarboScope family of data-based estimates of carbon-cycle variability) is based on observed sea surface pCO₂ from the Surface Ocean CO₂ Atlas (SOCAT; see above No. 1) (Bakker et al., 2014). It provides daily global fields of pCO₂ and sea-air CO₂ fluxes from 1957 to the year before present, on a resolution of 2.5×2 degrees. In the original method (Rödenbeck et al., 2013), a diagnostic model of the carbon balance in the ocean mixed layer is being fitted to the pCO₂ data, by adjusting the ocean-interior sources and sinks of carbon of the mixed layer. The multi-decadal trend is derived from the data-based Ocean Circulation Inverse Model (OCIM) estimate provided by DeVries et al. (2022). Since a later extension described in Rödenbeck et al. (2022), the variability in the ocean-interior sources and sinks is first regressed against variability in SST and wind speed. The regression step is followed by a correction step with explicit temporal variability, to also represent data variability not yet represented by the predictors of the regression. The CarboScope product is updated yearly. The results from current and previous releases can be downloaded from https://www.bgc-jena.mpg.de/CarboScope/.





- 32) UOEx-Watson: This product is an estimate of the atmosphere-ocean flux of CO₂ that takes into account near-surface temperature deviations (Watson et al., 2020). Most estimates use data on surface ocean pCO₂ without considering corrections due to temperature gradients within the uppermost few millimeters of the sea surface ("Skin temperature effects") or small effects due to changes in temperature that occur during sampling and measurement, especially when the measurement is from a commercial vessel rather than a research ship. This product takes these effects into account by recalculating pCO₂ from the SOCAT data base (v2019) using co-located satellite observations of skin temperature. The result is a substantial increase in the calculated net global uptake of CO₂. In other respects, the methodology for this data product follows the two-step neural network approach described by Landschützer et al. (2013, 2014). The gridded data set of sea surface fCO₂ adjusted to satellite-derived subskin surface temperature, is available at https://doi.org/10.1594/PANGAEA.905316. Ocean-atmosphere fluxes interpolated to monthly and 1° × 1° degree spatial resolution is available at OCADS (DOI: "10.25921/2dp5-xm29"): https://www.ncei.noaa.gov/data/oceans/ncei/ocads/metadata/0301544.html.
- 33) NIES-ML3: The National Institute for Environmental Studies (NIES-ML3) product includes monthly global surface ocean fCO₂ in 1982-2023 on a 1° × 1° grid. Using a leave-one-year-out (LOYO) validation method and three machine learning models, Zeng et al. (2022) found that the time variant trends of ocean CO₂ could be estimated approximately by a harmonic function fitting of the annual atmospheric CO₂. They removed the estimated trends from the ocean CO₂ and applied the LOYO to the trend-removed data to obtain the trend that could not be approximated by the fitting for trend correction. The trend-removed data by the corrected trends were used to train the models. The gap-filled CO₂ maps were constructed by adding the trends to model predictions. The product is available at NIES: https://doi.org/10.17595/20220311.001 (Zeng 2022).
- 34) CSIR-ML6: Provides monthly 1° × 1° estimates of surface pCO₂ (Gregor et al., 2019a). The approach uses the conceptual two-step approach of clustering and performing regressions for each cluster as Landschützer et al. (2016). CSIR-ML6 investigates the efficacy of various machine learning (ML) methods in estimating surface pCO₂, namely, feed-forward neural networks (FFNN), extremely randomized trees (ERT), gradient boosting machines (GBM), and support vector regression (SVR). It is found that the ensemble of all but the ERT method resulted in the best estimate, highlighting the fact that various ML methods do not produce the same outcome, particularly when data is sparse. Further, the variance between ensemble members can inform us about regions where uncertainty may be large due to methodological differences. Despite this, all methods achieve roughly the same uncertainty a barrier, or wall beyond which the community has yet to overcome. The data are available at OCADS (DOI: "10.25921/z682-mn47"): https://www.ncei.noaa.gov/data/oceans/ncei/ocads/metadata/0206205.html. The product is one of the six ensemble members of the SeaFlux dataset.





- 35) AOML-ET: Wanninkhof et al. (2024, 2025) developed a monthly global ocean data product of seawater pCO₂ and sea-air CO₂ fluxes, referred to as AOML-ET, using an extremely randomized trees (ET) machine learning technique. These maps are created on 1° × 1° spatial grids, providing global surface ocean coverages from 1998 to 2023. AOML-ET incorporates several predictor variables, including time, location, SST, SSS, MLD, and chlorophyll-a. The model was trained using the v2020 and v2023 releases of the SOCAT data product (No. 1). Sea-air CO₂ fluxes were calculated using the air-sea CO₂ partial pressure difference (ΔpCO₂) and a bulk gas transfer formulation incorporating windspeed. The dataset contains monthly 1° × 1° NetCDF files of the AOML-ET outputs, along with the predictor variables. The data are available at OCADS (DOI: "10.25921/0s8y-q287"): https://www.ncei.noaa.gov/data/oceans/ncei/ocads/metadata/0298989.html.
- 36) ULB-SOM-FFN-coastalv2.1: Roobaert et al. (2024) present high-resolution (0.25° × 0.25° grid) monthly maps showing the distribution of sea surface *p*CO₂ across the global coastal oceans, spanning from 1982 to 2020. This product (ULB-SOM-FFN-coastalv2.1) builds upon the work by Laruelle et al. (2017), incorporating a two-step methodology that utilizes Self Organizing Maps (SOM) and Feed Forward Networks (FFN). This updated product now captures temporal variability, enabling the assessment of interannual variability and long-term trends in coastal air-sea CO₂ exchange, unlike the product by Laruelle et al. (2017), which only offers a climatology for a short period (1998-2015). The enhancements include additional environmental predictors and an expanded dataset for training and validation, featuring approximately 18 million direct coastal observations from the Surface Ocean CO₂ Atlas (SOCAT) database, specifically the SOCATv2022 release (Bakker et al., 2016). The product is available at OCADS (DOI: "10.25921/4sde-p068"): https://www.ncei.noaa.gov/data/oceans/ncei/ocads/metadata/0279118.html (Roobaert et al., 2023).
 - 37) RFR-LME: Sharp et al. (2024b) developed a data product delineating the temporal trends of OA indicators mapped on a 0.25 °× 0.25° spatial grid, across eleven U.S. Large Marine Ecosystems (LMEs), with monthly coverage from 1998–2023. These indicators, which include the *p*CO₂, pH, Ω_{arag}, DIC, TA, Revelle Factors, among others, were derived from SOCATv2023, along with other oceanographic properties, e.g., SST, SSS, SSH, and MLD. The methodology combined Gaussian Mixture Models to categorize the data into environmentally similar subregions, Random Forest Regressions for the spatial and temporal extrapolation of observational *f*CO₂ data, and regressions to estimate TA (Carter et al. 2021) to provide a second carbonate system constraint. The resulting maps are available at OCADS (DOI: "10.25921/h8vw-e872"): https://www.ncei.noaa.gov/data/oceans/ncei/ocads/metadata/0287551.html (Sharp et al., 2024a), while an online portal at https://ecowatch.noaa.gov/thematic/ocean-acidification presents regionally averaged time series for three key indicators: the partial pressure of carbon dioxide, calcium carbonate saturation state with respect to aragonite, and seawater pH.



720

721

722

723

724

725

726

727

728

729

730

731

732

733

734

735

736

737

738739

740

741742

743

744

745

746

747

748749

750



- **38)** ReCAD-NAACOM- pCO_2 : Wu et al. (2025) developed a reconstructed pCO_2 product for the North American Atlantic Coastal Ocean Margins (NAACOM), spanning from the Gulf of Mexico/Gulf of America to the Grand Banks, called the Reconstructed Coastal Acidification Database-pCO₂ (ReCAD-NAACOM-pCO₂). This product employed a two-step approach combining random forest regression and linear regression to generate monthly pCO₂ data at 0.25° spatial resolution from 1993–2021. The model was trained using SOCAT v2023 observations as ground-truth values, incorporating various satellitederived and reanalysis environmental variables known to influence sea surface pCO_2 . The ReCAD-NAACOM-pCO₂ product demonstrates robust performance, with a coefficient of determination of 0.83, a root-mean-square error of 18.64 µatm, and an accumulative uncertainty of 23.83 µatm when compared against all SOCAT observation samples. This high accuracy was maintained across model training and validation phases. The model exhibits robust performance when validated against independent test data from a period excluded from both training and validation, underscoring the product's capability to reliably reconstruct pCO₂ in periods lacking direct observational data within the NAACOM. Significantly, the product enables detailed investigation of regional spatial differences, seasonal cycles, and decadal changes in pCO₂ across the NAACOM. The ReCAD-NAACOM-pCO₂ dataset is publicly accessible (https://doi.org/10.5281/zenodo.11500974) and will be updated regularly.
- 39) Gridded surface OA indicators, and air–sea CO₂ fluxes in the northern Caribbean Sea: This dataset contains a high-quality dataset of derived products from over a million observations of surface water partial pressure/fugacity of carbon dioxide (*p*CO₂w/*f*CO₂w), for the Caribbean Sea, Gulf of Mexico/Gulf of America and North-West Atlantic Ocean covering the timespan from 2002-01-01 to 2019-12-30. The derived quantities include total alkalinity (TA), acidity (pH), aragonite saturation state (Ω_{Ar}) and air-sea CO₂ flux (Wanninkhof et al., 2020). This data product is available at OCADS (DOI: "10.25921/2swk-9w56"): https://www.ncei.noaa.gov/data/oceans/ncei/ocads/metadata/0207749.html (Wanninkhof et al., 2019)
- 40) Ocean acidification data in the Gulf of Mexico/Gulf of America and wider Caribbean from 2014 to 2020: The Acidification, Climate, and Coral Reef Ecosystems Team (ACCRETE) Lab within AOML's Ocean Chemistry and Ecosystems Division (OCED) developed a data product for tracking ocean acidification in the Caribbean and Gulf of Mexico/Gulf of America (van Hooidonk, 2022). Utilizing satellite imagery and a data-assimilative hybrid model, the tool maps key indicators of the water's carbonate system, including pCO_2 , TA, pH, Ω_{arag} , and Ω_{calc} . This innovation builds upon an update to the experimental Ocean Acidification Product Suite (OAPS) developed by NOAA's Coral Reef Watch. The data product is available at OCADS (DOI: "10.25921/tt1c-dx53"): https://www.ncei.noaa.gov/data/oceans/ncei/ocads/metadata/0245950.html. (van Hooidonk, 2022)





41) Regional pCO₂ climatology of the Baltic Sea: Bittig et al. (2024) used biogeochemical model output to inform the mapping of sea surface pCO₂ observations in the Baltic Sea and to build a mean monthly climatology for the period 2003 to 2021 with 3 nautical mile resolution. In a first step, spatial patterns of variability were extracted from 20 years of model surface pCO₂ data by an EOF analysis. These spatial patterns were then used to map surface pCO₂ observations from the Surface Ocean CO₂ Atlas (SOCAT; see above No. 1) (Bakker et al., 2014) onto the Baltic Sea domain. By using an ensemble approach with varying number of EOF patterns, the spatial scales of the mapping were locally adjusted based on the observation's data density. Mapped monthly fields of pCO₂ from 2003-2021 were combined for the product into a mean monthly climatology and a spatially-resolved linear trend. The climatology product is available at PANGAEA (DOI: "10.1594/PANGAEA.961119"): https://doi.org/10.1594/PANGAEA.961119 (Bittig et al., 2023).

763 Table 3. Gridded and derived ocean carbonate chemistry data synthesis products in the surface ocean.

No.	Name	Open or coastal ocean	Spatial resolution	Temporal resolution	Methodology	Highlights	Reference
22	Updated Takahashi delta fCO ₂ and flux climatology	Open ocean	1°×1°	12-month climatology for a base year of 2010	Advection Scheme	Does not use proxy variables for extrapolation. Only produced as monthly climatology.	Fay et al. (2024)
23	MPI-ULB- SOM-FFN	Open + Coastal	0.25° × 0.25°	Monthly climatology (January through December) without reference year	2-step machine learning: Merged product of the SOM-FFN approach applied to the open ocean (Landschützer et al 2016) and the coastal ocean (Laruelle et al 2017)	Monthly gridded pCO ₂ without adjusting for a specific reference year, high-resolution coastal ocean coverage	Landschützer et al. (2020a)
24	VLIZ SOM-FFN	Open ocean	1° × 1°	Monthly from January 1982 onwards	2-step machine learning: Self organizing map clustering followed by a feed forward network (SOM-FFN)	Monthly gridded pCO ₂ from 1982 through near present	Landschützer et al. (2016)
25	JMA-MLR	Open ocean	1° × 1°	Monthly from January 1990 onwards	Multiple linear regressions	Temporal trends of DIC, TA, p CO ₂ , airsea CO ₂ flux, pH, and Ω_{arag}	lida et al. (2021)
26(a)	OceanSODA -ETHZv1	Open ocean	1° × 1°	Monthly from 1982 to 2023	Ensemble of 2-step members: K-means clustering with gradient boosting and SVR regression	Temporal trends of DIC, TA, p CO ₂ , pH, Ω_{arag} , and Ω_{calc}	Gregor and Gruber (2021)





26(b)	OceanSODA -ETHZv2	Open + Coastal ocean	0.25° × 0.25°	8-day from 1982 to 2022	FFNN	Highlighting fine- scale and short-term variability of the ocean carbon sink	Gregor, Shutler, and Gruber (2024)
27	LDEO-HPD fCO ₂ product	Open ocean	1° × 1°	Monthly from 1982	XGBoost algorithm	Temporal evolution of surface ocean fCO ₂ and air-sea CO ₂ exchange	Gloege et al. (2022)
28	LDEO HPD with extended temporal coverage	Open ocean	1° × 1°	Monthly from 1959	XGBoost algorithm	uses model-data misfit climatology to extend estimate back in time to 1959	Bennington et al (2022a)
29	LDEO fCO ₂ - Residual Method	Open ocean	1° × 1°	Monthly from 1982	XGBoost algorithm	Removes the temperature component before ML	Bennington et al (2022b)
30(a)	CMEMS -LSCEv1	Open + Coastal	1° × 1°	Monthly from 1985 to 2019	FFNN	seamless reconstruction from coastal to open ocean	Chau et al. (2022)
30(b)	CMEMS -LSCEv2	Open + Coastal	0.25° × 0.25°	Monthly from 1985 to 2021	FFNN	yearly extension of time series & monthly reconstruction at low latency	Chau et al. (2024)a,b
31	CarboScope (Jena-MLS)	Open ocean	2.5° × 2°	Daily from 1957	Multi-linear regression against long-term predictors, plus auto- regressive correction	Variability of pCO2 and sea-air CO ₂ fluxes since 1957, sensitivities to SST and wind speed variations	Rödenbeck et al. (2022)
32	UOEx-Watson	Open ocean	1° × 1°	Monthly from January 1992	Two-step neural network approach described by Landschützer et al.	air-sea fluxes of CO ₂ with adjusted skin temperature effect	Watson et al., 2020
33	NIES-ML3	Open ocean	1° × 1°	Monthly from 1982 to 2023	FNN, GBM, RF	The prediction of a ML method was obtained from ten trainings with different seeds. The mean of the three methods was taken as the final prediction.	Zeng (2022), Zeng et al. (2022)
34	CSIR-ML6	Open ocean	1°×1°	Monthly from 1982 to 2016	Ensemble: FFNN, SVR, ERT, Gradient Boosted Trees	Various ML methods produce different results when data is sparse, but all still achieving roughly the same uncertainty.	Gregor et al. (2019a)
35	AOML-ET	Open ocean	1° × 1°	Monthly from 1998 to 2023	Extremely randomized trees (ET) machine learning technique	Monthly global sea-air CO ₂ flux maps in modern era	Wanninkhof et al. (2015)





36	ULB-SOM-FFN -coastalv2.1	Coastal ocean	0.25° × 0.25°	Monthly from 1982 to 2020	2-step machine learning: Self organizing map clustering followed by a feed forward network (SOM-FFN)	Global temporal trends of coastal pCO ₂ and air-sea CO ₂ fluxes based on SOCATv2022 with data collected from 1982–2020	Roobaert et al. (2024)
37	RFR-LME	Coastal	0.25° × 0.25°	Monthly from 1998 to 2023	Gaussian mixture models and random forest regressions	Temporal trends of OA indicators and estimated uncertainties across 11 U.S. Large Marine Ecosystems (LMEs), with monthly coverage from 1998–2023.	Sharp et al. (2024b)
38	ReCAD -NAACOM -pCO ₂	Coastal	0.25° × 0.25°	Monthly from 1993 to 2021	2-step machine learning: random forest regression followed by linear regression	Sea surface pCO ₂ in the North American Atlantic Coastal Ocean Margins (NAACOM)	Wu et al. (2025)
39	Gridded surface OA indicators, and air–sea CO ₂ fluxes in the northern Caribbean Sea	Coastal	1° × 1°	Monthly from 2002 to 2019	Gridding of the observations of fCO ₂ , SST and SSS was performed by binning and averaging the data in (1° × 1° by month) cells	A 17-year record of f CO ₂ , TA, pH, Ω _{Ar} , and air-sea CO ₂ flux in the Caribbean Sea	Wanninkhof et al. (2020)
40	OA data in the Gulf of Mexico/Gulf of America and wider Caribbean from 2014 to 2020	Regional	0.088° × 0.88°	Monthly from 2014 to 2020	Utilizing satellite imagery and a data-assimilative hybrid model, the tool maps key indicators of the water's carbonate system, including pCO ₂ , TA, pH, Ωarag, and Ωcalc.	A new tool to monitor ocean acidification over the wider Caribbean and Gulf of Mexico/Gulf of America.	van Hooidonk (2022)
41	Regional pCO ₂ climatology of the Baltic Sea	Regional	0.1° × 0.05°	12-month climatology for a base year of 2013; linear trend 2003-2021	Extrapolation using model-based patterns of variability	Does not use proxy variables for extrapolation. Spatial scales adjust locally to data density	Bittig et al. (2024)

764 3.1.4 Gridded and derived data products – Interior ocean:

Although cruise data compilations are valuable for making data available in a uniform format, they often are constrained by their sampling strategies and can have significant gaps in space and time. Gridded and derived data products address this limitation by making some variables available at all grid points on a standardized spatial grid and at standardized depth levels through processes such as interpolation and gap filling.





- 42) Global interior ocean mapped climatology from GLODAPv2 (referenced to 2002): Lauvset et al. (2016) generated a comprehensive set of global interior ocean climatologies, mapping key biogeochemical variables on a 1°×1° grid for 33 depth levels from surface to 5500 m. These climatologies cover temperature, salinity, oxygen, nitrate, phosphate, silicate, DIC, TA, pH, and the saturation states of aragonite and calcite (Ω_{arag} and Ω_{calc}). This data product was created based on the quality-controlled and internally consistent GLODAPv2.2016 (Olsen et al., 2016) using the Data-Interpolating Variational Analysis (DIVA) method (Barth et al., 2014). The conceivably confounding temporal trends in DIC, pH, Ω_{arag} and Ω_{calc} due to anthropogenic influence were removed prior to mapping by normalizing their values to a reference year of 2002 using first-order calculations of anthropogenic carbon accumulation rates. For all variables, all data from the full 1972–2013 period were used, including data that did not receive full secondary quality control. This data product is not updated each year along with the main GLODAPv2 data product. The mapped data product is available at OCADS (DOI: "10.3334/cdiac/otg.ndp093_glodapv2"): https://www.ncei.noaa.gov/data/oceans/ncei/ocads/metadata/0286118.html (Lauvset et al., 2023b). It can also be accessed from the GLODAP website: https://glodap.info/.
- 43) Global aragonite saturation state climatology (referenced to 2000): Jiang et al. (2015a) developed a climatology of the derived variable, aragonite saturation state (Ω_{arag}) across the global interior ocean, on a 1° x 1° grid at 9 standardized depth levels from the surface down to 4000m. This was accomplished by integrating data from the first version of GLODAP (Key et al., 2004), CARINA (Key et al., 2010), and PACIFICA (Suzuki et al., 2013), along with additional recent cruise datasets up to 2012. Calculations of Ω_{arag} utilized a MATLAB version of the CO2SYS program (Orr et al., 2015), with the dissociation constants for carbonic acid of Lueker et al. [2000], potassium bisulfate (KHSO₄⁻) of Dickson [1990], hydrofluoric acid (HF) of Perez and Fraga (1987), and the total borate concentration equations of Lee et al. [2010]. Temporal adjustments were made to a reference year of 2000, accounting for an annual increase of fCO₂ of 1.6 μatm in the surface mixed layer (SML), with a rate that decreases linearly to zero μatm yr⁻¹ from the bottom of the SML to a depth of 1000 m (Sabine et al., 2008). The data product is available at OCADS (DOI: "10.1002/2015GB005198"): https://www.ncei.noaa.gov/data/oceans/ncei/ocads/metadata/0139360.html (Jiang et al., 2015b).
- 44) MOBO-DIC (Version 2020): Keppler et al. (2020) produced a global interior ocean DIC monthly climatology (average climatological values for January through December) on a 1° × 1° grid at 33 standardized depth levels from the surface to 2000 m. The Mapped Observation-Based Oceanic Dissolved Inorganic Carbon (MOBO-DIC) mapping method adapts and extends the SOM-FFN technique originally introduced by Landschützer et al. (2013). It starts by categorizing the ocean into clusters with comparable physical and biogeochemical characteristics using self-organizing maps (SOM). Subsequently, within each SOM-defined cluster, a feed-forward network (FFN) is employed to estimate and enforce the statistical correlation between the targeted dissolved inorganic carbon (DIC) data and the predictor data available in





- globally mapped fields. The product uses data from January 2004 to December 2017, and is thus centered around the years 2010/2011. The data product is available at OCADS (DOI: "10.25921/yvzj-zx46"): https://www.ncei.noaa.gov/access/ocean-carbon-acidification-data-system/oceans/ndp_104/ndp104.html.
- interior ocean TA climatology using a feed-forward neural network approach. This dataset offers a spatial resolution of 1° × 1° in the horizontal, spans 102 depth levels (ranging from 0–5500 m) in the vertical dimension, and features a temporal resolution that varies from monthly (0–1500 m) to annual (1550–5500 m). The development of this climatology was based on the analysis of TA in relation to several key predictor variables, including temperature, salinity, nutrients (phosphate, nitrate, and silicate), dissolved oxygen, and sampling position (coordinates and depth), as outlined in Velo et al. (2013). Both TA and these predictor variables were sourced from GLODAPv2 (version 2016) (Olsen et al., 2016). The global interior ocean TA climatology was constructed by leveraging the established relationships between TA and the predictor variables, as well as the monthly climatologies of temperature, salinity, and dissolved oxygen from the World Ocean Atlas 2013 (WOA13) (Locarnini et al., 2013; Zweng et al., 2013; Garcia et al., 2014), and nutrients data that were obtained through the CANYON-B neural network process, applied to the previously mentioned fields. The data product is available at OCADS (DOI: "10.25921/5p69-y471"): https://www.ncei.noaa.gov/data/oceans/ncei/ocads/metadata/0222470.html.
- 46) Monthly global interior ocean DIC climatology: Broullón et al. (2020) employed a feed-forward neural network approach to create a monthly global interior ocean DIC climatology, centered around the year 1995. This dataset offers a 1° × 1° spatial resolution in the horizontal domain, encompassing 102 depth levels ranging from 0–5500 m vertically. The temporal resolution varies, ranging from monthly (0–1500 m) to annual (1550–5500 m). In contrast to their previous work on TA (Broullón et al., 2019), this analysis includes the variable "year" to account for anthropogenic DIC pool changes. It also incorporates data from the Lamont–Doherty Earth Observatory (LDEO) pCO2 database (Takahashi et al., 2017) alongside GLODAPv2.2019 (Olsen et al., 2019) to establish relationships between DIC and its input variables: temperature, salinity, dissolved oxygen, as well as location, pressure, and time. The DIC climatology was derived using these relationships, along with monthly climatological data for temperature, salinity, and dissolved oxygen from the World Ocean Atlas 2013 (Locarnini et al., 2013; Zweng et al., 2013; Garcia et al., 2014), as well as phosphate, nitrate, and silicate values computed from the CANYON-B neural network fed with the aforementioned fields. The data product is available at OCADS (DOI: "10.25921/ndgj-jp24"): https://www.ncei.noaa.gov/data/oceans/ncei/ocads/metadata/0222469.html.
- **47) MOBO-DIC** (Version 2023): Keppler et al. (2023) extended the temporal resolution of MOBO-DIC to resolve monthly fields from January 2004 to December 2019, as opposed to the average climatological values in Keppler et al. (2020). This data product is on a 1° × 1° grid at 28 depth levels from the surface to 1500 m. The data product is available at OCADS (DOI: "10.25921/z31n-3m26"):



840

841

842

843

844

845

846847

848

849

850

851

852

853

854

855

856857

858

859

860

861

862

863

864

865

866867

868

869

870

871872



https://www.ncei.noaa.gov/data/oceans/ncei/ocads/metadata/0277099.html.

- 48) Metrics of acidification in the ocean interior: Fassbender et al. (2023) generated estimates of global interior ocean changes to pH, [H⁺], Ω_{Ar} , pCO₂, and the Revelle sensitivity factor driven by the accumulation of anthropogenic carbon (C_{ant}) from the preindustrial period to the year 2002, and quantified the component of those changes caused by nonlinearities in the carbonate system. For each OA metric, the dataset includes year 2002 values and quasi-preindustrial values, which were estimated by subtracting Cant from the year 2002 carbonate chemistry information and recomputing each OA metric without considering any warming, circulation, or biological changes that may have occurred since the preindustrial era. Data from the upper 2000 m of the GLODAPv2.2016b mapped data product (DOI: "10.3334/cdiac/otg.ndp093 glodapv2"), described in Lauvset et al., 2016, and from the preformed properties product of Carter et al., 2021 were used to make these estimates on the GLODAPv2.2016b 1° × 1° grid for 26 depth levels from surface to 2000 m. The provided uncertainties were estimated using a 1000-iteration Monte Carlo simulation. Calculation details are described in Fassbender et al. (2023). Year 2002 aragonite saturation state and pH values, and their uncertainties, are reproduced from the GLODAPv2.2016b mapped data product and are provided in this dataset for user convenience with the permission of the original data producer. This data product is available at OCADS (DOI: "10.25921/rdtr-9t74"): https://www.ncei.noaa.gov/data/oceans/ncei/ocads/metadata/0290073.html.
- 49) Anthropogenic CO₂ from 1994 to 2007: Gruber et al. (2019a) estimated decadal changes in the oceanic content of anthropogenic CO₂ (ΔCant) for the years 1994, 2004, and 2014. The results have been derived from the GLODAPv2.2016 product (Olsen et al., 2016), utilizing the eMLR(C*) methodology pioneered by Clement and Gruber (2018). All estimates are geospatially distributed on a horizontal grid with a resolution of 1° × 1°. Two primary files are available: one providing the complete three-dimensional distribution of ΔC_{ant}, and the other containing vertically integrated values, i.e., the column inventories. This data product is available at OCADS (DOI: "10.25921/wdn2-pt10"): https://www.ncei.noaa.gov/data/oceans/ncei/ocads/metadata/0186034.html (Gruber et al., 2019b).
- 50) Decadal trends in anthropogenic CO₂ from 1994 to 2014: Müller et al. (2023) extended the analysis by Gruber et al. (2019a) to reconstruct decadal trends in the oceanic storage of anthropogenic CO₂ (ΔC_{ant}) in the global ocean interior from 1994 to 2014. They applied the extended multiple linear regression (eMLR) method (Clement and Gruber 2018) to ship-borne observations of DIC and other biogeochemical variables from GLODAPv2.2021 (Lauvset et al., 2021). All estimates are provided on a 1° × 1° horizontal grid. Two principal data files are provided: one featuring the comprehensive three-dimensional distribution of ΔC_{ant}, and the other presenting the vertically integrated quantities, i.e., the column inventories. The data product is available at OCADS (DOI: "10.25921/ppcf-w020"): https://www.ncei.noaa.gov/data/oceans/ncei/ocads/metadata/0279447.html.



874

875

876

877

878

879

880

881

882

883

884

885

886

887

888

889

890

891

892

893 894

895

896

897 898

899

900



- anthropogenic carbon estimates for 1994 from Sabine et al. (2004) and the decadal changes between 1994 and 2014 reconstructed by Müller et al. (2023), Müller et al. (2024) quantified ocean interior acidification over the industrial era. To convert the increasing anthropogenic carbon concentrations into acidification estimates, their approach relied on time-invariant climatologies of ocean interior DIC, TA, temperature, salinity, and other relevant variables to determine the background state of the marine carbonate system. Hence, their estimates resolve exclusively the acidification driven by the anthropogenic carbon accumulation. In contrast to direct observations of acidification parameters—such as those collected at time series stations—this approach does not account for changes in the natural carbon cycle or the displacement of water masses. The approach by Müller et al. (2024) is conceptually similar to that of Fassbender et al. (2023), but provides temporally resolved estimates, enabling the tracking of both the spatial distribution and temporal evolution of ocean interior acidification. The data product is available at OCADS (DOI: "10.25921/tefm-x802"): https://www.ncei.noaa.gov/data/oceans/ncei/ocads/metadata/0298993.html
- 52) CODAP-NA climatology: Jiang et al. (2024) developed a coastal OA indicators climatology on a 1°×1° grid, covering North American ocean margins from surface to 500 m at 14 standardized depth levels: 0, 10, 20, 30, 50, 75, 100, 125, 150, 200, 250, 300, 400, and 500 m. This product includes 10 key oceanographic parameters: fugacity of carbon dioxide (fCO₂), pH, total hydrogen ion content, free hydrogen ion content, carbonate ion content ([CO₃²⁻]), Ω_{arag} , Ω_{calc} , DIC, TA, and Revelle Factor (RF), as well as temperature and salinity. The climatology was produced with the World Ocean Atlas (WOA) gridding technologies of the NOAA National Centers for Environmental Information (NCEI), based on the recently released Coastal Ocean Data Analysis Product in North America (CODAP-NA) (Jiang et al., 2021), along with GLODAPv2.2022 (Lauvset et al., 2022). The relevant variables were adjusted to the year of 2010 before the gridding. The first-guess fields for this analysis were calculated using ESPERs (Carter et al., 2021), based on the WOA (Version 2018) climatologies for salinity (Zweng et al., 2019), temperature (Locarnini et al., 2019) and dissolved oxygen (Garcia et al., 2018b). The data product is available in NetCDF at OCADS (DOI: "10.25921/g8pb-zy76"): https://www.ncei.noaa.gov/data/oceans/ncei/ocads/metadata/0270962.html. Additionally, maps of these indicators are available in jpeg at: https://www.ncei.noaa.gov/access/ocean-carbon-acidification-datasystem/synthesis/nacoastal.html (Jiang et al., 2022b).





Table 4. Gridded and derived ocean carbonate chemistry data synthesis products in the subsurface ocean.

No.	Name	Open or coastal ocean	Reso- lution	Temporal resolution	Methodology	Highlights	Reference
42	Global interior ocean mapped climatology from GLODAPv2	Open ocean	1° × 1°	adjusted to 2002	Data Interpolating Variational Analysis (DIVA)	Ocean interior climatology for multiple variables from surface to the bottom of the ocean (referenced to year 2002)	Lauvset et al. (2016)
43	Global aragonite saturation state climatology	Open ocean	1° × 1°	adjusted to 2000	Data Interpolating Variational Analysis (DIVA)	Ocean interior climatology for aragonite saturation state from surface to 4000 m (referenced to year 2000)	Jiang et al. (2015a)
44	MOBO-DIC (Version 2020)	Open ocean	1° × 1°	monthly climatology, centered around 2010/2011	Machine learning	Seasonal variability of DIC in the interior ocean from surface to 2000 m	Keppler et al. (2020)
45	Monthly global interior ocean TA climatology	Open ocean	1° × 1°	monthly climatology	Machine learning	Ocean interior climatology for TA from surface to bottom	Broullón et al. (2019)
46	Monthly global interior ocean DIC climatology	Open ocean	1° × 1°	monthly from 1957 to 2018	Machine learning	Ocean interior climatology for DIC from surface to bottom (referenced to year 1995)	Broullón et al. (2020)
47	MOBO-DIC (Version 2023)	Open ocean	1° × 1°	monthly from Jan 2004 to Dec 2019	Machine learning	Temporal trends and interannual variability of DIC in the interior ocean from surface to 1500 m	Keppler et al. (2023)
48	Metrics of acidification in the ocean interior	Open ocean	1° × 1°	2002 and preindustrial	Reproduced from GLODAPv2.2016b (Lauvset et al., 2016) and the preformed properties of Carter et al., (2021)	Metrics of acidification in the ocean interior (to 2000 m) and the component of those changes caused by carbonate system nonlinearities	Fassbender et al. (2023)
49	Anthropogenic CO ₂ from 1994 to 2007	Open ocean	1° × 1°	1994 and 2007	Extended multiple linear regression (eMLR)	The oceanic sink for anthropogenic CO ₂ over the period 1994 to 2007	Gruber et al. (2019a)
50	Decadal trends in anthropogenic CO ₂ From 1994 to 2014	Open ocean	1° × 1°	Decadal from 1994 to 2014	eMLR(C*) extended Multiple Linear Regression applied to the tracer C*	Temporal trends in the accumulation of anthropogenic CO ₂ in the interior ocean are resolved	Müller et al. (2023)
51	Progression of Ocean Interior Acidification over the Industrial Era	Open ocean	1° × 1°	1800 – 1994 – 2004 - 2014	Conversion of anthropogenic carbon accumulation into acidification rates	Temporal trends in the progression of acidification in the interior ocean are resolved	Müller et al. (2024)





52	CODAP-NA climatology	Coastal	1° × 1°	adjusted to 2010	Objective analysis approach of the World Ocean Atlas	The first discrete bottle based climatology in the North American ocean margins	Jiang et al. (2024)
----	-------------------------	---------	---------	------------------	--	---	---------------------

3.1.5 Multi-product analyses:

This section includes data products that have been generated by community synthesis efforts designed to inform global carbon budgets.

- 53) SeaFlux: Harmonization of air–sea CO₂ fluxes from surface *p*CO₂ data products using a standardized approach (Gregor and Fay, 2021). This resource provides an ensemble of six pCO₂ products with air-sea CO₂ fluxes computed consistently. The six included products are: CMEMS-FFNN, CSIR-ML6, JENA-MLS, JMA-MLR, MPI-SOMFFN, and NIES-FNN. First, missing areas of *p*CO₂ estimates (mostly high-latitude and marginal seas) are filled using a linear-regression approach, thus addressing differences in spatial coverage between the mapping products. Further, also accounts for methodological inconsistencies in flux calculations. Fluxes are calculated using three wind products (CCMPv2, ERA5, and JRA55) along with the application of a scaled gas exchange coefficient for each of the wind products. Through these steps, SeaFlux presents an product ensemble of interpolated global surface ocean pCO₂ and air–sea carbon flux estimates for the years 1990–2019. For more details, refer to Fay et al. (2021).
- Processes (RECCAP2), the ocean carbon community compiled, quality controlled and harmonized (in the sense of providing output on the same regular grid at the same spatial and temporal resolution) 12 global ocean biogeochemical model simulations, 11 pCO₂ products, one ocean interior DIC products, and three data assimilation models to constrain the ocean carbon sink between 1985 and 2018. The RECCAP2 synthesis effort stands as a distinct but complementary resource to the Global Carbon Budget (GCB) project (Friedlingstein et al., 2025), which primarily focuses on anthropogenically perturbed surface CO₂ fluxes from a global budgeting perspective. The individual chapters of RECCAP2 were published in this special issue of Global Biogeochemical Cycles:

 https://agupubs.onlinelibrary.wiley.com/doi/toc/10.1002/(ISSN)2169-8961.RECCAP2. The data products of this assessment are available on a 1° × 1° horizontal grid, with monthly resolution for surface ocean variables such as air-sea CO₂ fluxes, and annual resolution for interior ocean variables, such as DIC content. The data compilation, which is described in detail in DeVries et al. (2023), is available at: https://zenodo.org/records/7990823 (Müller, 2023).
- 55) Global Carbon Budget: The GCB collects annually updated estimates of the ocean carbon sink from currently nine fCO₂-products and ten Global Ocean Biogeochemical Models for the period 1959 to the past calendar year (Friedlingstein et al., 2025, https://globalcarbonbudget.org/gcb-2024). In contrast to Earth System Models, the GOBMs are here forced with atmospheric reanalysis that ingested atmosphere and





ocean observations and are thus thought to be closer to the observed climate. Gridded fields are provided on a 1° × 1° horizontal grid and monthly resolution. In addition, globally and regionally integrated air-sea CO₂ fluxes from the native model grids are provided. Globally integrated time-series are adjusted for full ocean coverage and model bias and drift and are available for each individual fCO₂-product and GOBM (https://globalcarbonbudget.org/download/1442/?tmstv=1731323337). The model data goes well beyond surface fluxes and includes data to analyze drivers of carbon fluxes, including several 3D variables. The model data request has been updated since RECCAP2 and also provides, for example, monthly interior ocean data of DIC, alkalinity, nutrients and oxygen. The GOBM data request was also updated to have all variables available that are needed to serve as a testbed for fCO₂-products (e.g., sea surface height). Gridded surface data of sea surface fugacity and air-sea CO₂ flux of all fCO₂-products and GOBMs as used in the latest release of GCB (2024) are published on Zenodo (https://zenodo.org/records/14639761, Hauck et al., 2025). All other GOBM output is available via https://globalcarbonbudgetdata.org/closed-access-requests.html.

Table 5. Ocean carbonate chemistry data product synthesis and harmonizations.

No.	Name	Open or coastal ocean	Surface or water column	Snafial	Temporal resolution		Highlights	Reference
53	SeaFlux	Open ocean + coastal	Surface only	1° × 1°	Monthly	Consistent flux calculations for 6 pCO ₂ products to produce an ensemble estimate	Careful consideration of flux calculation provides a resource and code to the community for independent flux calculations	Gregor and Fay (2021)
54	RECCAP2	Open ocean + coastal	Surface + Water column	1° × 1° (open) 0.25° x 0.25° (coastal)	Monthly	Harmonized compilation of surface fCO ₂ products, model simulations and ocean interior products	Quality controlled data compilation with a harmonised horizontal grid and temporal resolution	Müller (2023); DeVries et al. (2023) Resplandy et al (2024)
55	Global Carbon Budget	Open ocean + coastal	Surface + Water column	1° × 1°	Monthly	Harmonized compilation of surface fCO ₂ products, and global ocean biogeochemical model simulations		Friedlingstein et al., 2025

3.1.6 Model based and hybrid data products and analyses:

Model-based projections of biogeochemical variables are often available from global and regional models, such as those in the Sixth Coupled Model Intercomparison Project (Dunne et al., 2024; Durack et al., 2025). This section further includes hybrid data products, which adjust model estimates towards observation-based constraints.





- 56) Decadal trends in the ocean carbon sink: The DeVries et al. (2019) analysis examines decadal trends in global and regional air-sea CO₂ fluxes from a variety of ocean biogeochemical models that contributed to the Global Carbon Budget (see No. 55). Three sets of model simulations were performed. Simulation A uses variable climate forcing (e.g., variable wind stress, heat and freshwater fluxes) and observed atmospheric CO₂ forcing, Simulation B uses constant (repeated) climate forcing and observed atmospheric CO₂, and simulation C uses both constant climate forcing and constant atmospheric CO₂ concentrations. With these simulations, the authors partitioned decadal trends in ocean CO₂ uptake into those driven by climate variability and those driven by atmospheric CO₂. They found that climate variability drove a weakening trend of the ocean carbon sink during the 1990s, and a strengthening trend during the first decade of the 2000s. The magnitude of these trends agreed with those of an OCIM that was trained to replicate tracer data from the 1990s and 2000s (DeVries et al., 2017), indicating that the decadal trends may be driven by variability in ocean circulation. This data from this analysis is accessible through figshare at https://doi.org/10.6084/m9.figshare.8091161.v1.
- 57) ECCO-Darwin: Carroll et al. (2022) used the Estimating the Circulation and Climate of the Ocean-Darwin (ECCO-Darwin) global-ocean biogeochemistry state estimate to generate a data-constrained DIC budget and investigate how spatiotemporal variability in advection and mixing, air-sea CO₂ flux, and the biological pump have modulated the ocean sink for 1995–2018. ECCO-Darwin assimilates ocean circulation and physical tracers, including temperature, salinity, and sea ice, derived from the Estimating the Circulation and Climate of the Ocean (ECCO) LLC270 global-ocean and sea-ice data synthesis (Zhang et al., 2018). Additionally, it assimilates biogeochemical observations encompassing the cycling of carbon, nitrogen, phosphorus (PO₄), iron (Fe), silica (SiO₂), oxygen, and alkalinity. This inclusive approach enhances the model's fidelity by aligning it with a diverse array of observations. All ECCO-Darwin model output is available on the ECCO Data Portal: https://data.nas.nasa.gov/ecco/. The model code and platform-independent instructions for running ECCO-Darwin simulations can be found at: https://github.com/MITgcm-contrib/ecco darwin.
- 58) Global surface ocean pH, acidity, and Revelle factor from 1770 to 2100: Jiang et al. (2019a) produced a high-resolution (1°×1°) data product delineating regionally varying view of global surface ocean pH, acidity, and Revelle Factor (RF) from the beginning of the Industrial Revolution to the end of this century by amalgamating recent observational seawater CO₂ data from the SOCAT database (Version 6, 1991–2018, ~23 million observations) (Bakker et al., 2016), and temporal trends at individual locations of the global surface ocean from an Earth System Model, i.e., GFDL-ESM2M (Dunne et al., 2013). The calculations were conducted under historical atmospheric CO₂ levels (pre-2005) and four Representative Concentrations Pathways (post-2005) corresponding to the Intergovernmental Panel on Climate Change (IPCC)'s 5th Assessment Report, specifically RCP2.6, RCP4.5, RCP6.0, and RCP8.5. Surface ocean TA was calculated from SSS, SST using the updated locally interpolated alkalinity regression (LIARv2)





989 method (Carter et al., 2017). Surface ocean pH, acidity, and RF were then calculated using a MATLAB 990 version of the CO2SYS program (Orr et al., 2015). The data product is available at OCADS (DOI: 991 "10.25921/kggr-9h49"): https://www.ncei.noaa.gov/data/oceans/ncei/ocads/metadata/0206289.html (Jiang 992 et al., 2019b). 993 59) Global surface ocean acidification indicators from 1750 to 2100: Jiang et al. (2023) developed a 994 comprehensive model-data fusion product that delineates the trajectory of 10 OA indicators: fCO₂, pH, total 995 hydrogen ion content, free hydrogen ion content, $[CO_3^2]$, Ω_{arag} , Ω_{calc} , DIC, TA, and RF, as well as temperature and salinity at all locations of the global surface ocean from 1750 to 2100. This product marks 996 997 a significant breakthrough in OA forecasting by refining temporal trends with data from 14 Earth System 998 Models (ESMs) within the Coupled Model Intercomparison Project Phase 6 (CMIP6), and by applying bias 999 and drift corrections from three updated observational ocean carbon data products: SOCAT (Version 2022) (Bakker et al., 2016), GLODAPv2.2022 (Lauvset et al., 2022), and CODAP-NA (Jiang et al., 2021). This 1000 1001 dataset offers 10-year averages on a 1° × 1° global surface ocean grid, capturing trends from preindustrial 1002 times (1750), through historical conditions (1850-2010), and projects future conditions to 2100 across five 1003 Shared Socioeconomic Pathways: SSP1-1.9, SSP1-2.6, SSP2-4.5, SSP3-7.0, and SSP5-8.5. The gridded 1004 data product is available in NetCDF at OCADS (DOI: "10.25921/9ker-1005 bc48"): https://www.ncei.noaa.gov/data/oceans/ncei/ocads/metadata/0259391.html, and global maps of 1006 these indicators are available in jpeg at: https://www.ncei.noaa.gov/access/ocean-carbon-acidification-1007 data-system/synthesis/surface-oa-indicators.html (Jiang et al., 2022c). 1008 60) Simulated and constrained ocean carbon sink from 1850 to 2100 for the global ocean and the 1009 Southern Ocean: These two datasets include spatially-integrated and annually averaged values for the 1010 ocean carbon sink from 1850 to 2100 for different scenarios over the 21st century for the global ocean 1011 (Terhaar et al., 2022a, 2022b) and the Southern Ocean (Terhaar et al., 2021b, 2021c). All results are based 1012 on CMIP5 and CMIP6 models. For the global ocean carbon sink, values are available for SSP1-2.6, SSP2-1013 4.5, and SSP5-8.5. For the Southern Ocean, values are also available for SSP1-2.6, SSP2-4.5, and SSP5-8.5 1014 and additionally also for RCP2.6, RCP4.5, and RCP8.5. In addition, to the raw simulated values, 1015 constrained estimates of the annually averaged ocean carbon sink estimates are available. These 1016 constrained estimates adjusted the simulated carbon sink estimates for biases on the ocean's circulation and 1017 surface carbonate chemistry (see Terhaar et al., 2021b, 2022a for details). It is recommended to use the 1018 constrained estimates. The datasets are available at https://doi.org/10.17882/103934 and

https://doi.org/10.17882/103938.





1020 Table 6. Model based data synthesis products and analyses for ocean carbonate chemistry.

No.	Name	Open or coastal ocean	Surface or water column	Spatial resolution	Temporal resolution	Highlights	Reference
56	Decadal trends in the ocean carbon sink	Open ocean	Surface	Variable	Decadal	Climate variability drove weakened ocean CO ₂ uptake in the 1990s, and strengthened CO ₂ uptake in the 2000s	DeVries et al. (2019)
57	ECCO-Darwin	Open + Coastal	Water column	1/3° × 1/3°	3-hourly, daily, and month fields available	Model-data synthesis product based on the Estimating the Circulation and Climate of the Ocean (ECCO) ocean state estimate. Fully-closed, physically-consistent 3-D biogeochemical budgets.	Carroll et al. (2020, 2022, 2024)
58	Global surface ocean pH, acidity, and buffer capacity from 1770 to 2100	Open ocean	Surface	1° × 1°	Decadal	A model-observation fusion product for pH, acidity and Revelle Factor, leveraging GFDL-ESM2M and SOCATv6	Jiang et al. (2019)
59	Global surface ocean acidification indicators from 1750 to 2100	Open ocean	Surface	1°×1°	Decadal	A model-observation fusion product for all major OA indicators, leveraging a consortium of 14 Earth System Models and 3 observational data products	Jiang et al. (2023)
60	Simulated and constrained ocean carbon sink from 1850 to 2100 for the global ocean and the Southern Ocean	Open ocean	Surface	Spatially integrated	Annual (1850- 2100)	A constrained estimate of the ocean carbon sink based on the simulated carbon sink from CMIP5 and CMIP6 models and constrained with observations of the ocean physics and carbonate chemistry	Terhaar et al. (2021b, 2022a)

1021 3.2 Overlaps and history

Many of the data products described above exhibit significant overlap in various forms. In some cases, one or more products are used to generate new ones, while in others, the same collection-level cruise datasets underpin multiple products. There are a few foundational data products, such as GLODAPv2 and SOCAT, which are widely utilized to develop other data products, including their respective gridded products (e.g., Lauvset et al., 2016). For instance, SOCAT forms the backbone of nearly all derived products listed in Table 3, serving as a key resource for product development or validation. Some derived products, such as the JMA-MLR (No. 25) and OceanSODA-ETHZv1 (No. 26), incorporate both SOCAT and GLODAPv2 during development. Having overlaps in data and derived products has provided opportunities for data quality control and intercomparison of different approaches to gap filling that would not have been available otherwise. Additional overlaps between these data products are provided below:



1032

1050



3.2.1 SOCAT and LDEO:

1033 colleagues at the Lamont-Doherty Earth Observatory (LDEO) in Palisades, New York. His pioneering work led to 1034 the creation of the LDEO Surface pCO₂ Database (No. 2), which focused on high-quality data collected by his team 1035 and from various U.S. and international expeditions. Over time, this data set expanded to include contributions from other laboratories, resulting in a highly influential collection of pCO2 data and several seminal papers on global 1036 1037 surface ocean CO₂ variations and air-sea CO₂ fluxes (Takahashi et al., 1997; 2002; 2009). The last update to the 1038 LDEO database was in 2019, following Dr. Takahashi's passing, and no further updates are anticipated (Takahashi 1039 et al., 2021). 1040 The Surface CO₂ Atlas (SOCAT) project was developed to address questions around the current and future drivers 1041 of CO₂ fluxes raised at the 2007 Surface Ocean CO₂ Variability and Vulnerability (SOCOVV) workshop in Paris, 1042 France (Metzl et al., 2007). SOCAT was developed to synthesize all of the publicly available, discoverable, and citable surface CO2 data. Following the GLODAP model, there was a strong emphasis on an open and transparent 1043 1044 secondary quality control process to ensure the highest data quality. The first data release came in 2011 (Pfeil et al., 1045 2013; Sabine et al, 2013) and included contributions from numerous laboratories, as well as the freely available CO2 1046 data from the LDEO database. As of 2024, SOCAT contains ~40 million data points, with new observations added 1047 annually. All data are rigorously standardized, and recalculated as fCO2. SOCAT represents an ongoing global 1048 community effort, with participants from all continents contributing data and to the quality control process. Initially 1049 new versions were released every other year, but automation allowed annual public releases since version 4.

The quality control and synthesis of global surface ocean CO2 data began in 1997 with Dr. Taro Takahashi and his

3.2.2 GLODAPv2 and Java OceanAtlas (JOA) Suite:

1051 Starting in the late 1980s, the World Ocean Circulation Experiment (WOCE), Joint Global Ocean Flux Study 1052 (JGOFS), and the NOAA Ocean-Atmosphere Exchange Study (OACES) collaborated in a multinational effort to 1053 conduct a decadal global hydrographic survey of unparalleled quality and quantity. At the conclusion of the survey 1054 at the end of the 1990s, the Global Ocean Data Analysis Project (GLODAP) combined and publicly released all of 1055 the available hydrographic data with high-quality carbon measurements as a single database (Key et al., 2004; 1056 Sabine et al., 2005). The data were subjected to extensive secondary quality control checks where cruise tracks 1057 intersected one another, making it the most comprehensive and highest-quality ocean inorganic carbon dataset ever 1058 generated. A gridded, full-depth global ocean carbon climatology was also created and released as part of the 1059 project. These data and associated climatology have been extensively used to evaluate carbon distributions as well as 1060 the accumulation of anthropogenic CO₂ in the ocean. Other regional datasets, like CARINA (CARbon dioxide IN 1061 the Atlantic Ocean) data synthesis project, an international collaborative effort of the European Union CARBOOCEAN program (Key et al., 2010; Tanhua et al., 2010) and PACIFICA (PACIFic ocean Interior CArbon), 1062 1063 an international synthesis of Pacific Ocean data organized through the North Pacific Marine Science Organization (PICES) (Ishii et al., 2011b; Suzuki et al., 2013), were combined with GLODAP after its initial release. The 1064





1065 GLODAP database is continuing to grow with new data collected as part of the Global Ocean Ship-Based 1066 Hydrographic Investigations Program (GO-SHIP). 1067 For discrete bottle measurements spanning the entire oceanic water column, GLODAPv2 (No. 3) and the Java 1068 Ocean Atlas (JOA, No. 4) are the primary data products. Most cruise datasets contributing to these two data products 1069 overlap, but the key difference lies in their approach to data adjustment. The former applies crossover and inversion analysis for bias correction, while the latter presents the data without such adjustments. GLODAPv2 achieves 1070 1071 consistency by applying adjustments based on deep-ocean offsets, whereas JOA provides the data in its original form. While there is substantial overlap between the two, data from a specific expedition might differ slightly due to 1072 GLODAPv2's secondary quality control adjustments. Both GLODAPv2 and JOA offer global coverage, but several 1073 1074 independent regional data products are also available, such as SNAPO-CO2 (No. 6), CODAP-NA (No. 8), AZMP 1075 Carbon (No. 9), MOCHA (No. 10), and ARIOS (No. 11). Data from these regional products often partially or fully 1076 overlap with GLODAPv2 and JOA. 1077 a) GLODAPv2 and CODAP-NA: 1078 All cruise datasets contributing to CODAP-NA were forwarded to the GLODAPv2 quality control team in 2022. 1079 Data from select cruises with deep-water sampling (>1500 m), enabling crossover analysis, were subsequently 1080 incorporated into the GLODAPv2.2022 data product update (Lauvset et al., 2022). 1081 b) GLODAPv2 and SPOTS: 1082 Some time-series data are included in both GLODAPv2 and the Synthesis Product for Ocean Time-Series (SPOTS). 1083 Usually, data present in both products have not been measured on dedicated time-series cruises but rather collected 1084 as part of a larger cruise passing by a time series location. As the quality control of SPOTS is restricted to assigning 1085 method flags, adjustments that are applied as a result of the QC of GLODAP are not present in SPOTS. Additional 1086 crossover analyses between SPOTS and GLODAP have revealed a good consistency (Lange et al., 2024). 1087 3.2.3 RECCAP2 and GCB: 1088 RECCAP2 and GCB are not data products themselves, but analyses and syntheses of data-based and model-based 1089 products. Users should be aware that there is a large degree of overlap between the fCO₂- products and GOBMs that 1090 contributed to both RECCAP2 and GCB. However, RECCAP2 and GCB serve different purposes. GCB is updated annually to the latest complete calendar year and its main purpose is to present and estimate of the magnitude (and 1091 1092 uncertainty) of the ocean CO2 sink for that year, while RECCAP2 is presents a deeper analysis of the magnitude, 1093 trends, and variability of the ocean CO₂ sink over the period 1985-2018.



1095

1096

1097

1098

1099

1101

1102



3.2.4 Jiang et al. (2019) and Jiang et al. (2023):

Both products contain the projection of surface ocean pH, total hydrogen ion content, and buffer capacity from 1750 to 2100. However, the former is based on one GFDL model ESM2M, while the latter is based on a consortium of 14 Earth system models, and additional observational data. The latter also contains the projection of seven other OA variables, including carbonate ions, aragonite saturation state, calcite saturation state, fCO2, DIC, and TA.

4 Data availability

1100 Access links for all data products mentioned in this paper are provided in their respective paragraphs. Additionally, their access links are available in Table 7 below.

Table 7. Access links for the compiled ocean carbonate chemistry data products. N/A is short for not applicable.

No.	Name	Data access link	DOI	Reference
1	SOCAT	https://socat.info/	https://doi.org/10.25921/9w pn-th28	Bakker et al. (2016, 2024)
2	LDEO Surface pCO ₂ Database	https://www.ncei.noaa.gov/data/ocean s/ncei/ocads/metadata/0160492.html	https://doi.org/10.3334/cdiac/ otg.ndp088(v2015)	Takahashi et al. (2017)
3	GLODAPv2	https://glodap.info/	https://doi.org/10.25921/zyrq- ht66	Lauvset et al. (2023a, 2024)
4	JOA Suite	https://joa.ucsd.edu/	N/A	Swift and Osborne (2022)
5	WOD	https://www.ncei.noaa.gov/products/world-ocean-database	https://doi.org/10.25923/z885- h264	Mishonov et al. (2024)
6	SNAPO-CO ₂	https://www.ncei.noaa.gov/data/ocean s/ncei/ocads/metadata/0285681.html	https://doi.org/10.17882/954 14	Metzl et al (2023, 2024)
7	Arctic Ocean anthropogenic carbon estimates	https://www.seanoe.org/data/00927/10 3920/	https://doi.org/10.17882/103 920	Terhaar et al. (2024)
8	CODAP-NA	https://www.ncei.noaa.gov/data/ocean s/ncei/ocads/metadata/0219960.html	https://doi.org/10.25921/531n -c230	Jiang et al. (2020, 2021)
9	AZMP Carbon	N/A	https://doi.org/10.20383/102 .0673	Cyr et al. (2022)
10	МОСНА	https://www.ncei.noaa.gov/data/ocean s/ncei/ocads/metadata/0277984.html	https://doi.org/10.25921/2vve- fh39	Kennedy et al., (2024)
11	ARIOS	https://digital.csic.es/handle/10261/2051 35	https://doi.org/10.20350/dig italCSIC/12498	Pérez et al. (2020)
12	Marine inorganic carbon chemistry observations in the northern Gulf of Alaska	https://www.ncei.noaa.gov/data/ocean s/ncei/ocads/metadata/0277034.html	https://doi.org/10.25921/x9sg- 9b08	Monacci et al. (2023, 2024)





13	Coral Reef Carbonate Chemistry Off the Florida Keys	https://www.ncei.noaa.gov/access/met adata/landing- page/bin/iso?id=gov.noaa.nodc:NCR MP-CO3-Atlantic	https://doi.org/10.25921/vfz0- dg77	Manzello et al. (2018)
14	Salish cruise data package and multi-stressor data product	https://www.ncei.noaa.gov/access/oce an-carbon-acidification-data- system/oceans/SalishCruise_DataPack age.html, https://www.ncei.noaa.gov/access/oce an-carbon-acidification-data- system/oceans/SalishCruises_DataPro duct.html	https://doi.org/10.25921/zgk5- ep63, https://doi.org/10.25921/5g29 -q841	Alin et al. (2021, 2023, 2024a, 2024b)
15	BATS	https://demo.bco- dmo.org/project/2124	https://doi.org/10.26008/191 2/bco-dmo.894099.4, https://doi.org/10.26008/191 2/bco-dmo.893182.4, https://doi.org/10.26008/191 2/bco-dmo.926534.4, https://doi.org/10.26008/191 2/bco-dmo.893521.6, https://doi.org/10.26008/191 2/bco-dmo.917255.5, https://doi.org/10.26008/191 2/bco-dmo.939210.7, https://doi.org/10.26008/191 2/bco-dmo.3782.6, https://doi.org/10.26008/191 2/bco-dmo.3918.8, https://doi.org/10.26008/191 2/bco-dmo.881861.5	Bates et al., 2024a,b,c,d,e; Johnson et al., 2024a,b,c; Steinberg and Cope, 2024
16	НОТ	https://www.bco-dmo.org/project/2101, https://dhoi.org/10.5281/zenodo.15060 930	https://doi.org/10.1575/1912/b co-dmo.3773.1, https://doi.org/10.5281/zenod o.15060931	Winn et al. (1994, 1998); Dore et al. (2003, 2009, 2014, 2025); Knor et al. (2023)





17	ESTOC	N/A	https://doi.org/10.1594/PANG AEA.959856, https://doi.pangaea.de/10.159 4/PANGAEA.856590, https://doi.pangaea.de/10.159 4/PANGAEA.856615, https://doi.pangaea.de/10.159 4/PANGAEA.856608, https://doi.pangaea.de/10.159 4/PANGAEA.856616, https://doi.pangaea.de/10.159 4/PANGAEA.856593, https://doi.pangaea.de/10.159 4/PANGAEA.856612, https://doi.pangaea.de/10.159 4/PANGAEA.856614, https://doi.pangaea.de/10.159 4/PANGAEA.856617, https://doi.pangaea.de/10.159 4/PANGAEA.856607, https://doi.pangaea.de/10.159 4/PANGAEA.856607,	González- Dávila and Santana-Casiano (2023)
18	Point B Time- series	N/A	https://doi.org/10.1594/P ANGAEA.727120	Gattuso et al. (2021b)
19	Ny-Ålesund Time-series	N/A	https://doi.org//10.1594/P ANGAEA.957028	Gattuso et al. (2023)
20	SPOTS	https://www.bco- dmo.org/dataset/896862	https://doi.org/10.26008/1912/ bco-dmo.896862.2	Lange et al. (2024a, 2024b)
21	Autonomous pCO ₂ and pH time series from 40 surface buoys	https://www.ncei.noaa.gov/data/ocean s/ncei/ocads/metadata/0173932.html	https://doi.org/10.7289/v5db8 043	Sutton et al. (2018)
22	Updated Takahashi delta fCO ₂ and flux climatology	https://www.ncei.noaa.gov/data/ocean s/ncei/ocads/metadata/0282251.html	https://doi.org/10.25921/295g -sn13	Fay et al. (2023)
23	MPI-ULB-SOM- FFN	https://www.ncei.noaa.gov/data/ocean s/ncei/ocads/metadata/0209633.html	https://doi.org/10.25921/qb25 -f418	Landschützer et al. (2020a, 2020b)
24	VLIZ SOM-FFN	https://www.ncei.noaa.gov/data/ocean s/ncei/ocads/metadata/0160558.html	https://doi.org/10.7289/V5Z8 99N6	Landschützer et al. (2016), Jersild et al. (2017)
25	JMA-MLR	https://www.data.jma.go.jp/kaiyou/eng lish/co2_flux/co2_flux_data_en.html	N/A	lida et al. (2021)
26(a)	OceanSODA -ETHZv1	https://www.ncei.noaa.gov/data/ocean s/ncei/ocads/ metadata/0220059.html	https://doi.org/10.25921/m5w x-ja34	Gregor et al. (2020)
26(b)	OceanSODA -ETHZv2	N/A	https://doi.org/10.5281/zeno do.11206365	Gregor et al. (2024b)
27	LDEO-HPD fCO2 product	https://zenodo.org/records/4760205	https://doi.org/10.5281/zenod o.4760205	Gloege et al. (2022)





28	LDEO HPD with extended temporal coverage	https://zenodo.org/records/13891722	https://doi.org/10.5281/zenod o.13891722	Bennington et al. (2022a)
29	LDEO fCO2 - Residual Method	https://zenodo.org/records/13941548	https://doi.org/10.5281/zenod o.13941548	Bennington et al. (2022b)
30(a)	CMEMS -LSCEv1	https://data.ipsl.fr/catalog/srv/eng/catal og.search#/metadata/a2f0891b-763a- 49e9-af1b-78ed78b16982	https://doi.org/10.14768/a 2f0891b-763a-49e9-af1b- 78ed78b16982	Chau et al. (2022)
30(b)	CMEMS -LSCEv2	https://data.marine.copernicus.eu/prod uct/MULTIOBS_GLO_BIO_CARBO N_SURFACE_MYNRT_015_008/ser vices	https://doi.org/10.48670/ moi-00047	Chau et al. (2024a, 2024b)
31	CarboScope (Jena-MLS)	https://www.bgc- jena.mpg.de/CarboScope/?ID=oc	10.17871/CarboScope- oc_v2024E (or analogously for previous and upcoming releases)	Rödenbeck et al. (2022)
32	UOEx-Watson	https://www.ncei.noaa.gov/data/ocean s/ncei/ocads/metadata/0301544.html	https://doi.org/10.25921/2dp5 -xm29	Watson et al. (2025)
33	NIES-ML3	https://db.cger.nies.go.jp/DL/10.17595 /20220311.001.html.en	https://doi.org/10.17595/202 20311.001	Zeng (2022), Zeng et al. (2022)
34	CSIR-ML6	https://www.ncei.noaa.gov/data/ocean s/ncei/ocads/metadata/0206205.html	https://doi.org/10.25921/z682- mn47	Gregor et al. (2019b)
35	AOML-ET	https://www.ncei.noaa.gov/data/ocean s/ncei/ocads/metadata/0298989.html	https://doi.org/10.25921/0s8y- q287	Wanninkhof et al. (2024, 2025)
36	ULB-SOM-FFN -coastalv2.1	https://www.ncei.noaa.gov/data/ocean s/ncei/ocads/metadata/0279118.html	https://doi.org/10.25921/4sde- p068	Roobaert et al. (2023, 2024)
37	RFR-LME	https://www.ncei.noaa.gov/data/ocean s/ncei/ocads/metadata/0287551.html	https://doi.org/10.25921/h8vw -e872	Sharp et al. (2024a, 2024b)
38	ReCAD -NAACOM -pCO2	https://zenodo.org/records/14038561	https://doi.org/10.5281/zeno do.1150097.	Wu et al. (2025)
39	Gridded surface OA indicators, and air–sea CO2 fluxes in the northern Caribbean Sea	https://www.ncei.noaa.gov/data/ocean s/ncei/ocads/metadata/0207749.html	https://doi.org/10.25921/2swk -9w56	Wanninkhof et al. (2019)
40	OA data in the Gulf of Mexico/Gulf of America and wider Caribbean from 2014 to 2020	https://www.ncei.noaa.gov/data/ocean s/ncei/ocads/metadata/0245950.html	https://doi.org/10.25921/tt1c- dx53	van Hooidonk (2022)
41	Regional pCO ₂ climatology of the Baltic Sea	N/A	https://doi.org/10.1594/PAN GAEA.961119	Bittig et al. (2023)





Global interior ocean mapped climatology from GLODAPv2	https://www.ncei.noaa.gov/data/ocean s/ncei/ocads/metadata/0286118.html	https://doi.org/10.3334/cdiac/ otg.ndp093_glodapv2	Lauvset et al. (2016, 2023b)
Global aragonite saturation state climatology	https://www.ncei.noaa.gov/data/ocean s/ncei/ocads/metadata/0139360.html	https://doi.org/10.7289/v5q81 b4p	Jiang et al. (2015a, 2015b)
MOBO-DIC (Version 2020)	https://www.ncei.noaa.gov/access/oce an-carbon-acidification-data- system/oceans/ndp_104/ndp104.html	https://doi.org/10.25921/yvzj-zx46	Keppler et al. (2020)
Monthly global interior ocean TA climatology	https://www.ncei.noaa.gov/data/ocean s/ncei/ocads/metadata/0222470.html	http://doi.org/10.20350/DIGI TALCSIC/8564	Broullon et al., (2019)
Monthly global interior ocean DIC climatology	https://www.ncei.noaa.gov/data/ocean s/ncei/ocads/metadata/0222469.html	http://doi.org/10.20350/digital CSIC/10551	Broullon et al., (2020)
MOBO-DIC (Version 2023)	https://www.ncei.noaa.gov/data/ocean s/ncei/ocads/metadata/0277099.html	https://doi.org/10.25921/z31n- 3m26	Keppler et al. (2023)
Metrics of acidification in the ocean interior	https://www.ncei.noaa.gov/data/ocean s/ncei/ocads/metadata/0290073.html	https://doi.org/10.25921/rdtr- 9t74	Fassbender et al. (2023), Fassbender (2024)
Anthropogenic CO ₂ from 1994 to 2007	https://www.ncei.noaa.gov/data/ocean s/ncei/ocads/metadata/0186034.html	https://doi.org/10.25921/wdn2 -pt10	Gruber et al. (2019a, 2019b)
Decadal trends in anthropogenic CO2 From 1994 to 2014	https://www.ncei.noaa.gov/data/ocean s/ncei/ocads/metadata/0279447.html	https://doi.org/10.25921/ppcf- w020	Müller et al. (2023)
Progression of Ocean Interior Acidification over the Industrial Era	https://www.ncei.noaa.gov/data/ocean s/ncei/ocads/metadata/0298993.html	https://doi.org/10.25921/tefm- x802	Müller et al. (2024)
CODAP-NA climatology	https://www.ncei.noaa.gov/data/ocean s/ncei/ocads/metadata/0270962.html	https://doi.org/10.25921/g8pb -zy76	Jiang et al. (2022b), Jiang et al. (2024)
SeaFlux	https://zenodo.org/records/8280457	https://doi.org/10.5281/zenod o.5482547	Gregor & Fay. (2021)
RECCAP2	https://zenodo.org/records/7990823	https://doi.org/10.5281/zenod o.7990823	Müller (2023)
Global Carbon Budget	https://zenodo.org/records/14639761	https://doi.org/10.5281/zenod o.14639761	Hauck et al. (2025)
Decadal trends in the ocean carbon sink	N/A	https://doi.org/10.6084/m 9.figshare.8091161.v1	DeVries et al. (2019)
ECCO-Darwin	https://data.nas.nasa.gov/ecco/	N/A	Carroll et al. (2020)
	ocean mapped climatology from GLODAPv2 Global aragonite saturation state climatology MOBO-DIC (Version 2020) Monthly global interior ocean TA climatology Monthly global interior ocean DIC climatology MOBO-DIC (Version 2023) Metrics of acidification in the ocean interior CO2 from 1994 to 2007 Decadal trends in anthropogenic CO2 From 1994 to 2014 Progression of Ocean Interior Acidification over the Industrial Era CODAP-NA climatology SeaFlux RECCAP2 Global Carbon Budget Decadal trends in the ocean carbon sink	ocean mapped climatology from GLODAPv2 Global aragonite saturation state climatology MOBO-DIC (Version 2020) Monthly global interior ocean TA climatology MoBO-DIC (Version 2020) Morbin global interior ocean TA climatology Morbin global interior ocean DIC climatology Morbin global interior ocean bit global interior ocean DIC climatology Morbin global interior ocean s/ncei/ocads/metadata/0222470.html Metrics of acidification in the ocean interior Anthropogenic CO ₂ from 1994 to 2007 Decadal trends in anthropogenic CO2 From 1994 to 2014 Progression of Ocean Interior Acidification over the Industrial Era CODAP-NA climatology https://www.ncei.noaa.gov/data/ocean s/ncei/ocads/metadata/0279447.html Netrics of acidification over the Industrial Era CODAP-NA climatology https://www.ncei.noaa.gov/data/ocean s/ncei/ocads/metadata/0279447.html SeaFlux https://www.ncei.noaa.gov/data/ocean s/ncei/ocads/metadata/0279962.html https://www.ncei.noaa.gov/data/ocean s/ncei/ocads/metadata/0270962.html https://www.ncei.noaa.gov/data/ocean s/ncei/ocads/metadata/0270962.html https://zenodo.org/records/8280457 RECCAP2 https://zenodo.org/records/14639761 N/A	https://www.ncei.noaa.gov/data/ocean s/ncei/ocads/metadata/0286118.html https://doi.org/10.3334/cdiac/otg.ndp093_glodapv2





58	Global surface ocean pH, acidity, and buffer capacity from 1770 to 2100	https://www.ncei.noaa.gov/data/ocean s/ncei/ocads/metadata/0206289.html	https://doi.org/10.25921/kgqr- 9h49	Jiang et al. 2019(a), Jiang et al. (2019b)
59	Global surface ocean acidification indicators from 1750 to 2100	https://www.ncei.noaa.gov/data/ocean s/ncei/ocads/metadata/0259391.html	https://doi.org/10.25921/9ker- bc48	Jiang et al. (2022c), Jiang et al. (2023)
60	Simulated and constrained ocean carbon sink from 1850 to 2100 for the global ocean and the Southern Ocean	https://www.seanoe.org/data/00927/10 3934/, https://www.seanoe.org/data/00927/10 3938/	https://doi.org/10.17882/103 934, https://doi.org/10.17882/103 938	Terhaar et al. (2021c), Terhaar et al. (2022b)

5 Summary

The synthesis and gridded data products presented here reflect significant community-based efforts that have been made to advance understanding of the ocean's role in global carbon cycling. This synthesis provides a comprehensive overview of key data compilations and gridded data products essential for coastal and global ocean carbonate chemistry research. It highlights the key features of each product, serving as a resource for researchers seeking the necessary data for their work.

Author contributions

L-QJ prepared the initial draft. All authors contributed to the writing of the manuscript. The first 20 authors are listed based on their contributions, while the remaining authors are listed alphabetically by their last names.

Competing interests

One of the (co-)authors, Anton Velo (Instituto de Investigacions Mariñas, IIM - CSIC, Vigo, Spain), is a member of the editorial board of the Earth System Science Data.

Acknowledgements

We extend our gratitude to all scientists who collected and measured the original data and those who compiled and quality controlled these data products. We thank Bronte Tilbrook (CSIRO Oceans and Atmosphere and Australian Antarctic Program Partnership, University of Tasmania, Australia), and Dwight Gledhill (NOAA/OAR Ocean Acidification Program, United States) for their contributions to the writing of this paper. We also thank Pierre Friedlingstein (University of Exeter, Exeter, UK) for his valuable insights and discussions, which helped shape the



1123



vision of this paper. This is PMEL contribution 5728.

Financial support

1124 Funding for L-QJ was from NOAA Ocean Acidification Program (https://ror.org/02bfn4816) and NOAA grant 1125 NA24NESX432C0001 (Cooperative Institute for Satellite Earth System Studies - CISESS) at the Earth System 1126 Science Interdisciplinary Center, University of Maryland. The authors acknowledge funding from the United States 1127 National Science Foundation (grant no. OCE-2140395) to the Scientific Committee on Oceanic Research (SCOR, 1128 United States) for the International Ocean Carbon Coordination Project (IOCCP). SKL and NL acknowledge 1129 funding by the Horizon Europe research and innovation program under grant agreement 101083922 (OceanICU Improving Carbon Understanding). Funding for GLODAPv2 was provided by the EU FP7 project CarboChange 1130 1131 (grant agreement 264879) and the Research Council of Norway project DECApH (grant agreement 214513), and the 1132 2019-2023 updates were funded by the EU Horizon 2020 innovation action EuroSea (grant agreement 862626). 1133 AJF, SRA, and RAF were supported by the NOAA Pacific Marine Environmental Laboratory. GAM was funded by 1134 NOAA NA24OARX431G0151-T1-01. JPG was supported by the Service d'Observation Rade de Villefranche (SO-Rade), the Service d'Observation en Milieu Littoral (SOMLIT/CNRS-INSU), the Coastal Observing System for 1135 1136 Northern and Arctic Seas (COSYNA), the two Helmholtz large-scale infrastructure projects ACROSS and MOSES, 1137 the French Polar Institute (IPEV), and the European Commission, Horizon 2020 Framework Programme (grant nos. 1138 871153, 951799, 727890 and 869154). Discrete samples reported by JPG were analyzed for CT and AT by the Service National d'Analyse des Paramètres Océaniques du CO₂. AV and FFP was supported by BOCATS2 1139 1140 (PID2019-104279GB-C21) project funded by MICIU/AEI/10.13039/501100011033, by FICARAM+ (PID2023-1141 148924OB-100) and by EuroGO-SHIP project (Horizon Europe #101094690). NM and CLM acknowledge Institut 1142 National des Sciences de l'Univers du Centre National de la Recherche Scientifique (INSU/CNRS) and 1143 Observatoire des Science de l'Univers (OSU ECCE-Terra) for supporting the SNAPO-CO2 facility housed by the 1144 LOCEAN laboratory in Paris/France. The AZMP Carbon dataset is a contribution to Fisheries and Oceans Canada 1145 Atlantic Zone Monitoring Program. Funding for the HOT program and WHOTS mooring maintenance were provided by the National Science Foundation (grant no. OCE-9617409). CMEMS-LSCE is supported by the 1146 1147 European Copernicus Marine Environment Monitoring Service (CMEMS, grant no. 83-CMEMSTAC-MOB). The 1148 work of LGr was supported by the ESA OceanHealth-OA project (contract number 4000137603/22/I-DT), the 1149 European Space Agency (OceanSODA project, grant no. 4000112091/14/I-LG), the European Commission 1150 (COMFORT project, grant no. 820989), and the Horizon 2020 (4C project, grant no. 821003). JH received funding 1151 from the Initiative and Networking Fund of the Helmholtz Association (Helmholtz Young Investigator Group Marine Carbon and Ecosystem Feedbacks in the Earth System [MarESys], Grant VH-NG-1301), and from the ERC-1152 1153 2022-STG OceanPeak (Grant 101077209). AK was funded by the NOAA Global Ocean Monitoring and Observing 1154 program (https://ror.org/037bamf06). J.T. was funded by the Swiss National Science Foundation under grant # 1155 PZ00P2 209044 (ArcticECO). HCB acknowledges funding by the German Federal Ministry of Education and Research under grants no. 03F0877D (C-SCOPE project) and 03F0773A (BONUS INTEGRAL project). TD 1156





- 1157 acknowledges support from the US National Science Foundation through Grant # 1948955. RW, LB, AJS, SRA, and
- 1158 RAF acknowledge support from the Office of Oceanic and Atmospheric Research of NOAA, U.S. Department of
- 1159 Commerce, including resources from the Global Ocean Monitoring and Observing Program and the Ocean
- 1160 Acidification Program (Open Funder Registry numbers 100018302 and 100018228, respectively). SRA and RAF
- acknowledge support from the Washington Ocean Acidification Center.

References

- Alin, S.R., Newton, J. A., Greeley, D., Curry, B., Herndon, J., Kozyr, A., and Feely, R. A.: A Compiled Data
- 1164 Product of Profile, Discrete Biogeochemical Measurements from 35 Individual Cruise Data Sets Collected from a
- 1165 Variety of Ships in the Southern Salish Sea and Northern California Current System (Washington State Marine
- 1166 Waters) from 2008-02-04 to 2018-10-19 (NCEI Accession 0238424), NOAA National Centers for Environmental
- Information, Dataset, https://doi.org/10.25921/zgk5-ep63, 2022.
- Alin, S.R., Newton, J. A., Feely, R. A., Greeley, D., Herndon, J., and Kozyr, A.: A Multi-Stressor Data Product for
- Marine Heatwave, Hypoxia, and Ocean Acidification Research, Including Calculated Inorganic Carbon Parameters
- 1170 from the Southern Salish Sea and Northern California Current System from 2008-02-04 to 2018-10-19 (NCEI
- 1171 Accession 0283266), NOAA National Centers for Environmental Information, Dataset,
- 1172 https://doi.org/10.25921/5g29-q841, 2023.
- Alin, S. R., Newton, J. A., Feely, R. A., Greeley, D., Curry, B., Herndon, J., and Warner, M.: A decade-long cruise
- time series (2008–2018) of physical and biogeochemical conditions in the southern Salish Sea, North America,
- 1175 Earth Syst. Sci. Data, 16, 837–865, https://doi.org/10.5194/essd-16-837-2024, 2024a.
- Alin, S. R., Newton, J. A., Feely, R. A., Siedlecki, S., and Greeley, D.: Seasonality and response of ocean
- 1177 acidification and hypoxia to major environmental anomalies in the southern Salish Sea, North America (2014–
- 1178 2018), Biogeosciences, 21, 1639–1673, https://doi.org/10.5194/bg-21-1639-2024, 2024b.
- 1179 Archer, D., Eby, M., Brovkin, V., Ridgwell, A., Cao, L., Mikolajewicz, U., Caldeira, K., Matsumoto, K., Munhoven,
- 1180 G., Montenegro, A., and Tokos, K.: Atmospheric lifetime of fossil fuel carbon dioxide, Annu. Rev. Earth Planet.
- 1181 Sci., 37(1), 117–134, https://doi.org/10.1146/annurev.earth.031208.100206, 2009.
- 1182 Archer, D.: The Global Carbon Cycle, Princeton University Press, JSTOR, https://doi.org/10.2307/j.ctvcm4hx8,
- 1183 2010.
- Bach, L. T., Gill, S. J., Rickaby, R. E., Gore, S., and Renforth, P.: CO₂ removal with enhanced weathering and ocean
- alkalinity enhancement: Potential risks and co-benefits for marine pelagic ecosystems, Front. clim., 1,
- 1186 https://doi.org/10.3389/fclim.2019.00007, 2019.
- 1187 Bakker, D. C. E., Pfeil, B., Smith, K., Hankin, S., Olsen, A., Alin, S. R., Cosca, C., Harasawa, S., Kozyr, A., Nojiri,
- 1188 Y., O'Brien, K. M., Schuster, U., Telszewski, M., Tilbrook, B., Wada, C., Akl, J., Barbero, L., Bates, N. R., Boutin,





- 1189 J., Bozec, Y., Cai, W.-J., Castle, R. D., Chavez, F. P., Chen, L., Chierici, M., Currie, K., de Baar, H. J. W., Evans,
- 1190 W., Feely, R. A., Fransson, A., Gao, Z., Hales, B., Hardman-Mountford, N. J., Hoppema, M., Huang, W.-J., Hunt,
- 1191 C. W., Huss, B., Ichikawa, T., Johannessen, T., Jones, E. M., Jones, S. D., Jutterström, S., Kitidis, V., Körtzinger,
- 1192 A., Landschützer, P., Lauvset, S. K., Lefèvre, N., Manke, A. B., Mathis, J. T., Merlivat, L., Metzl, N., Murata, A.,
- 1193 Newberger, T., Omar, A. M., Ono, T., Park, G.-H., Paterson, K., Pierrot, D., Ríos, A. F., Sabine, C. L., Saito, S.,
- 1194 Salisbury, J., Sarma, V. V. S. S., Schlitzer, R., Sieger, R., Skjelvan, I., Steinhoff, T., Sullivan, K. F., Sun, H., Sutton,
- 1195 A. J., Suzuki, T., Sweeney, C., Takahashi, T., Tjiputra, J., Tsurushima, N., van Heuven, S. M. A. C., Vandemark,
- D., Vlahos, P., Wallace, D. W. R., Wanninkhof, R., and Watson, A. J.: An update to the Surface Ocean CO₂ Atlas
- 1197 (SOCAT version 2), Earth Syst. Sci. Data, 6, 69–90, https://doi.org/10.5194/essd-6-69-2014, 2014.
- 1198 Bakker, D. C. E., Pfeil, B., Landa, C. S., Metzl, N., O'Brien, K. M., Olsen, A., Smith, K., Cosca, C., Harasawa, S.,
- Jones, S. D., Nakaoka, S., Nojiri, Y., Schuster, U., Steinhoff, T., Sweeney, C., Takahashi, T., Tilbrook, B., Wada,
- 1200 C., Wanninkhof, R., Alin, S. R., Balestrini, C. F., Barbero, L., Bates, N. R., Bianchi, A. A., Bonou, F., Boutin, J.,
- 1201 Bozec, Y., Burger, E. F., Cai, W.-J., Castle, R. D., Chen, L., Chierici, M., Currie, K., Evans, W., Featherstone, C.,
- 1202 Feely, R. A., Fransson, A., Goyet, C., Greenwood, N., Gregor, L., Hankin, S., Hardman-Mountford, N. J., Harlay, J.,
- 1203 Hauck, J., Hoppema, M., Humphreys, M. P., Hunt, C. W., Huss, B., Ibánhez, J. S. P., Johannessen, T., Keeling, R.,
- 1204 Kitidis, V., Körtzinger, A., Kozyr, A., Krasakopoulou, E., Kuwata, A., Landschützer, P., Lauvset, S. K., Lefèvre, N.,
- 1205 Lo Monaco, C., Manke, A., Mathis, J. T., Merlivat, L., Millero, F. J., Monteiro, P. M. S., Munro, D. R., Murata, A.,
- 1206 Newberger, T., Omar, A. M., Ono, T., Paterson, K., Pearce, D., Pierrot, D., Robbins, L. L., Saito, S., Salisbury, J.,
- 1207 Schlitzer, R., Schneider, B., Schweitzer, R., Sieger, R., Skjelvan, I., Sullivan, K. F., Sutherland, S. C., Sutton, A. J.,
- 1208 Tadokoro, K., Telszewski, M., Tuma, M., van Heuven, S. M. A. C., Vandemark, D., Ward, B., Watson, A. J., and
- 1209 Xu, S. (2016). A multi-decade record of high-quality fCO₂ data in version 3 of the Surface Ocean CO₂ Atlas
- 1210 (SOCAT), Earth Syst. Sci. Data, 8, 383–413, https://doi.org/10.5194/essd-8-383-2016.
- 1211 Bakker, D. C. E., Alin, S. R., Bates, N., Becker, M.; Gkritzalis, T., Jones, Steve D., Kozyr, A., Lauvset, S. K., Metzl,
- 1212 N., Nakaoka, S.-i., O'Brien, K. M., Olsen, A., Pierrot, D., Steinhoff, T., Sutton, A. J., Takao, S., Tilbrook, B., Wada,
- 1213 C., Wanninkhof, R., Akl, J., Arbilla, L. A., Arruda, R., Azetsu-Scott, K., Barbero, L., Beatty, C. M., Berghoff, C. F.,
- 1214 Bittig, H. C., Burger, E. F., Campbell, K., Cardin, V., Collins, A., Coppola, L., Cronin, M., Cross, J. N., Currie, K.
- 1215 I., Emerson, S. R., Enright, M. P., Enyo, K., Evans, W., Feely, R. A., Flohr, A., Gehrung, M., Glockzin, M.,
- 1216 González-Dávila, M., Hamnca, S., Hartman, S., Howden, S. D., Kam, K., Kamb, L., Körtzinger, A., Kosugi, N.,
- 1217 Lefèvre, N., Lo Monaco, C., Macovei, V. A., Maenner Jones, S., Manalang, D., Martz, T. R., Mdokwana, B.,
- 1218 Monacci, N. M., Monteiro, P. M. S., Mordy, C., Morell, J. M., Murata, A., Neill, C., Noh, J.-H., Nojiri, Y., Ohman,
- 1219 M. D., Olivier, O., Ono, T., Petersen, W., Plueddemann, A. J., Prytherch, J., Rehder, G., Rutgersson, A., Santana-
- 1220 Casiano, J. M., Schlitzer, R., Send, U., Skjelvan, I., Sullivan, K. F., T'Jampens, M., Tadokoro, K., Telszewski, M.,
- 1221 Theetaert, H., Tsanwani, M., Vandemark, D., van Ooijen, E., Veccia, M. H., Voynova, Y. G., Wang, H., Weller, R.
- 1222 A., Woosley, R. J. (2024). Surface Ocean CO2 Atlas Database Version 2024 (SOCATv2024) (NCEI Accession
- 1223 0293257). NOAA National Centers for Environmental Information. Dataset. https://doi.org/10.25921/9wpn-th28,





- 1224 2024.
- 1225 Barth, A., Beckers, J.-M., Troupin, C., Alvera-Azcárate, A., and Vandenbulcke, L.: DIVAnd-1.0: n-dimensional
- 1226 variational data analysis for ocean observations, Geosci. Model Dev., 7, 225-241, https://doi.org/10.5194/gmd-7-
- 1227 225-2014, 2014.
- 1228 Bates, N.R., and Johnson, R.J.: Forty years of ocean acidification observations (1983-2023) in the Sargasso Sea at
- 1229 the Bermuda Atlantic Time-series Study (BATS) site, Frontiers in Marine Science, 10,
- 1230 https://doi.org/10.3389/fmars.2023.1289931, 2023.
- 1231 Bates, N., Johnson, R. J., Lomas, M.W., Steinberg, D.K., Lopez, P., Hayden, M., May, R., Derbyshire, L., Lethaby,
- 1232 P. J., Smith, D., and Lomas, D.: Determination of carbon, nitrogen, and phosphorus content in sinking particles at
- 1233 the Bermuda Atlantic Time-series Study (BATS) site from December 1988 to December 2023 using a Particle
- 1234 Interceptor Trap System (PITS). Biological and Chemical Oceanography Data Management Office (BCO-DMO).
- 1235 (Version 4) Version Date 2024-11-14 [if applicable, indicate subset used]. doi:10.26008/1912/bco-dmo.894099.4
- 1236 [access date], 2024a.
- 1237 Bates, N., Johnson, R. J., Lethaby, P. J., Smith, D., and Medley, C.: Primary productivity estimates from the
- 1238 incubation of seawater collected at the Bermuda Atlantic Time-series Study (BATS) site from December 1988
- 1239 through December 2023. Biological and Chemical Oceanography Data Management Office (BCO-DMO). (Version
- 1240 4) Version Date 2024-11-14 [if applicable, indicate subset used]. doi:10.26008/1912/bco-dmo.893182.4 [access
- 1241 date], 2024b.
- 1242 Bates, N., Johnson, R. J., Lethaby, P. J., Smith, D., and Medley, C.: HPLC and fluorometric derived phytoplankton
- 1243 pigment concentrations from seawater collected on BATS Validation cruises from June 1996 to June 2023.
- 1244 Biological and Chemical Oceanography Data Management Office (BCO-DMO). (Version 4) Version Date 2024-09-
- 1245 18 [if applicable, indicate subset used]. doi:10.26008/1912/bco-dmo.926534.4 [access date], 2024c.
- 1246 Bates, N., Johnson, R. J., Lethaby, P. J., Medley, C., and Smith, D.: HPLC and fluorometric derived phytoplankton
- 1247 pigment concentrations from seawater collected at the Bermuda Atlantic Time-series Study (BATS) site from
- 1248 October 1988 through December 2023. Biological and Chemical Oceanography Data Management Office (BCO-
- DMO). (Version 6) Version Date 2023-09-13 [if applicable, indicate subset used]. doi:10.26008/1912/bco-
- 1250 dmo.893521.6 [access date], 2024d.
- Bates, N., Johnson, R. J., Smith, D., Lethaby, P. J., Lomas, M.W., and Lomas, D.: Discrete bottle samples collected
- 1252 during BATS Validation (BVAL) cruises from April 1991 through June 2023. Biological and Chemical
- 1253 Oceanography Data Management Office (BCO-DMO). (Version 5) Version Date 2024-10-01 [if applicable, indicate
- subset used]. doi:10.26008/1912/bco-dmo.917255.5 [access date], 2024e.
- 1255 Bennington, V., Gloege, L., and McKinley, G. A.: Variability in the global ocean carbon sink from 1959 to 2020 by
- 1256 correcting models with observations, Geophys. Res. Lett., 49(14), https://doi.org/10.1029/2022gl098632, 2022a.





- 1257 Bennington, V., Galjanic, T., and McKinley, G. A.: Explicit physical knowledge in machine learning for Ocean
- 1258 Carbon Flux Reconstruction: The pCO₂-residual method. J. Adv. Model. Earth Syst., 14(10),
- 1259 https://doi.org/10.1029/2021ms002960, 2022b.
- 1260 Bertin, C., Carroll, D., Menemenlis, D., Dutkiewicz, S., Zhang, H., Matsuoka, A., Tank, S., Manizza, M., Miller, C.
- 1261 E., Babin, M., Mangin, A., and Le Fouest, V.: Biogeochemical River runoff drives intense coastal Arctic Ocean CO₂
- outgassing, Geophys. Res. Lett., 50(8), https://doi.org/10.1029/2022g1102377, 2023.
- 1263 Bittig, H. C., Steinhoff, T., Claustre, H., Fiedler, B., Williams, N. L., Sauzède, R., Körtzinger, A., and Gattuso, J.-P.:
- 1264 An alternative to static climatologies: Robust estimation of open ocean CO₂ variables and nutrient concentrations
- from T, S, and O₂ data using Bayesian Neural Networks, Frontiers in Marine Science, 5,
- 1266 https://doi.org/10.3389/fmars.2018.00328, 2018.
- 1267 Bittig, H. C., Jacobs, E., Neumann, T., and Rehder, G.: A regional pCO2 climatology of the Baltic Sea, PANGAEA
- 1268 [data set], https://doi.org/10.1594/PANGAEA.961119, 2023.
- 1269 Bittig, H.C., Jacobs, E., Neumann, T., and Rehder, G.: A regional pCO₂ climatology of the Baltic Sea from in situ
- pCO2 observations and a model-based extrapolation approach, Earth Syst. Sci. Data, 16(2), 753–773,
- 1271 https://doi.org/10.5194/essd-16-753-2024, 2024.
- 1272 Boyer, T. P., Garcia, H. E., Locarnini, R. A., Zweng, M. M., Mishonov, A. V., Reagan, J. R., Weathers, K. A.,
- 1273 Baranova, O. K., Seidov, D., Smolyar, I. V.: World Ocean Atlas 2018, NOAA National Centers for Environmental
- 1274 Information, https://www.ncei.noaa.gov/archive/accession/NCEI-WOA18, 2018.
- 1275 Brett, A., Leape, J., Abbott, M., Sakaguchi, H., Cao, L., Chand, K., Golbuu, Y., Martin, T. J., Mayorga, J., and
- 1276 Myksvoll, M. S.: Ocean Data Need a sea change to help navigate the Warming World. Nature, 582(7811), 181–183,
- 1277 https://doi.org/10.1038/d41586-020-01668-z, 2020.
- 1278 Broecker W. S.: Glacial to interglacial changes in ocean chemistry, Prog. Oceanogr., 11(2), 151–97,
- 1279 https://doi.org/10.1016/0079-6611(82)90007-6, 1982.
- 1280 Broullón, D., Pérez, F. F., Velo, A., Hoppema, M., Olsen, A., Takahashi, T., Key, R. M., Tanhua, T., González-
- 1281 Dávila, M., Jeansson, E., Kozyr, A., and van Heuven, S. M. A. C.: A global monthly climatology of total alkalinity:
- 1282 a neural network approach, Earth Syst. Sci. Data, 11, 1109–1127, https://doi.org/10.5194/essd-11-1109-2019, 2019.
- 1283 Broullón, D., Pérez, F. F., Velo, A., Hoppema, M., Olsen, A., Takahashi, T., Key, R. M., Tanhua, T., Santana-
- 1284 Casiano, J. M., and Kozyr, A.: A global monthly climatology of oceanic total dissolved inorganic carbon: A Neural
- 1285 Network approach, Earth Syst. Sci. Data, 12(3), 1725-1743, https://doi.org/10.5194/essd-12-1725-2020, 2020.
- 1286 Cai, W.-J., Hu, X., Huang, W.-J., Murrell, M. C., Lehrter, J. C., Lohrenz, S. E., Chou, W.-C., Zhai, W., Hollibaugh,
- 1287 J. T., Wang, Y., Zhao, P., Guo, X., Gundersen, K., Dai, M., and Gong, G.-C.: Acidification of subsurface coastal





- waters enhanced by eutrophication, Nature Geoscience, 4(11), 766–770, https://doi.org/10.1038/ngeo1297, 2011.
- 1289 Carroll, D., Menemenlis, D., Adkins, J. F., Bowman, K. W., Brix, H., Dutkiewicz, S., Fenty, I., Gierach, M. M.,
- 1290 Hill, C., Jahn, O., Landschützer, P., Lauderdale, J. M., Liu, J., Manizza, M., Naviaux, J. D., Rödenbeck, C., Schimel,
- 1291 D. S., Van der Stocken, T., and Zhang, H.: The ECCO-Darwin data-assimilative global ocean biogeochemistry
- 1292 model: Estimates of seasonal to multidecadal surface ocean pCO2 and air-sea CO2 flux, J. Adv. Model. Earth Syst.,
- 1293 12(10), https://doi.org/10.1029/2019ms001888, 2020.
- 1294 Carroll, D., Menemenlis, D., Dutkiewicz, S., Lauderdale, J. M., Adkins, J. F., Bowman, K. W., Brix, H., Fenty, I.,
- 1295 Gierach, M. M., Hill, C., Jahn, O., Landschützer, P., Manizza, M., Mazloff, M. R., Miller, C. E., Schimel, D. S.,
- 1296 Verdy, A., Whitt, D. B., and Zhang, H.: Attribution of space-time variability in global-ocean dissolved Inorganic
- 1297 Carbon, Global Biogeochemical Cycles, 36(3), https://doi.org/10.1029/2021gb007162, 2022.
- 1298 Carroll, D., Menemenlis, D., Zhang, H., Mazloff, M., McKinley, G., Fay, A., Dutkiewicz, S., Lauderdale, J., and
- 1299 Fenty, I.: Evaluation of the ECCO-Darwin Ocean Biogeochemistry State Estimate vs. In-situ Observations (ver 1.0),
- 1300 Zenodo, https://doi.org/10.5281/zenodo.10627664, 2024.
- 1301 Carter, B. R., Williams, N. L., Gray, A. R., and Feely, R. A.: Locally interpolated alkalinity regression for global
- alkalinity estimation, Limnology and Oceanography: Methods, 14(4), 268–277, https://doi.org/10.1002/lom3.10087,
- 1303 2016.
- 1304 Carter, B. R., Feely, R. A., Williams, N. L., Dickson, A. G., Fong, M. B., and Takeshita, Y.: Updated methods for
- 1305 global locally interpolated estimation of alkalinity, ph, and nitrate, Limnology and Oceanography: Methods, 16(2),
- 1306 119–131, https://doi.org/10.1002/lom3.10232, 2017.
- 1307 Carter, B. R., Bittig, H. C., Fassbender, A. J., Sharp, J. D., Takeshita, Y., Xu, Y.-Y., et al.: New and updated global
- 1308 empirical seawater property estimation routines, Limnol. and Oceanogr.: Methods, 19(12), 785–809,
- 1309 https://doi.org/10.1002/lom3.10461, 2021.
- 1310 Chau, T.-T.-T., Gehlen, M., and Chevallier, F.: A seamless ensemble-based reconstruction of surface ocean pCO₂
- and air–sea CO₂ fluxes over the global coastal and open oceans. Biogeosciences, 19(4), 1087–1109,
- 1312 https://doi.org/10.5194/bg-19-1087-2022, 2022.
- 1313 Chau, T.-T.-T., Gehlen, M., Metzl, N., and Chevallier, F.: CMEMS-LSCE: a global, 0.25°, monthly reconstruction
- 1314 of the surface ocean carbonate system, Earth Syst. Sci. Data, 16, 121–160, https://doi.org/10.5194/essd-16-121-
- 1315 2024, 2024a.
- 1316 Chau, T.-T.-T., Chevallier, F. and Gehlen, M.: Global analysis of surface ocean CO₂ fugacity and air-sea fluxes with
- low latency, Geophys. Res. Lett., https://doi.org/10.1029/2023GL106670, 2024b.
- 1318 Chen, C.-T. A., Lui, H.-K., Hsieh, C.-H., Yanagi, T., Kosugi, N., Ishii, M., and Gong, G.-C.: Deep oceans may





- acidify faster than anticipated due to global warming, Nat. Clim. Change., 7(12), 890–894,
- 1320 https://doi.org/10.1038/s41558-017-0003-y, 2017.
- 1321 Clement, D., and Gruber, N.: The EMLR(C*) method to determine decadal changes in the global ocean storage of
- 1322 Anthropogenic CO₂. Global Biogeochemical Cycles, 32(4), 654–679, https://doi.org/10.1002/2017gb005819, 2018.
- 1323 Cooley, S. R., and Doney, S. C.: Anticipating ocean acidification's economic consequences for commercial
- 1324 fisheries. Environmental Research Letters, 4(2), 024007, https://doi.org/10.1088/1748-9326/4/2/024007, 2009.
- 1325 Crisp, D., Dolman, H., Tanhua, T., McKinley, G. A., Hauck, J., Bastos, A., Sitch, S., Eggleston, S., and Aich, V.:
- How well do we understand the land-ocean-atmosphere carbon cycle? Reviews of Geophysics, 60(2),
- 1327 https://doi.org/10.1029/2021RG000736, 2022.
- 1328 Cyr, F., Gibb, O., Azetsu-Scott, K., Chassé, J., Galbraith, P., Maillet, G., Pepin, P., Punshon, S., and Starr, M.:
- 1329 Ocean carbonate parameters on the Canadian Atlantic Continental Shelf, Federated Research Data Repository,
- 1330 https://doi.org/10.20383/102.0673, 2022.
- 1331 Delaigue, L., Sulpis, O., Reichart, G.-J., and Humphreys, M. P.: The changing biological carbon pump of the South
- 1332 Atlantic Ocean. Global Biogeochemical Cycles, 38(9), https://doi.org/10.1029/2024gb008202, 2024.
- 1333 DeVries, T., Holzer, M. and Primeau, F.: Recent increase in oceanic carbon uptake driven by weaker upper-ocean
- overturning, Nature, 542, 215–218, https://doi.org/10.1038/nature21068, 2017.
- 1335 DeVries, T., Le Quéré, C., Andrews, O., Berthet, S., Hauck, J., Ilyina, T., Landschützer, P., Lenton, A., Lima, I. D.,
- 1336 Nowicki, M., Schwinger, J., and Séférian, R.: Decadal trends in the ocean carbon sink, Proceedings of the National
- 1337 Academy of Sciences, 116(24), 11646–11651, https://doi.org/10.1073/pnas.1900371116, 2019.
- 1338 DeVries, T.: The Ocean Carbon Cycle, Annual Review of Environment and Resources, 47(1), 317–341,
- 1339 https://doi.org/10.1146/annurev-environ-120920-111307, 2022.
- 1340 DeVries, T., Yamamoto, K., Wanninkhof, R., Gruber, N., Hauck, J., Müller, J. D., Bopp, L., Carroll, D., Carter, B.,
- Chau, T., Doney, S. C., Gehlen, M., Gloege, L., Gregor, L., Henson, S., Kim, J. H., Iida, Y., Ilyina, T.,
- 1342 Landschützer, P., Le Quéré, C., Munro, D., Nissen, C., Patara, L., Pérez, F. F., Resplandy, L., Rodgers, K. B.,
- 1343 Schwinger, J., Séférian, R., Sicardi, V., Terhaar, J., Triñanes, J., Tsujino, H., Watson, A., Yasunaka, S., Zeng, J.
- 1344 (2023). Magnitude, trends, and variability of the Global Ocean Carbon Sink from 1985 to 2018. Global
- 1345 Biogeochemical Cycles, 37(10). https://doi.org/10.1029/2023gb007780, 2023.
- Dickson, A. G.: Standard potential of the reaction: AgCl(s) + 1/2 H2(g) = Ag(s) + HCl(aq), and the standard acidity
- 1347 constant of the ion HSO4- in synthetic seawater from 273.15 to 318.15K, Journal of Chemical Thermodynamics,
- 1348 22(2), 113–127, https://doi.org/10.1016/0021-9614(90)90074-Z, 1990.



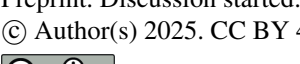


- Doney, S. C., Busch, D. S., Cooley, S. R., and Kroeker, K. J.: The impacts of ocean acidification on marine
- 1350 ecosystems and reliant human communities, Annual Review of Environment and Resources, 45(1), 83–112,
- 1351 https://doi.org/10.1146/annurev-environ-012320-083019, 2020.
- 1352 Dore, J. E., Lukas, R., Sadler, D. W., and Karl, D. M.: Climate-driven changes to the atmospheric CO₂ sink in the
- subtropical North Pacific Ocean, Nature, 424, 754-757, https://doi.org/10.1038/nature01885, 2003.
- 1354 Dore, J. E., Lukas, R., Sadler, D. W., Church, M. J., and Karl, D. M.: Physical and biogeochemical modulation of
- ocean acidification in the central North Pacific, Proc. Natl. Acad. Sci., 106, 12235-12240,
- 1356 https://doi.org/10.1073/pnas.0906044106, 2009.
- Dore, J. E., Church, M. J., Karl, D. M., Sadler, D. W., and Letelier, R. M.: Paired windward and leeward
- 1358 biogeochemical time series reveal consistent surface ocean CO₂ trends across the Hawaiian Ridge, Geophys. Res.
- 1359 Lett., 41, 6459-6467, https://doi.org/10.1002/2014GL060725, 2014.
- 1360 Dore, J.E., White, A.E., and Karl, D.M.: Hawaii Ocean Time-series (HOT) Carbon Dioxide (Version 1) [Data set].
- 1361 Zenodo. https://doi.org/10.5281/zenodo.15060931, 2025.
- Dunne, John P., John, J. G., Shevliakova, E., Stouffer, R. J., Krasting, J. P., Malyshev, S. L., Milly, P. C., Sentman,
- 1363 L. T., Adcroft, A. J., Cooke, W., Dunne, K. A., Griffies, S. M., Hallberg, R. W., Harrison, M. J., Levy, H.,
- Wittenberg, A. T., Phillips, P. J., and Zadeh, N.: GFDL's ESM2 global coupled climate-carbon earth system
- models. part II: Carbon system formulation and baseline simulation characteristics, Journal of Climate, 26(7), 2247-
- 1366 2267, https://doi.org/10.1175/jcli-d-12-00150.1, 2013.
- Dunne, J. P., Hewitt, H. T., Arblaster, J., Bonou, F., Boucher, O., Cavazos, T., Durack, P. J., Hassler, B., Juckes, M.,
- 1368 Miyakawa, T., Mizielinski, M., Naik, V., Nicholls, Z., O'Rourke, E., Pincus, R., Sanderson, B. M., Simpson, I. R.,
- and Taylor, K. E.: An Evolving Coupled Model Intercomparison Project Phase 7 (CMIP7) and Fast Track in
- 1370 Support of Future Climate Assessment, https://doi.org/10.5194/egusphere-2024-3874, 2024.
- 1371 Durack, P. J., Taylor, K. E., Gleckler, P. J., Meehl, G. A., Lawrence, B. N., Covey, C., Stouffer, R. J., Levavasseur,
- 1372 G., Ben-Nasser, A., Denvil, S., Stockhause, M., Gregory, J. M., Juckes, M., Ames, S. K., Antonio, F., Bader, D. C.,
- Dunne, J. P., Ellis, D., Eyring, V., Fiore, S. L., Joussaume, S. Kershaw, P., Lamarque, J.-F., Lautenschlager, M.,
- 1374 Lee, J., Mauzey, C. F., Mizielinski, M., Nassisi, P., Nuzzo, A., O'Rourke, E., Painter, J., Potter, G. L., Rodriguez,
- 1375 S., Williams, D. N.: The Coupled Model Intercomparison Project (CMIP): Reviewing Project History, Evolution,
- 1376 Infrastructure and Implementation, https://doi.org/10.5194/egusphere-2024-3729, 2025.
- 1377 Edmond, J. M.: High precision determination of titration alkalinity and total carbon dioxide content of sea water by
- 1378 potentiometric titration, Deep Sea Research and Oceanographic Abstracts, 17(4), 737–750,
- 1379 https://doi.org/10.1016/0011-7471(70)90038-0, 1970.





- 1380 Fassbender, A. J., Carter, B. R., Sharp, J. D., Huang, Y., Arroyo, M. C., and Frenzel, H.: Amplified subsurface
- signals of ocean acidification, Global Biogeochemical Cycles, 37, e2023GB007843,
- 1382 https://doi.org/10.1029/2023GB007843, 2023.
- 1383 Fay, A. R., Gregor, L., Landschützer, P., McKinley, G. A., Gruber, N., Gehlen, M., Iida, Y., Laruelle, G. G.,
- 1384 Rödenbeck, C., Roobaert, A., and Zeng, J.: SeaFlux: harmonization of air–sea CO₂ fluxes from surface pCO₂ data
- products using a standardized approach, Earth Sys. Sci. Data, 13(10), 4693-4710, https://doi.org/10.5194/essd-13-
- 1386 4693-2021, 2021.
- 1387 Fay, A. R., and McKinley, G. A.: Observed regional fluxes to constrain modelled estimates of the Ocean Carbon
- 1388 Sink, Geophysical Res. Lett., 48(20), https://doi.org/10.1029/2021gl095325, 2021.
- 1389 Fay, A. R., Munro, D. R., McKinley, G. A., Pierrot, D., Sutherland, S. C., Sweeney, C., and Wanninkhof, R.:
- 1390 Updated climatological mean Δ/CO₂ and net sea-air CO₂ flux over the global open ocean regions, Earth Syst. Sci.
- 1391 Data, 16, 2123–2139, https://doi.org/10.5194/essd-16-2123-2024, 2024.
- 1392 Feely, R. A., Jiang, L.-Q., Wanninkhof, R., Carter, B. R., Alin, S. A., Bednaršek, N., and Cosca, C. E.: Acidification
- of the global surface ocean: What we have learned from observations, Oceanography, 36, 120-129,
- 1394 https://doi.org/10.5670/oceanog.2023.222, 2023.
- 1395 Fennel, K., Mattern, J. P., Doney, S. C., Bopp, L., Moore, A. M., Wang, B., and Yu, L.: Ocean biogeochemical
- 1396 modelling, Nat. Rev. Methods Primers, 2, 76, https://doi.org/10.1038/s43586-022-00154-2, 2022.
- 1397 Freeland, H.: A short history of ocean station papa and line P. Progress in Oceanography, 75(2), 120–125,
- 1398 https://doi.org/10.1016/j.pocean.2007.08.005, 2007.
- 1399 Friedlingstein, P., O'Sullivan, M., Jones, M. W., Andrew, R. M., Bakker, D. C. E., Hauck, J., Landschützer, P., Le
- 1400 Quéré, C., Luijkx, I. T., Peters, G. P., Peters, W., Pongratz, J., Schwingshackl, C., Sitch, S., Canadell, J. G., Ciais,
- 1401 P., Jackson, R. B., Alin, S. R., Anthoni, P., Barbero, L., Bates, N. R., Becker, M., Bellouin, N., Decharme, B., Bopp,
- 1402 L., Brasika, I. B. M., Cadule, P., Chamberlain, M. A., Chandra, N., Chau, T.-T.-T., Chevallier, F., Chini, L. P.,
- 1403 Cronin, M., Dou, X., Enyo, K., Evans, W., Falk, S., Feely, R. A., Feng, L., Ford, D. J., Gasser, T., Ghattas, J.,
- Gkritzalis, T., Grassi, G., Gregor, L., Gruber, N., Gürses, Ö., Harris, I., Hefner, M., Heinke, J., Houghton, R. A.,
- Hurtt, G. C., Iida, Y., Ilyina, T., Jacobson, A. R., Jain, A., Jarníková, T., Jersild, A., Jiang, F., Jin, Z., Joos, F., Kato,
- 1406 E., Keeling, R. F., Kennedy, D., Klein Goldewijk, K., Knauer, J., Korsbakken, J. I., Körtzinger, A., Lan, X.,
- 1407 Lefèvre, N., Li, H., Liu, J., Liu, Z., Ma, L., Marland, G., Mayot, N., McGuire, P. C., McKinley, G. A., Meyer, G.,
- 1408 Morgan, E. J., Munro, D. R., Nakaoka, S.-I., Niwa, Y., O'Brien, K. M., Olsen, A., Omar, A. M., Ono, T., Paulsen,
- 1409 M., Pierrot, D., Pocock, K., Poulter, B., Powis, C. M., Rehder, G., Resplandy, L., Robertson, E., Rödenbeck, C.,
- 1410 Rosan, T. M., Schwinger, J., Séférian, R., Smallman, T. L., Smith, S. M., Sospedra-Alfonso, R., Sun, Q., Sutton, A.
- 1411 J., Sweeney, C., Takao, S., Tans, P. P., Tian, H., Tilbrook, B., Tsujino, H., Tubiello, F., van der Werf, G. R., van
- Ooijen, E., Wanninkhof, R., Watanabe, M., Wimart-Rousseau, C., Yang, D., Yang, X., Yuan, W., Yue, X., Zaehle,





- 1413 S., Zeng, J., and Zheng, B.: Global Carbon Budget 2023, Earth Syst. Sci. Data, 15, 5301–5369,
- 1414 https://doi.org/10.5194/essd-15-5301-2023, 2023.
- 1415 Friedlingstein, P., O'Sullivan, M., Jones, M. W., Andrew, R. M., Hauck, J., Landschützer, P., Le Quéré, C., Li, H.,
- 1416 Luijkx, I. T., Olsen, A., Peters, G. P., Peters, W., Pongratz, J., Schwingshackl, C., Sitch, S., Canadell, J. G., Ciais,
- 1417 P., Jackson, R. B., Alin, S. R., Arneth, A., Arora, V., Bates, N. R., Becker, M., Bellouin, N., Berghoff, C. F., Bittig,
- 1418 H. C., Bopp, L., Cadule, P., Campbell, K., Chamberlain, M. A., Chandra, N., Chevallier, F., Chini, L. P., Colligan,
- 1419 T., Decayeux, J., Djeutchouang, L. M., Dou, X., Duran Rojas, C., Enyo, K., Evans, W., Fay, A. R., Feely, R. A.,
- 1420 Ford, D. J., Foster, A., Gasser, T., Gehlen, M., Gkritzalis, T., Grassi, G., Gregor, L., Gruber, N., Gürses, Ö., Harris,
- 1421 I., Hefner, M., Heinke, J., Hurtt, G. C., Iida, Y., Ilyina, T., Jacobson, A. R., Jain, A. K., Jarníková, T., Jersild, A.,
- 1422 Jiang, F., Jin, Z., Kato, E., Keeling, R. F., Klein Goldewijk, K., Knauer, J., Korsbakken, J. I., Lan, X., Lauvset, S.
- 1423 K., Lefèvre, N., Liu, Z., Liu, J., Ma, L., Maksyutov, S., Marland, G., Mayot, N., McGuire, P. C., Metzl, N.,
- 1424 Monacci, N. M., Morgan, E. J., Nakaoka, S.-I., Neill, C., Niwa, Y., Nützel, T., Olivier, L., Ono, T., Palmer, P. I.,
- 1425 Pierrot, D., Qin, Z., Resplandy, L., Roobaert, A., Rosan, T. M., Rödenbeck, C., Schwinger, J., Smallman, T. L.,
- 1426 Smith, S. M., Sospedra-Alfonso, R., Steinhoff, T., Sun, Q., Sutton, A. J., Séférian, R., Takao, S., Tatebe, H., Tian,
- 1427 H., Tilbrook, B., Torres, O., Tourigny, E., Tsujino, H., Tubiello, F., van der Werf, G., Wanninkhof, R., Wang, X.,
- Yang, D., Yang, X., Yu, Z., Yuan, W., Yue, X., Zaehle, S., Zeng, N., and Zeng, J.: Global Carbon Budget 2024, 1428
- 1429 Earth Syst. Sci. Data, 17, 965–1039, https://doi.org/10.5194/essd-17-965-2025, 2025.
- 1430 Garcia, H. E., Locarnini, R. A., Boyer, T. P., Antonov, J. I., Baranova, O. K., Zweng, M. M., Reagan, J. R., and
- 1431 Johnson, D. R.: World Ocean Atlas 2013, Volume 3: Dissolved Oxygen, Apparent Oxygen Utilization, and Oxygen
- 1432 Saturation, edited by: Levitus, S. and Mishonov, A., Technical Ed., NOAA Atlas NES-DIS 75, 27 pp., 2014.
- 1433 Garcia, H. E., Weathers, K., Paver, C. R., Smolyar, I., Boyer, T. P., Locarnini, R. A., Zweng, M. M., Mishonov, A.
- 1434 V., Baranova, O. K., Seidov, D., and Reagan, J. R.: World Ocean Atlas 2018, Volume 4: Dissolved Inorganic
- 1435 Nutrients (phosphate, nitrate and nitrate+nitrite, silicate), A. Mishonov Technical Ed., NOAA Atlas NESDIS 84,
- 1436 35pp, 2018a.
- 1437 Garcia H. E., Weathers, K. W., Paver, C. R., Smolyar, I.V., Boyer, T. P., Locarnini, R. A., Zweng, M. M.,
- 1438 Mishonov, A. V., Baranova, O.K., and Reagan, J. R.: World Ocean Atlas 2018, Volume 3: Dissolved Oxygen,
- Apparent Oxygen Utilization, and Oxygen Saturation, Mishonov, A., Technical Editor, NOAA Atlas NESDIS 83, 1439
- 1440 2018b.
- 1441 Garcia H. E., Boyer, T. P., Locarnini, R. A., Reagan, J. R., Mishonov, A. V., Baranova, O. K., Paver, C. R., Wang,
- 1442 Z., Bouchard, C. N., Cross, S. L., Seidov, D., and Dukhovskoy, D.: World Ocean Database 2023: User's Manual.
- 1443 A.V. Mishonov, Technical Ed., NOAA Atlas NESDIS 98, pp 129. https://doi.org/10.25923/j8gq-eee82, 2024.
- 1444 Gattuso, J.-P., and Hansson, L.: Ocean acidification, Oxford University Press, pp. 326, 2011.
- 1445 Gattuso, J.-P., Epitalon, J.-M., Lavigne, H., and Orr, J.: seacarb: Seawater Carbonate Chemistry, R Package





- 1446 (Version 3.2.16), https://CRAN.R-project.org/package=seacarb, 2021a.
- 1447 Gattuso, J.-P., Alliouane, S., Mousseau, L.: Seawater carbonate chemistry in the Bay of Villefranche, Point B
- 1448 (France), January 2007 June 2023 [dataset], PANGAEA, https://doi.org/10.1594/PANGAEA.727120, 2021b.
- Gattuso, J.-P., Alliouane, S., and Fischer, P.: High-frequency, year-round time series of the carbonate chemistry in a
- 1450 high-Arctic fjord (Svalbard), Earth Syst. Sci. Data, 15, 2809–2825, https://doi.org/10.5194/essd-15-2809-2023,
- 1451 2023a.
- 1452 Gattuso, J.-P., Alliouane, S., and Fischer, P.: High-frequency, year-round time series of the carbonate chemistry in a
- high-Arctic fjord (Svalbard) [dataset], PANGAEA, https://doi.org/10.1594/PANGAEA.957028, 2023b.
- Gibb, O., Cyr, F., Azetsu-Scott, K., Chassé, J., Childs, D., Gabriel, C.-E., Galbraith, P. S., Maillet, G., Pepin, P.,
- 1455 Punshon, S., and Starr, M.: Spatiotemporal variability in pH and carbonate parameters on the Canadian Atlantic
- 1456 continental shelf between 2014 and 2022, Earth Syst. Sci. Data, 15, 4127–4162, https://doi.org/10.5194/essd-15-
- 1457 4127-2023, 2023.
- 1458 Gloege, L., Yan, M., Zheng, T., and McKinley, G. A.: Improved quantification of ocean carbon uptake by using
- machine learning to merge global models and pCO₂ data, Journal of Advances in Modeling Earth Systems, 14(2),
- 1460 https://doi.org/10.1029/2021ms002620, 2022.
- 1461 González-Dávila, M. and Santana-Casiano J. M.: Long-term trends of pH and inorganic carbon in the Eastern North
- 1462 Atlantic: the ESTOC site, Front. Mar. Sci., 10, 1236214, https://doi.org/10.3389/fmars.2023.1236214, 2023.
- 1463 Gregor, L., Lebehot, A. D., Kok, S., and Monteiro, P. M. S.: A comparative assessment of the uncertainties of
- Global Surface Ocean CO₂ Estimates using a machine-learning ensemble (CSIR-ML6 version 2019a) have we hit
- the wall? Geoscientific Model Development, 12(12), 5113-5136, https://doi.org/10.5194/gmd-12-5113-2019, 2019a.
- 1466 Gregor, L., Lebehot, A. D., Kok, S., Monteiro, P. M. S.: Global surface-ocean partial pressure of carbon dioxide
- 1467 (pCO₂) estimates from a machine learning ensemble: CSIR-ML6 v2019a (NCEI Accession 0206205), NOAA
- National Centers for Environmental Information, Dataset, https://doi.org/10.25921/z682-mn47, 2019b.
- 1469 Gregor, L., and Gruber, N.: OceanSODA-ETHZ: A global gridded dataset of the surface ocean carbonate system for
- seasonal to decadal studies of ocean acidification (v2023) (NCEI Accession 0220059), NOAA National Centers for
- Environmental Information, Dataset, https://doi.org/10.25921/m5wx-ja34, 2020.
- 1472 Gregor, L.: luke-gregor/OceanSODA-ETHZ: code, Zenodo, https://doi.org/10.5281/zenodo.4455354, 2021.
- 1473 Gregor, L. and Fay, A.: SeaFlux: harmonised sea-air CO₂ fluxes from surface pCO₂ data products using a
- standardised approach [Data set], Zenodo, https://doi.org/10.5281/zenodo.5482547, 2021.
- 1475 Gregor, L., and Gruber, N.: Oceansoda-ETHZ: A global gridded data set of the surface ocean carbonate system for





- seasonal to decadal studies of ocean acidification, Earth System Science Data, 13(2), 777-808,
- 1477 https://doi.org/10.5194/essd-13-777-2021, 2021.
- 1478 Gregor, L., and Gruber, N.: OceanSODA-ETHZ: A global gridded dataset of the surface ocean carbonate system for
- 1479 seasonal to decadal studies of ocean acidification (v2023) (NCEI accession 0220059) [Dataset], NOAA National
- 1480 Centers for Environmental Information, https://doi.org/10.25921/m5wx-ja34, 2023.
- 1481 Gregor, L., Shutler, J., and Gruber, N.: High-resolution variability of the Ocean Carbon Sink, Global
- 1482 Biogeochemical Cycles, 38(8), https://doi.org/10.1029/2024gb008127, 2024a.
- 1483 Gregor, L., Shutler, J., and Gruber, N.: OceanSODA-ETHZ-v2: Surface ocean sea-air CO₂ fluxes from 1982 to 2022
- 1484 (8-day by 0.25° x 0.25°) (v2.2024r01), [Data set], Zenodo, https://zenodo.org/records/11206366, 2024b.
- Gruber, N., Clement, D., Carter, B. R., Feely, R. A., van Heuven, S., Hoppema, M., Ishii, M., Key, R. M., Kozyr,
- 1486 A., Lauvset, S. K., Lo Monaco, C., Mathis, J. T., Murata, A., Olsen, A., Perez, F. F., Sabine, C. L., Tanhua, T., and
- Wanninkhof, R.: The oceanic sink for anthropogenic CO₂ from 1994 to 2007, Science, 363(6432), 1193–1199,
- 1488 https://doi.org/10.1126/science.aau5153, 2019a.
- Gruber, N., Clement, D., Carter, B. R., Feely, R. A., van Heuven, S., Hoppema, M., Ishii, M., Key, R. M., Kozyr,
- 1490 A., Lauvset, S. K., Lo Monaco, C., Mathis, J. T., Murata, A., Olsen, A., Perez, F. F., Sabine, C. L., Tanhua, T., and
- Wanninkhof, R.: The oceanic sink for anthropogenic CO2 from 1994 to 2007 the data (NCEI Accession 0186034),
- $NOAA\ National\ Centers\ for\ Environmental\ Information,\ Dataset,\ https://doi.org/10.25921/wdn2-pt10,\ 2019b.$
- Gruber, N., Bakker, D. C. E., DeVries, T., Gregor, L., Hauck, J., Landschützer, P., McKinley, G. A., and Müller, J.
- D.: Trends and variability in the ocean carbon sink, Nature Reviews Earth and Environment, 4(2), 119–134,
- 1495 https://doi.org/10.1038/s43017-022-00381-x, 2023.
- 1496 Hauck, J., Mayot, N., Landschützer, P., & Jersild, A. (2025). Global Carbon Budget 2024, surface ocean fugacity of
- 1497 CO₂ (fCO₂) and air-sea CO₂ flux of individual global ocean biogeochemical models and surface ocean fCO₂-based
- data-products [Data set]. Zenodo. https://doi.org/10.5281/zenodo.14639761
- 1499 Holzer, M., and DeVries, T.: Source-labeled anthropogenic carbon reveals a large shift of preindustrial carbon from
- the ocean to the atmosphere, Global Biogeochemical Cycles, 36(10), https://doi.org/10.1029/2022gb007405, 2022.
- Humphreys, M. P., Lewis, E. R., Sharp, J. D., and Pierrot, D.: PyCO2SYS v1.8: Marine carbonate system
- 1502 calculations in Python, Geoscientific Model Development, 15(1), 15-43, https://doi.org/10.5194/gmd-15-15-2022,
- 1503 2022.
- 1504 Iida, Y., Takatani, Y., Kojima, A., and Ishii, M.: Global trends of ocean CO₂ sink and ocean acidification: An
- observation-based reconstruction of surface ocean inorganic carbon variables, Journal of Oceanography, 77(2), 323-
- 1506 358, https://doi.org/10.1007/s10872-020-00571-5, 2021.





- 1507 IPCC: Climate Change 2023: Synthesis Report, Contribution of Working Groups I, II and III to the Sixth
- 1508 Assessment Report of the Intergovernmental Panel on Climate Change [Core Writing Team, H. Lee and J. Romero
- 1509 (eds.)], IPCC, Geneva, Switzerland, pp. 35-115, https://doi.org/10.59327/IPCC/AR6-9789291691647, 2023.
- 1510 Ishii, M., Kosugi, N., Sasano, D., Saito, S., Midorikawa, T., & Inoue, H. Y.: Ocean acidification off the south coast
- 1511 of Japan: A result from time series observations of CO₂ Parameters from 1994 to 2008. Journal of Geophysical
- 1512 Research, 116(C6), https://doi.org/10.1029/2010jc006831, 2011a.
- 1513 Ishii, M., Suzuki, T., and Key, R.: Pacific Ocean Interior Carbon Data Synthesis, PACIFICA, in Progress, PICES
- 1514 Press, 19(1), 20-23, https://www.pices.int/publications/pices press/volume19/v19 n1/pp 20-23 PACIFICA f.pdf,
- 1515 2011b.
- 1516 Jersild, A., Landschützer, P., Gruber, N., Bakker, D. C. E.: An observation-based global monthly gridded sea surface
- 1517 pCO₂ and air-sea CO₂ flux product from 1982 onward and its monthly climatology (NCEI Accession 0160558),
- NOAA National Centers for Environmental Information, Dataset, https://doi.org/10.7289/v5z899n6, 2017.
- 1519 Jiang, L.-Q., Feely, R. A., Carter, B. R., Greeley, D. J., Gledhill, D. K., and Arzayus, K. M.: Climatological
- distribution of aragonite saturation state in the global oceans, Global Biogeochemical Cycles, 29(10), 1656–1673,
- 1521 https://doi.org/10.1002/2015GB005198, 2015a.
- 1522 Jiang, L-Q., Feely, R. A.: Aragonite saturation state gridded to 1x1 degree latitude and longitude at depth levels of 0,
- 1523 50, 100, 200, 500, 1000, 2000, 3000, and 4000 meters in the global oceans (NCEI Accession 0139360), NOAA
- National Centers for Environmental Information, Dataset, https://doi.org/10.7289/v5q81b4p, 2015b.
- 1525 Jiang, L.-Q., Carter, B. R., Feely, R. A., Lauvset, S., and Olsen, A.: Surface ocean pH and buffer capacity: Past,
- 1526 present and future, Scientific Reports, 9(1), 18624, https://doi.org/10.1038/s41598-019-55039-4, 2019a.
- 1527 Jiang, L.-Q., Carter, B. R., Feely, R. A., Lauvset, S., and Olsen, A.: Global surface ocean pH, acidity, and Revelle
- 1528 Factor on a 1x1 degree global grid from 1770 to 2100 (NCEI Accession 0206289), NOAA National Centers for
- Environmental Information, Dataset, https://doi.org/10.25921/kgqr-9h49, 2019b.
- 1530 Jiang, L.-Q., Feely, R. A., Wanninkhof, R., Greeley, D., Barbero, L., Alin, S., Carter, B. R., Pierrot, D.,
- Featherstone, C., Hooper, J., Melrose, C., Monacci, N., Sharp, J. D., Shellito, S., Xu, Y.-Y., Kozyr, A., Byrne, R. H.,
- 1532 Cai, W.-J., Cross, J., Johnson, G. C., Hales, B., Langdon, C., Mathis, J., Salisbury, J., and Townsend, D. W.: Coastal
- 1533 Ocean Data Analysis Product in North America (CODAP-NA, Version 2021) (NCEI Accession 0219960), NOAA
- National Centers for Environmental Information, Dataset,. https://doi.org/10.25921/531n-c230, 2020.
- 1535 Jiang, L.-Q., Feely, R. A., Wanninkhof, R., Greeley, D., Barbero, L., Alin, S., Carter, B. R., Pierrot, D.,
- Featherstone, C., Hooper, J., Melrose, C., Monacci, N., Sharp, J. D., Shellito, S., Xu, Y.-Y., Kozyr, A., Byrne, R. H.,
- 1537 Cai, W.-J., Cross, J., Johnson, G. C., Hales, B., Langdon, C., Mathis, J., Salisbury, J., and Townsend, D. W.: Coastal





- 1538 Ocean Data Analysis Product in North America (CODAP-NA) an internally consistent data product for discrete
- inorganic carbon, oxygen, and nutrients on the North American ocean margins, Earth Syst. Sci. Data, 13, 2777–
- 2799, https://doi.org/10.5194/essd-13-2777-2021, 2021.
- 1541 Jiang, L.-Q., Pierrot, D., Wanninkhof, R., Feely, R. A., Tilbrook, B., Alin, S., Barbero, L., Byrne, R. H., Carter, B.
- 1542 R., Dickson, A. G., Gattuso, J.-P., Greeley, D., Hoppema, M., Humphreys, M. P., Karstensen, J., Lange, N.,
- Lauvset, S. K., Lewis, E. R., Olsen, A., Perez, F. F., Sabine, C., Sharp, J. D., Tanhua, T., Trull, T. W., Velo, A.,
- Allegra, A. J., Barker, P., Burger, E., Cai, W.-J., Chen, C.-T. A., Cross, J., Garcia, H., Hernandez-Ayon, J. M., Hu,
- 1545 X., Kozyr, A., Langdon, C., Lee, K., Salisbury, J., Wang, Z. A., and Xue, L.: Best practice data standards for
- discrete chemical oceanographic observations. Frontiers in Marine Science, 8,
- 1547 https://doi.org/10.3389/fmars.2021.705638, 2022a.
- 1548 Jiang, L.-Q., Boyer, T. P., Paver, C. R., Yoo, H., Reagan, J. R., Alin, S. R., Barbero, L., Carter, B. R., Feely, R. A.,
- 1549 and Wanninkhof, R.: Climatological distribution of ocean acidification indicators from surface to 500 meters water
- depth on the North American ocean margins from 2003-12-06 to 2018-11-22 (NCEI Accession 0270962), NOAA
- National Centers for Environmental Information, Dataset, https://doi.org/10.25921/g8pb-zy76, 2022b.
- 1552 Jiang, L., Dunne, J., Carter, B. R., Tjiputra, J. F., Terhaar, J., Sharp, J. D., Olsen, A., Alin, S., Bakker, D. C., Feely,
- 1553 R. A., Gattuso, J., Hogan, P., Ilyina, T., Lange, N., Lauvset, S. K., Lewis, E. R., Lovato, T., Palmieri, J., Santana-
- 1554 Falcón, Y., Schwinger, J., Séférian, R., Strand, G., Swart, N., Tanhua, T., Tsujino, H., Wanninkhof, R., Watanabe,
- 1555 M., Yamamoto, A., and Ziehn, T.: Global surface ocean acidification indicators from 1750 to 2100 (NCEI
- 1556 Accession 0259391), NOAA National Centers for Environmental Information, Dataset,
- 1557 https://doi.org/10.25921/9ker-bc48, 2022c.
- 1558 Jiang, L., Dunne, J., Carter, B. R., Tjiputra, J. F., Terhaar, J., Sharp, J. D., Olsen, A., Alin, S., Bakker, D. C., Feely,
- 1559 R. A., Gattuso, J., Hogan, P., Ilyina, T., Lange, N., Lauvset, S. K., Lewis, E. R., Lovato, T., Palmieri, J., Santana-
- 1560 Falcón, Y., Schwinger, J., Séférian, R., Strand, G., Swart, N., Tanhua, T., Tsujino, H., Wanninkhof, R., Watanabe,
- 1561 M., Yamamoto, A., and Ziehn, T.: Global surface ocean acidification indicators from 1750 to 2100, Journal of
- 1562 Advances in Modeling Earth Systems, 15(3), https://doi.org/10.1029/2022ms003563, 2023.
- 1563 Jiang, L.-Q., Boyer, T. P., Paver, C. R., Yoo, H., Reagan, J. R., Alin, S. R., Barbero, L., Carter, B. R., Feely, R. A.,
- and Wanninkhof, R.: Climatological distribution of ocean acidification variables along the North American ocean
- 1565 margins, Earth System Science Data, 16(7), 3383–3390, https://doi.org/10.5194/essd-16-3383-2024, 2024.
- 1566 Johnson, G. C., Robbins, P. E., and Hufford, G. E. (2001). Systematic adjustments of hydrographic sections for
- internal consistency. Journal of Atmospheric and Oceanic Technology, 18(7), 1234–1244, 2001.
- 1568 Kapsenberg, L., Alliouane, S., Gazeau, F., Mousseau, L., and Gattuso, J.-P.: Coastal ocean acidification and
- increasing total alkalinity in the northwestern Mediterranean Sea, Ocean Sci., 13, 411–426,
- $1570 \qquad https://doi.org/10.5194/os-13-411-2017, \, 2017.$





- 1571 Karl, D., Dore, J., Lukas, R., Michaels, A., Bates, N., and Knap, A.: Building the long-term picture: The U.S.
- 1572 JGOFS Time-series programs. Oceanography, 14(4), 6–17, https://doi.org/10.5670/oceanog.2001.02, 2001.
- 1573 Karl, D. M., and Lukas, R.: The Hawaii Ocean Time-series (HOT) program: Background, rationale and field
- 1574 implementation, Deep Sea Research Part II, 43(2–3), 129–156, https://doi.org/10.1016/0967-0645(96)00005-7,
- 1575 1996.
- 1576 Kennedy, E. G., Zulian, M., Hamilton, S. L., Hill, T. M., Delgado, M., Fish, C. R., Gaylord, B., Kroeker, K. J.,
- 1577 Palmer, H. M., Ricart, A. M., Sanford, E., Spalding, A. K., Ward, M., Carrasco, G., Elliott, M., Grisby, G. V.,
- 1578 Harris, E., Jahncke, J., Rocheleau, C. N., Westerink, S., and Wilmot, M. I.: Multistressor Observations of Coastal
- 1579 Hypoxia and Acidification (MOCHA) Synthesis (NCEI Accession 0277984), NOAA National Centers for
- Environmental Information, Dataset, https://doi.org/10.25921/2vve-fh39, 2023.
- 1581 Kennedy, E. G., Zulian, M., Hamilton, S. L., Hill, T. M., Delgado, M., Fish, C. R., Gaylord, B., Kroeker, K. J.,
- Palmer, H. M., Ricart, A. M., Sanford, E., Spalding, A. K., Ward, M., Carrasco, G., Elliott, M., Grisby, G. V.,
- 1583 Harris, E., Jahncke, J., Rocheleau, C. N., Westerink, S., and Wilmot, M. I.: A high-resolution synthesis dataset for
- multistressor analyses along the US West Coast, Earth Syst. Sci. Data, 16, 219–243, https://doi.org/10.5194/essd-
- 1585 16-219-2024, 2024.
- 1586 Keppler, L., Landschützer, P., Gruber, N., Lauvset, S. K., and Stemmler, I.: Seasonal carbon dynamics in the near-
- 1587 global ocean, *Global Biogeochemical Cycles*, 34(12), e2020GB006571, https://doi.org/10.1029/2020GB006571,
- 1588 2020.
- 1589 Keppler, L., Landschützer, P., Lauvset, S. K., and Gruber, N.: Recent trends and variability in the oceanic storage of
- dissolved inorganic carbon, Global Biogeochemical Cycles, 37(5), https://doi.org/10.1029/2022gb007677, 2023.
- 1591 Key, R. M., Kozyr, A., Sabine, C. L., Lee, K., Wanninkhof, R., Bullister, J. L., Feely, R. A., Millero, F. J., Mordy,
- 1592 C., and Peng, T.-H.: A global ocean carbon climatology: Results from Global Data Analysis Project (GLODAP),
- 1593 Global Biogeochemical Cycles, 18(4), https://doi.org/10.1029/2004gb002247, 2004.
- 1594 Key, R. M., Tanhua, T., Olsen, A., Hoppema, M., Jutterström, S., Schirnick, C., van Heuven, S., Kozyr, A., Lin, X.,
- 1595 Velo, A., Wallace, D. W. R., and Mintrop, L.: The CARINA data synthesis project: introduction and overview,
- 1596 Earth Syst, Sci, Data, 2, 105–121, https://doi.org/10.5194/essd-2-105-2010, 2010.
- 1597 Key, R. M., Olsen, A., van Heuven, S., Lauvset, S. K., Velo, A., Lin, X., Schirnick, C., Kozyr, A., Tanhua, T.,
- 1598 Hoppema, M., Jutterström, S., Steinfeldt, R., Jeansson, E., Ishi, M., Perez, F. F., and Suzuki, T.: Global Ocean Data
- 1599 Analysis Project, Version 2 (GLODAPv2), ORNL/CDIAC-162, ND-P093, Carbon Dioxide Information Analysis
- 1600 Center, Oak Ridge National Laboratory, U. S. Department of Energy, Oak Ridge, Tennessee,
- 1601 https://doi.org/10.3334/CDIAC/OTG.NDP093 GLODAPv2, 2015.





- 1602 Kheshgi, H. S.: Sequestering atmospheric carbon dioxide by increasing ocean alkalinity, Energy, 20(9), 915–922,
- 1603 https://doi.org/10.1016/0360-5442(95)00035-f, 1995.
- 1604 Knor, L. A. C. M., Sabine, C. L., Sutton, A. J., White, A. E., Potemra, J., and Weller, R. A.: Quantifying net
- 1605 community production and calcification at Station ALOHA near Hawai'i: Insights and limitations from a dual tracer
- 1606 carbon budget approach, Global Biogeochemical Cycles, 37, e2022GB007672,
- 1607 https://doi.org/10.1029/2022GB007672, 2023.
- 1608 Kwiatkowski, L., Torres, O., Bopp, L., Aumont, O., Chamberlain, M., Christian, J. R., Dunne, J. P., Gehlen, M.,
- 1609 Ilyina, T., John, J. G., Lenton, A., Li, H., Lovenduski, N. S., Orr, J. C., Palmieri, J., Santana-Falcón, Y., Schwinger,
- 1610 J., Séférian, R., Stock, C. A., Tagliabue, A., Takano, Y., Tjiputra, J., Toyama, K., Tsujino, H., Watanabe, M.,
- 1611 Yamamoto, A., Yool, A., and Ziehn, T.: Twenty-first century ocean warming, acidification, deoxygenation, and
- 1612 upper-ocean nutrient and primary production decline from CMIP6 model projections, Biogeosciences, 17, 3439–
- 1613 3470, https://doi.org/10.5194/bg-17-3439-2020, 2020.
- 1614 Landschützer, P., Gruber, N., Bakker, D. C. E., Schuster, U., Nakaoka, S., Payne, M. R., Sasse, T., and Zeng, J.: A
- 1615 neural network-based estimate of the seasonal to inter-annual variability of the Atlantic Ocean carbon sink,
- 1616 Biogeosciences, 10, 7793–7815, https://doi.org/10.5194/bg-10-7793-2013, 2013.
- 1617 Landschützer, P., Gruber, N., Bakker, D. C. E., and Schuster, U.: Recent variability of the Global Ocean Carbon
- 1618 Sink, Global Biogeochemical Cycles, 28(9), 927–949, https://doi.org/10.1002/2014gb004853, 2014.
- 1619 Landschützer, P., Gruber, N., and Bakker, D. C. E.: Decadal variations and trends of the Global Ocean Carbon Sink,
- 1620 Global Biogeochemical Cycles, 30(10), 1396–1417. https://doi.org/10.1002/2015gb005359, 2016.
- 1621 Landschützer, P., Laruelle, G. G., Roobaert, A., and Regnier, P.: A uniform pCO2 climatology combining open and
- 1622 coastal oceans, Earth Syst. Sci. Data, 12, 2537–2553, https://doi.org/10.5194/essd-12-2537-2020, 2020a.
- 1623 Landschützer, P., Laruelle, G. G., Roobaert, A., and Regnier, P.: A combined global ocean pCO2 climatology
- 1624 combining open ocean and coastal areas (NCEI Accession 0209633), NOAA National Centers for Environmental
- 1625 Information, Dataset, https://doi.org/10.25921/qb25-f418, 2020b.
- 1626 Lange, N., Tanhua, T., Pfeil, B., Bange, H. W., Lauvset, S. K., Grégoire, M., Bakker, D. C., Jones, S. D., Fiedler, B.,
- 1627 O'Brien, K. M., and Körtzinger, A.: A status assessment of selected data synthesis products for ocean
- $1628 \qquad \text{biogeochemistry, Frontiers in Marine Science, } 10, \text{https://doi.org/} 10.3389/\text{fmars.} 2023.1078908, 2023.$
- Lange, N., Fiedler, B., Álvarez, M., Benoit-Cattin, A., Benway, H., Buttigieg, P. L., Coppola, L., Currie, K., Flecha,
- 1630 S., Gerlach, D. S., Honda, M., Huertas, I. E., Lauvset, S. K., Muller-Karger, F., Körtzinger, A., O'Brien, K. M.,
- 1631 Ólafsdóttir, S. R., Pacheco, F. C., Rueda-Roa, D., Skjelvan, I., Wakita, M., White, A., and Tanhua, T.: Synthesis
- product for ocean time series (spots) a ship-based biogeochemical pilot, Earth System Science Data, 16(4), 1901–





- 1633 1931, https://doi.org/10.5194/essd-16-1901-2024, 2024a.
- Lange, N., Fiedler, B., Álvarez, M., Benoit-Cattin, A., Benway, H., Buttigieg, P. L., Coppola, L., Currie, K. I.,
- 1635 Flecha, S., Gerlach, D. S., Honda, M. C., Huertas, E. I., Kinkade, D., Muller-Karger, F., Lauvset, S. K., Körtzinger,
- 1636 A., O'Brien, K. M., Ólafsdóttir, S., Pacheco, F. C., Rueda-Roa, D., Skjelvan, I., Wakita, M., White, A. E., Tanhua,
- 1637 T.: Synthesis Product for Ocean Time Series (SPOTS), Biological and Chemical Oceanography Data Management
- 1638 Office (BCO-DMO), (Version 2) Version Date 2024-02-22, https://doi.org/10.26008/1912/bco-dmo.896862.2,
- 1639 2024b.
- 1640 Laruelle, G. G., Landschützer, P., Gruber, N., Tison, J.-L., Delille, B., and Regnier, P.: Global high-resolution
- monthly pCO_2 climatology for the coastal ocean derived from neural network interpolation, Biogeosciences, 14,
- 4545–4561, https://doi.org/10.5194/bg-14-4545-2017, 2017.
- 1643 Lauvset, S. K., and Tanhua, T.: A toolbox for secondary quality control on ocean chemistry and Hydrographic Data,
- Limnology and Oceanography: Methods, 13(11), 601–608, https://doi.org/10.1002/lom3.10050, 2015.
- 1645 Lauvset, S. K., Key, R. M., Olsen, A., van Heuven, S., Velo, A., Lin, X., Schirnick, C., Kozyr, A., Tanhua, T.,
- Hoppema, M., Jutterström, S., Steinfeldt, R., Jeansson, E., Ishii, M., Perez, F. F., Suzuki, T., and Watelet, S.: A new
- 1647 global interior ocean mapped climatology: The 1° × 1° GLODAP version 2, Earth System Science Data, 8(2), 325–
- 1648 340, https://doi.org/10.5194/essd-8-325-2016, 2016.
- Lauvset, S. K., Lange, N., Tanhua, T., Bittig, H. C., Olsen, A., Kozyr, A., Álvarez, M., Becker, S., Brown, P. J.,
- 1650 Carter, B. R., Cotrim da Cunha, L., Feely, R. A., van Heuven, S., Hoppema, M., Ishii, M., Jeansson, E., Jutterström,
- 1651 S., Jones, S. D., Karlsen, M. K., Lo Monaco, C., Michaelis, P., Murata, A., Pérez, F. F., Pfeil, B., Schirnick, C.,
- 1652 Steinfeldt, R., Suzuki, T., Tilbrook, B., Velo, A., Wanninkhof, R., Woosley, R. J., and Key, R. M.: An updated
- version of the global interior ocean biogeochemical data product, GLODAPv2.2021, Earth Syst. Sci. Data, 13,
- 1654 5565–5589, https://doi.org/10.5194/essd-13-5565-2021, 2021.
- Lauvset, S. K., Lange, N., Tanhua, T., Bittig, H. C., Olsen, A., Kozyr, A., Alin, S., Álvarez, M., Azetsu-Scott, K.,
- 1656 Barbero, L., Becker, S., Brown, P. J., Carter, B. R., da Cunha, L. C., Feely, R. A., Hoppema, M., Humphreys, M. P.,
- 1657 Ishii, M., Jeansson, E., Jiang, L.-Q., Jones, S. D., Lo Monaco, C., Murata, A., Müller, J. D., Pérez, F. F., Pfeil, B.,
- 1658 Schirnick, C., Steinfeldt, R., Suzuki, T., Tilbrook, B., Ulfsbo, A., Velo, A., Woosley, R. J., and Key, R. M.:
- 1659 GLODAPv2.2022: the latest version of the global interior ocean biogeochemical data product, Earth Syst. Sci. Data,
- 1660 14, 5543–5572, https://doi.org/10.5194/essd-14-5543-2022, 2022.
- Lauvset, S. K., Lange, N., Tanhua, T., Bittig, H. C., Olsen, A., Kozyr, A., Álvarez, M., Azetsu-Scott, K., Becker, S.,
- 1662 Brown, P. J., Carter, B. R., Cotrim da Cunha, L., Feely, R. A., Hoppema, M., Humphreys, M. P., Ishii, M., Jeansson,
- 1663 E., Jones, S. D., Lo Monaco, C. Murata, A., Müller, J. D., Pérez, F. F., Schirnick, C., Steinfeldt, R., Suzuki, T.,
- Tilbrook, B., Ulfsbo, A., Velo, A., Woosley, R. J., Key, R. M.: Global Ocean Data Analysis Project version 2.2023
- 1665 (GLODAPv2.2023) (NCEI Accession 0283442), NOAA National Centers for Environmental Information, Dataset,





- 1666 https://doi.org/10.25921/zyrq-ht66, 2023a.
- Lauvset, S. K., Key, R. M., Olsen, A., van Heuven, S. M. A. C., Velo, A., Lin, X., Schirnick, C., Kozyr, A., Tanhua,
- 1668 T., Hoppema, M., Jutterström, S., Steinfeldt, R., Jeansson, E., Ishii, M., Pérez, F. F., Suzuki, T., Watelet, S.: A new
- 1669 global interior ocean mapped climatology: the 1° × 1° GLODAP version 2 from 1972-01-01 to 2013-12-31 (NCEI
- 1670 Accession 0286118), NOAA National Centers for Environmental Information, Dataset,
- 1671 https://doi.org/10.3334/cdiac/otg.ndp093 glodapv2, 2023b.
- Lauvset, S. K., Lange, N., Tanhua, T., Bittig, H. C., Olsen, A., Kozyr, A., Álvarez, M., Azetsu-Scott, K., Brown, P.
- 1673 J., Carter, B. R., Cotrim da Cunha, L., Hoppema, M., Humphreys, M. P., Ishii, M., Jeansson, E., Murata, A., Müller,
- 1674 J. D., Pérez, F. F., Schirnick, C., Steinfeldt, R., Suzuki, T., Ulfsbo, A., Velo, A., Woosley, R. J., and Key, R. M.:
- 1675 The annual update GLODAPv2.2023: the global interior ocean biogeochemical data product, Earth Syst. Sci. Data,
- 1676 16, 2047–2072, https://doi.org/10.5194/essd-16-2047-2024, 2024.
- 1677 Lee, K., Tong, L. T., Millero, F. J., Sabine, C. L., Dickson, A. G., Goyet, C., Park, G., Wanninkhof, R., Feely, R. A.,
- 1678 and Key, R. M.: Global relationships of total alkalinity with salinity and temperature in surface waters of the world's
- oceans, Geophysical Research Letters, 33(19), https://doi.org/10.1029/2006gl027207, 2006.
- 1680 Lee, K., Kim, T.-W., Byrne, R. H., Millero, F. J., Feely, R. A., and Liu, Y.-M.: The universal ratio of boron to
- 1681 chlorinity for the North Pacific and North Atlantic oceans, Geochimica et Cosmochimica Acta, 74(6), 1801–1811,
- 1682 https://doi.org/10.1016/j.gca.2009.12.027, 2010.
- 1683 Lewis, E., and Wallace, D. W. R.: Program Developed for CO₂ System Calculations, ORNL/CDIAC-105, Carbon
- 1684 Dioxide Information Analysis Center, Oak Ridge National Laboratory, Oak Ridge, TN, 1998.
- 1685 Locarnini, R. A., Mishonov, A. V., Antonov, J. I., Boyer, T. P., Garcia, H. E., Baranova, O. K., Zweng, M. M.,
- 1686 Paver, C. R., Reagan, J. R., Johnson, D. R., Hamilton, M., and Seidov, D.: World Ocean Atlas 2013, Volume 1:
- 1687 Temperature, edited by: Levitus, S. and Mishonov, A., NOAA Atlas NESDIS 73, 40 pp., 2013.
- 1688 Locarnini, R. A., Mishonov, A. V., Baranova, O. K., Boyer, T., P., Zweng, M. M., Garcia, H. E., Reagan, J. R.,
- 1689 Seidov, D., Weathers, K. W., Paver, C. R., Smolyar, I. V.: World Ocean Atlas 2018, Volume 1: Temperature,
- 1690 Mishonov, A. [Technical Editor], NOAA Atlas NESDIS 81, 2019.
- Lueker, T. J., Dickson, A. G., and Keeling, C. D.: Ocean pCO₂ calculated from dissolved inorganic carbon,
- 1692 alkalinity, and equations for K1 and K2: Validation based on laboratory measurements of CO2 in gas and seawater at
- 1693 equilibrium, Marine Chemistry, 70(1-3), 105-119, https://doi.org/10.1016/s0304-4203(00)00022-0, 2000.
- 1694 Ma, D., Gregor, L., and Gruber, N. (2023). Four decades of trends and drivers of global surface ocean acidification,
- 1695 Global Biogeochemical Cycles, 37(7), https://doi.org/10.1029/2023gb007765, 2023.
- 1696 Manzello, D. P., Enochs, I. C., Hendee, J. C.: National Coral Reef Monitoring Program: Carbonate chemistry data





- 1697 collected in the Atlantic Ocean, NOAA National Centers for Environmental Information, Dataset,
- 1698 https://doi.org/10.25921/vfz0-dg77, 2018.
- 1699 Mercier, H., Desbruyères, D., Lherminier, P., Velo, A., Carracedo, L., Fontela, M., & Pérez, F. F.: New insights into
- the eastern subpolar North Atlantic Meridional overturning circulation from OVIDE. Ocean Science, 20(3), 779–
- 1701 797, https://doi.org/10.5194/os-20-779-2024, 2024.
- 1702 Metzl, N., Tilbrook, B., Bakker, D., le Quéré, C., Doney, S., Feely, R., Hood, M., and Dargaville, R.: Surface Ocean
- 1703 CO₂ variability and Vulnerability Workshop, Paris, France, 11–14 April 2007. Eos, Transactions American
- 1704 Geophysical Union, 88(28), 287–287, https://doi.org/10.1029/2007eo280005, 2007.
- 1705 Metzl, N., Fin, J., Lo Monaco, C., Mignon, C., Alliouane, S., Antoine, D., Bourdin, G., Boutin, J., Bozec, Y.,
- 1706 Conan, P., Coppola, L., Diaz, F., Douville, E., Durrieu de Madron, X., Gattuso, J.-P., Gazeau, F., Golbol, M.,
- 1707 Lansard, B., Lefèvre, D., Lefèvre, N., Lombard, F., Louanchi, F., Merlivat, L., Olivier, L., Petrenko, A., Petton, S.,
- 1708 Pujo-Pay, M., Rabouille, C., Reverdin, G., Ridame, C., Tribollet, A., Vellucci, V., Wagener, T., and Wimart-
- 1709 Rousseau, C.: A synthesis of ocean total alkalinity and dissolved inorganic carbon measurements from 1993 to
- 1710 2022: the SNAPO-CO2-v1 dataset, Earth Syst. Sci. Data, 16, 89–120, https://doi.org/10.5194/essd-16-89-2024,
- 1711 2024.
- 1712 Metzl, Nicolas; Fin, Jonathan; Lo Monaco, Claire; Mignon, Claude; Alliouane, Samir; Antoine, David; Bourdin,
- 1713 Guillaume; Boutin, Jacqueline; Bozec, Yann; Conan, Pascal; Coppola, Laurent; Diaz, Frédéric; Douville, Eric;
- 1714 Durrieu de Madron, Xavier; Gattuso, Jean-Pierre; Gazeau, Frédéric; Golbol, Melek; Lansard, Bruno; Lefèvre,
- 1715 Dominique; Lefèvre, Nathalie; Lombard, Fabien; Louanchi, Férial; Merlivat, Liliane; Olivier, Léa; Petrenko, Anne;
- 1716 Petton, Sébastien; Pujo-Pay, Mireille; Rabouille, Christophe; Reverdin, Gilles; Ridame, Céline; Tribollet, Aline;
- 1717 Vellucci, Vincenzo; Wagener, Thibaut; Wimart-Rousseau, Cathy (2023). A synthesis of ocean total alkalinity and
- 1718 dissolved inorganic carbon measurements in the Global Ocean and Mediterranean Sea from 1993 to 2022: the
- 1719 SNAPO-CO2-v1 dataset (NCEI Accession 0285681). [indicate subset used]. NOAA National Centers for
- 1720 Environmental Information. Unpublished Dataset. https://www.ncei.noaa.gov/archive/accession/0285681, 2023.
- 1721 Mishonov, A. V., Boyer, T. P., Baranova, O. K., Bouchard, C. N., Cross, S. L., Garcia H. E., Locarnini, R. A., Paver,
- 1722 C. R., Wang, Z., Seidov, D., Grodsky, A. I., Beauchamp, J. G.: World Ocean Database 2023, C. Bouchard, Technical
- 1723 Ed., NOAA Atlas NESDIS 97, 206 pp., https://doi.org/10.25923/z885-h264, 2024.
- Monacci, N. M., Cross, J. N., Danielson, S. L., Evans, W., Hopcroft, R. R., Mathis, J. T., Mordy, C. W., Naber, D.
- 1725 D., Shake, K. L., Trahanovsky, K., Wang, H., Weingartner, T. J., Whitledge, T. E.: Marine carbonate system
- discrete profile data from the Gulf of Alaska (GAK) Seward Line cruises between 2008 and 2017 (NCEI Accession
- 1727 0277034). NOAA National Centers for Environmental Information. Dataset. https://doi.org/10.25921/x9sg-9b08,
- 1728 2023.





- 1729 Monacci, N. M., Cross, J. N., Evans, W., Mathis, J. T., and Wang, H.: A decade of marine inorganic carbon
- 1730 chemistry observations in the northern Gulf of Alaska insights into an environment in transition, Earth Syst. Sci.
- Data, 16, 647–665, https://doi.org/10.5194/essd-16-647-2024, 2024.
- 1732 Müller, J. D., Gruber, N., Carter, B., Feely, R., Ishii, M., Lange, N., Lauvset, S. K., Murata, A., Olsen, A., Pérez, F.
- 1733 F., Sabine, C., Tanhua, T., Wanninkhof, R., and Zhu, D.: Decadal trends in the oceanic storage of anthropogenic
- 1734 carbon from 1994 to 2014, AGU Advances, 4(4), https://doi.org/10.1029/2023av000875, 2023.
- Müller, J. D.: RECCAP2-ocean data collection, https://doi.org/10.5281/zenodo.7990823, 2023.
- 1736 Müller, J. D., and Gruber, N.: Progression of ocean interior acidification over the industrial era, Science Advances,
- 1737 10(48), https://doi.org/10.1126/sciadv.ado3103, 2024.
- Olsen, A., Key, R. M., van Heuven, S., Lauvset, S. K., Velo, A., Lin, X., Schirnick, C., Kozyr, A., Tanhua, T.,
- Hoppema, M., Jutterström, S., Steinfeldt, R., Jeansson, E., Ishii, M., Pérez, F. F., and Suzuki, T.: The Global Ocean
- 1740 Data Analysis Project version 2 (GLODAPv2) an internally consistent data product for the world ocean, Earth
- 1741 Syst. Sci. Data, 8, 297–323, https://doi.org/10.5194/essd-8-297-2016, 2016.
- Olsen, A., Lange, N., Key, R. M., Tanhua, T., Álvarez, M., Becker, S., Bittig, H. C., Carter, B. R., Cotrim da Cunha,
- 1743 L., Feely, R. A., van Heuven, S., Hoppema, M., Ishii, M., Jeansson, E., Jones, S. D., Jutterström, S., Karlsen, M. K.,
- 1744 Kozyr, A., Lauvset, S. K., Lo Monaco, C., Murata, A., Pérez, F. F., Pfeil, B., Schirnick, C., Steinfeldt, R., Suzuki,
- 1745 T., Telszewski, M., Tilbrook, B., Velo, A., and Wanninkhof, R.: GLODAPv2.2019 an update of GLODAPv2,
- 1746 Earth Syst. Sci. Data, 11, 1437–1461, https://doi.org/10.5194/essd-11-1437-2019, 2019.
- Olsen, A., Lange, N., Key, R. M., Tanhua, T., Bittig, H. C., Kozyr, A., Álvarez, M., Azetsu-Scott, K., Becker, S.,
- Brown, P. J., Carter, B. R., Cotrim da Cunha, L., Feely, R. A., van Heuven, S., Hoppema, M., Ishii, M., Jeansson,
- 1749 E., Jutterström, S., Landa, C. S., Lauvset, S. K., Michaelis, P., Murata, A., Pérez, F. F., Pfeil, B., Schirnick, C.,
- 1750 Steinfeldt, R., Suzuki, T., Tilbrook, B., Velo, A., Wanninkhof, R., and Woosley, R. J.: An updated version of the
- global interior ocean biogeochemical data product, GLODAPv2.2020, Earth Syst. Sci. Data, 12, 3653–3678,
- 1752 https://doi.org/10.5194/essd-12-3653-2020, 2020.
- Orr, J. C., Fabry, V. J., Aumont, O., Bopp, L., Doney, S. C., Feely, R. A., Gnanadesikan, A., Gruber, N., Ishida, A.,
- 1754 Joos, F., Key, R. M., Lindsay, K., Maier-Reimer, E., Matear, R., Monfray, P., Mouchet, A., Najjar, R. G., Plattner,
- 1755 G.-K., Rodgers, K. B., Sabine, C. L., Sarmiento, J. L., Schlitzer, R., Slater, R. D., Totterdell, I. J., Weirig, M.-F.,
- 1756 Yamanaka, Y., and Yool, A.: Anthropogenic ocean acidification over the twenty-first century and its impact on
- 1757 calcifying organisms, Nature, 437(7059), 681–686, https://doi.org/10.1038/nature04095, 2005.
- 1758 Orr, J. C., Epitalon, J.-M., and Gattuso, J.-P.: Comparison of ten packages that compute ocean carbonate chemistry,
- 1759 Biogeosciences, 12, 1483–1510, https://doi.org/10.5194/bg-12-1483-2015, 2015.
- 1760 Orr, J. C., Epitalon, J.-M., Dickson, A. G., and Gattuso, J.-P.: Routine uncertainty propagation for the Marine





- 1761 Carbon Dioxide System, Marine Chemistry, 207, 84–107. https://doi.org/10.1016/j.marchem.2018.10.006, 2018.
- Oschlies, A., Bach, L. T., Fennel, K., Gattuso, J.-P., and Mengis, N.: Perspectives and challenges of marine carbon
- dioxide removal, Frontiers in Climate, 6, https://doi.org/10.3389/fclim.2024.1506181, 2025.
- 1764 Padin, X. A., Velo, A., & Pérez, F. F.: Arios: A database for ocean acidification assessment in the Iberian Upwelling
- 1765 System (1976–2018), Earth System Science Data, 12(4), 2647–2663, https://doi.org/10.5194/essd-12-2647-2020,
- 1766 2020.
- 1767 Palacio-Castro, A. M., Enochs, I. C., Besemer, N., Boyd, A., Jankulak, M., Kolodziej, G., Hirsh, H. K., Webb, A. E.,
- 1768 Towle, E. K., Kelble, C., Smith, I., and Manzello, D. P.: Coral Reef carbonate chemistry reveals interannual,
- seasonal, and spatial impacts on ocean acidification off Florida, Global Biogeochemical Cycles, 37(12),
- 1770 https://doi.org/10.1029/2023gb007789, 2023.
- 1771 Perez, F. F., and Fraga, F.: Association constant of fluoride and hydrogen ions in seawater. Marine Chemistry,
- 1772 21(2), 161–168, https://doi.org/10.1016/0304-4203(87)90036-3, 1987.
- 1773 Pérez, F. F., Velo, A., Padin, X. A., Doval, M. D., and Prego, R.: ARIOS Database: An Acidification Ocean
- 1774 Database for the Galician Upwelling Ecosystem, Instituto de Investigaciones Marinas, Consejo Superior de
- 1775 Investigaciones Cientificas (CSIC), https://doi.org/10.20350/digitalCSIC/12498, 2020.
- 1776 Pfeil, B., Olsen, A., Bakker, D. C. E., Hankin, S., Koyuk, H., Kozyr, A., Malczyk, J., Manke, A., Metzl, N., Sabine,
- 1777 C. L., Akl, J., Alin, S. R., Bates, N., Bellerby, R. G. J., Borges, A., Boutin, J., Brown, P. J., Cai, W.-J., Chavez, F.
- 1778 P., Chen, A., Cosca, C., Fassbender, A. J., Feely, R. A., González-Dávila, M., Goyet, C., Hales, B., Hardman-
- 1779 Mountford, N., Heinze, C., Hood, M., Hoppema, M., Hunt, C. W., Hydes, D., Ishii, M., Johannessen, T., Jones, S.
- D., Key, R. M., Körtzinger, A., Landschützer, P., Lauvset, S. K., Lefèvre, N., Lenton, A., Lourantou, A., Merlivat,
- 1781 L., Midorikawa, T., Mintrop, L., Miyazaki, C., Murata, A., Nakadate, A., Nakano, Y., Nakaoka, S., Nojiri, Y.,
- 1782 Omar, A. M., Padin, X. A., Park, G.-H., Paterson, K., Perez, F. F., Pierrot, D., Poisson, A., Ríos, A. F., Santana-
- 1783 Casiano, J. M., Salisbury, J., Sarma, V. V. S. S., Schlitzer, R., Schneider, B., Schuster, U., Sieger, R., Skjelvan, I.,
- 1784 Steinhoff, T., Suzuki, T., Takahashi, T., Tedesco, K., Telszewski, M., Thomas, H., Tilbrook, B., Tjiputra, J.,
- 1785 Vandemark, D., Veness, T., Wanninkhof, R., Watson, A. J., Weiss, R., Wong, C. S., and Yoshikawa-Inoue, H.: A
- uniform, quality controlled Surface Ocean CO₂ Atlas (SOCAT), Earth Syst. Sci. Data, 5, 125–143,
- 1787 https://doi.org/10.5194/essd-5-125-2013, 2013.
- $1788 \qquad \text{Qi, D., Ouyang, Z., Chen, L., Wu, Y., Lei, R., Chen, B., Feely, R. A., Anderson, L. G., Zhong, W., Lin, H., Chen, C$
- 1789 Polukhin, A., Zhang, Y., Zhang, Y., Bi, H., Lin, X., Luo, Y., Zhuang, Y., He, J., Chen, J. and Cai, W.-J.: Climate
- change drives rapid decadal acidification in the Arctic Ocean from 1994 to 2020, Science, 377, 1544-1550,
- 1791 doi:10.1126/science.abo0383, 2022.
- 1792 Resplandy, L., Hogikyan, A., Müller, J. D., Najjar, R. G., Bange, H. W., Bianchi, D., Weber, T., Cai, W. -J., Doney,





- 1793 S. C., Fennel, K., Gehlen, M., Hauck, J., Lacroix, F., Landschützer, P., Le Quéré, C., Roobaert, A., Schwinger, J.,
- 1794 Berthet, S., Bopp, L., Chau, T. T. T., Dai, M., Gruber, N., Ilyina, T., Kock, A., Manizza, M., Lachkar, Z., Laruelle,
- 1795 G. G., Liao, E., Lima, I. D., Nissen, C., Rödenbeck, C., Séférian, R., Toyama, K., Tsujino, H., and Regnier, P.: A
- 1796 synthesis of global coastal Ocean Greenhouse Gas Fluxes, Global Biogeochemical Cycles, 38(1),
- 1797 https://doi.org/10.1029/2023gb007803, 2024.
- 1798 Revelle, R., and Suess, H. E.: Carbon dioxide exchange between atmosphere and ocean and the question of an
- increase of atmospheric CO₂ during the past decades. Tellus, 9(1), 18–27, https://doi.org/10.1111/j.2153-
- 1800 3490.1957.tb01849.x, 1957.
- 1801 Rödenbeck, C., Keeling, R. F., Bakker, D. C., Metzl, N., Olsen, A., Sabine, C., and Heimann, M.: Global surface-
- 1802 ocean pCO₂ and sea-air CO₂ flux variability from an observation-driven ocean mixed-layer scheme, Ocean Science,
- 1803 9(2), 193–216, https://doi.org/10.5194/os-9-193-2013, 2013.
- 1804 Rödenbeck, Christian, DeVries, T., Hauck, J., Le Quéré, C., & Keeling, R. F.: Data-based estimates of interannual
- 1805 sea-air CO₂ flux variations 1957-2020 and their relation to environmental drivers, Biogeosciences, 19(10), 2627-
- 1806 2652, https://doi.org/10.5194/bg-19-2627-2022, 2022.
- 1807 Roobaert, A.: Regnier, P., Landschützer, P., Laruelle, G. G.: A novel sea surface partial pressure of carbon dioxide
- 1808 (pCO₂) data product for the global coastal ocean resolving trends over the 1982-2020 period (NCEI Accession
- 1809 0279118), NOAA National Centers for Environmental Information, Dataset, https://doi.org/10.25921/4sde-p068,
- 1810 2023.
- 1811 Roobaert, A., Regnier, P., Landschützer, P., and Laruelle, G. G.: A novel sea surface pCO₂-product for the global
- 1812 coastal ocean resolving trends over 1982–2020, Earth System Science Data, 16(1), 421–441,
- 1813 https://doi.org/10.5194/essd-16-421-2024, 2024.
- 1814 Sabine, C. L., Feely, R. A., Gruber, N., Key, R. M., Lee, K., Bullister, J. L., Wanninkhof, R., Wong, C. S., Wallace,
- D. W., Tilbrook, B., Millero, F. J., Peng, T.-H., Kozyr, A., Ono, T., and Rios, A. F.: The oceanic sink for
- anthropogenic CO₂, Science, 305(5682), 367–371, https://doi.org/10.1126/science.1097403, 2004.
- 1817 Sabine, C. L., Key, R. M., Kozyr, A., Feely, R. A., Wanninkhof, R., Millero, F. J., Peng, T.-H., Bullister, J. L., and
- 1818 Lee, K.: Global Ocean Data Analysis Project (GLODAP): Results and data. ORNL/CDIAC-145, NDP-083, Carbon
- 1819 Dioxide Information Analysis Center, Oak Ridge National Laboratory, U.S. Department of Energy, Oak Ridge, TN,
- 1820 110 pp. plus 6 Appendices, 2005.
- 1821 Sabine, C. L., Feely, R. A., Millero, F. J., Dickson, A. G., Langdon, C., Mecking, S., and Greeley, D.: Decadal
- changes in Pacific Carbon, Journal of Geophysical Research: Oceans, 113(C7),
- 1823 https://doi.org/10.1029/2007jc004577, 2008.





- 1824 Sabine, C. L., Hankin, S., Koyuk, H., Bakker, D. C. E., Pfeil, B., Olsen, A., Metzl, N., Kozyr, A., Fassbender, A.,
- Manke, A., Malczyk, J., Akl, J., Alin, S. R., Bellerby, R. G. J., Borges, A., Boutin, J., Brown, P. J., Cai, W.-J.,
- 1826 Chavez, F. P., Chen, A., Cosca, C., Feely, R. A., González-Dávila, M., Goyet, C., Hardman-Mountford, N., Heinze,
- 1827 C., Hoppema, M., Hunt, C. W., Hydes, D., Ishii, M., Johannessen, T., Key, R. M., Körtzinger, A., Landschützer, P.,
- 1828 Lauvset, S. K., Lefèvre, N., Lenton, A., Lourantou, A., Merlivat, L., Midorikawa, T., Mintrop, L., Miyazaki, C.,
- Murata, A., Nakadate, A., Nakano, Y., Nakaoka, S., Nojiri, Y., Omar, A. M., Padin, X. A., Park, G.-H., Paterson, K.,
- 1830 Perez, F. F., Pierrot, D., Poisson, A., Ríos, A. F., Salisbury, J., Santana-Casiano, J. M., Sarma, V. V. S. S., Schlitzer,
- 1831 R., Schneider, B., Schuster, U., Sieger, R., Skjelvan, I., Steinhoff, T., Suzuki, T., Takahashi, T., Tedesco, K.,
- Telszewski, M., Thomas, H., Tilbrook, B., Vandemark, D., Veness, T., Watson, A. J., Weiss, R., Wong, C. S., and
- 1833 Yoshikawa-Inoue, H.: Surface Ocean CO₂ Atlas (SOCAT) gridded data products, Earth Syst. Sci. Data, 5, 145–153,
- 1834 https://doi.org/10.5194/essd-5-145-2013, 2013.
- 1835 Sarma, V. V. S. S., Krishna, M. S., Paul, Y. S., and Murty, V. S. N.: Observed changes in ocean acidity and carbon
- dioxide exchange in the coastal bay of Bengal—A link to air pollution, Tellus B: Chemical and Physical
- 1837 Meteorology, 67(1), 24638, https://doi.org/10.3402/tellusb.v67.24638, 2015.
- 1838 Schimel, D. S., and Carroll, D.: Carbon cycle-climate feedbacks in the post-paris world, Annual Review of Earth
- and Planetary Sciences, 52(1), https://doi.org/10.1146/annurev-earth-031621-081700, 2024.
- 1840 Schoderer, M., Bittig, H., Klein, B., Hägele, R., Steinhoff, T., Castro-Morales, K., Cotrim da Cunha, L., Hornidge,
- 1841 A., and Körtzinger, A.: From individual observations to global assessments: Tracing the Marine Carbon Knowledge
- 1842 Value Chain, Ocean and Society, 2, https://doi.org/10.17645/oas.8891, 2024.
- Sharp, J. D., Pierrot, D., Humphreys, M. P., Epitalon, J.-M., Orr, J. C., Lewis, E. R., Wallace, D. W. R.: CO2SYSv3
- 1844 for MATLAB (Version v3.2.1), Zenodo, http://doi.org/10.5281/zenodo.3950562, 2023.
- 1845 Sharp, J. D., Jiang, L-Q., Carter, B. R., Lavin, P. D., Yoo, H., Cross, S. L. RFR-LME Ocean Acidification Indicators
- 1846 from 1998 to 2023 (NCEI Accession 0287551). NOAA National Centers for Environmental Information. Dataset.
- 1847 https://doi.org/10.25921/h8vw-e872, 2024a...
- 1848 Sharp, J. D., Jiang, L.-Q., Carter, B. R., Lavin, P. D., Yoo, H., and Cross, S. L.: A mapped dataset of surface ocean
- acidification indicators in large marine ecosystems of the United States, Sci. Data, 11, 715,
- 1850 https://doi.org/10.1038/s41597-024-03530-7, 2024b.
- 1851 Sridevi, B., and Sarma, V. V. S. S.: Role of river discharge and warming on ocean acidification and pco2 levels in
- the Bay of Bengal, Tellus B: Chemical and Physical Meteorology, 73 (1), 1–20,
- 1853 https://doi.org/10.1080/16000889.2021.1971924, 2021.
- Sutton, A. J., Feely, R. A., Maenner-Jones, S., Musielwicz, S., Osborne, J., Dietrich, C., Monacci, N., Cross, J.,
- 1855 Bott, R., Kozyr, A.: Autonomous seawater partial pressure of carbon dioxide (pCO2) and pH time series from 40





- 1856 surface buoys between 2004 and 2017 (NCEI Accession 0173932), NOAA National Centers for Environmental
- 1857 Information, Dataset, https://doi.org/10.7289/v5db8043, 2018.
- Sutton, A. J., Feely, R. A., Maenner-Jones, S., Musielwicz, S., Osborne, J., Dietrich, C., Monacci, N., Cross, J.,
- 1859 Bott, R., Kozyr, A., Andersson, A. J., Bates, N. R., Cai, W.-J., Cronin, M. F., De Carlo, E. H., Hales, B., Howden, S.
- D., Lee, C. M., Manzello, D. P., McPhaden, M. J., Meléndez, M., Mickett, J. B., Newton, J. A., Noakes, S. E., Noh,
- 1861 J. H., Olafsdottir, S. R., Salisbury, J. E., Send, U., Trull, T. W., Vandemark, D. C., and Weller, R. A.: Autonomous
- seawater pCO₂ and pH time series from 40 surface buoys and the emergence of anthropogenic trends, Earth Syst.
- 1863 Sci. Data, 11, 421–439, https://doi.org/10.5194/essd-11-421-2019, 2019.
- 1864 Suzuki, T., M. Ishii, M. Aoyama, J. R. Christian, K. Enyo, T. Kawano, R. M. Key, N. Kosugi, A. Kozyr, L. A.
- 1865 Miller, A. Murata, T. Nakano, T. Ono, T. Saino, K. Sasaki, D. Sasano, Y. Takatani, M. Wakita and C. Sabine:
- 1866 PACIFICA Data Synthesis Project. ORNL/CDIAC-159, NDP-092. Carbon Dioxide Information Analysis Center,
- Oak Ridge National Laboratory, U.S. Department of Energy, Oak Ridge, Tennessee. doi:
- 1868 10.3334/CDIAC/OTG.PACIFICA NDP092, 2013.
- Swift, J. (2022), Java OceanAtlas Data, https://joa.ucsd.edu/Data_homepage (Last accessed: 2025-02-08).
- 1870 Takahashi, T., Feely, R. A., Weiss, R. F., Wanninkhof, R. H., Chipman, D. W., Sutherland, S. C., and Takahashi, T.
- 1871 T.: Global Air-Sea Flux of CO₂: An estimate based on measurements of sea-air pCO₂ difference, Proceedings of the
- 1872 National Academy of Sciences, 94(16), 8292–8299, https://doi.org/10.1073/pnas.94.16.8292, 1997.
- 1873 Takahashi, T., Sutherland, S. C., Sweeney, C., Poisson, A., Metzl, N., Tilbrook, B., Bates, N., Wanninkhof, R.,
- Feely, R. A., Sabine, C., Olafsson, J., and Nojiri, Y.: Global sea-air CO₂ flux based on climatological surface ocean
- 1875 pCO₂, and seasonal biological and temperature effects, Deep Sea Research Part II: Topical Studies in
- 1876 Oceanography, 49(9–10), 1601–1622, https://doi.org/10.1016/s0967-0645(02)00003-6, 2002.
- 1877 Takahashi, T., Sutherland, S. C., Wanninkhof, R., Sweeney, C., Feely, R. A., Chipman, D. W., Hales, B., Friederich,
- 1878 G., Chavez, F., Sabine, C., Watson, A., Bakker, D. C. E., Schuster, U., Metzl, N., Yoshikawa-Inoue, H., Ishii, M.,
- 1879 Midorikawa, T., Nojiri, Y., Körtzinger, A., Steinhoff, T., and de Baar, H. J. W.: Climatological mean and decadal
- change in Surface Ocean pCO₂, and net sea-air CO₂ flux over the Global Oceans, Deep Sea Research Part II:
- Topical Studies in Oceanography, 56(8–10), 554–577, https://doi.org/10.1016/j.dsr2.2008.12.009, 2009.
- 1882 Takahashi, T., Sutherland, S. C., Kozyr, A.: LDEO Database (Version 2019): Global Ocean Surface Water Partial
- 1883 Pressure of CO2 Database: Measurements Performed During 1957-2019 (NCEI Accession 0160492), NOAA
- National Centers for Environmental Information, Dataset, https://doi.org/10.3334/cdiac/otg.ndp088(v2015), 2017.
- 1885 Takahashi, T., Sutherland, S. C., and Kozyr, A.: Global Ocean Surface Water Partial Pressure of CO₂ Database:
- 1886 Measurements Performed During 1957–2019 (LDEO Database Version 2019) (NCEI Accession 0160492), Version
- 9.9, NOAA National Centers for Environmental Information [data set],





- 1888 https://doi.org/10.3334/CDIAC/OTG.NDP088(V2015), 2021.
- Tanhua, T., Jones, E. P., Jeansson, E., Jutterström, S., Smethie, W. M., Wallace, D. W., and Anderson, L. G.:
- 1890 Ventilation of the Arctic Ocean: Mean ages and inventories of Anthropogenic CO2 and CFC-11, Journal of
- 1891 Geophysical Research: Oceans, 114(C1), https://doi.org/10.1029/2008jc004868, 2009.
- Tanhua, T., van Heuven, S., Key, R. M., Velo, A., Olsen, A., and Schirnick, C.: Quality control procedures and
- 1893 methods of the CARINA database, Earth Syst. Sci. Data, 2, 35-49, https://doi.org/10.5194/essd-2-35-2010, 2010.
- 1894 Tans, P., and Keeling, R.: Trends in atmospheric carbon dioxide, NOAA Global Monitoring Laboratory (Boulder,
- 1895 Colorado, USA) and Scripps Institution of Oceanography (LaJolla, California, USA),
- https://gml.noaa.gov/ccgg/trends/ and https://scrippsco2.ucsd.edu/, 2025.
- 1897 Terhaar, J., Orr, J. C., Ethé, C., Regnier, P., and Bopp, L.: Simulated Arctic Ocean response to doubling of riverine
- 1898 carbon and nutrient delivery, Global Biogeochemical Cycles, 33, 1048–1070,
- 1899 https://doi.org/10.1029/2019GB006200, 2019.
- 1900 Terhaar, J., Tanhua, T., Stöven, T., Orr, J. C., and Bopp, L.: Evaluation of data-based estimates of anthropogenic
- 1901 carbon in the Arctic Ocean, Journal of Geophysical Research: Oceans, 125(6),
- 1902 https://doi.org/10.1029/2020jc016124, 2020.
- 1903 Terhaar, J., Torres, O., Bourgeois, T., and Kwiatkowski, L.: Arctic Ocean acidification over the 21st century co-
- driven by anthropogenic carbon increases and freshening in the CMIP6 model ensemble, Biogeosciences, 18, 2221–
- 1905 2240, https://doi.org/10.5194/bg-18-2221-2021, 2021a.
- 1906 Terhaar, Jens, Frölicher, T. L., & Joos, F.: Southern Ocean anthropogenic carbon sink constrained by sea surface
- 1907 salinity, Science Advances, 7(18), https://doi.org/10.1126/sciadv.abd5964, 2021b.
- 1908 Terhaar Jens, Frölicher Thomas L., Joos Fortunat (2021c). Simulated and constrained Southern Ocean carbon sink
- 1909 from 1850 to 2100 based on CMIP5 and CMIP6 models. SEANOE. https://doi.org/10.17882/103938
- 1910 Terhaar, J., Frölicher, T. L., and Joos, F.: Observation-constrained estimates of the Global Ocean Carbon Sink from
- $1911 \qquad \text{earth system models, Biogeosciences, } 19(18), 4431-4457, \\ \text{https://doi.org/} 10.5194/bg-19-4431-2022, 2022a.$
- 1912 Terhaar Jens, Frölicher Thomas Lukas, Joos Fortunat (2022b). Simulated and constrained ocean carbon sink from
- 1913 1850 to 2100 based on CMIP6 models. SEANOE. https://doi.org/10.17882/103934
- 1914 Terhaar, J., Frölicher, T. L., and Joos, F.: Ocean acidification in emission-driven temperature stabilization scenarios:
- 1915 The role of TCRE and non-CO₂ greenhouse gases, Environmental Research Letters, 18(2), 02403,
- 1916 https://doi.org/10.1088/1748-9326/acaf91, 2023.
- 1917 Terhaar Jens, Tanhua Toste, Stöven Tim, Orr James C, Bopp Laurent (2024). Observation-based anthropogenic





- carbon estimates in the Arctic Ocean. SEANOE. https://doi.org/10.17882/103920
- van Heuven, S., Pierrot, D., Rae, J. W. B., Lewis, E., Wallace, D. W. R.: MATLAB Program Developed for CO₂
- 1920 System Calculations, ORNL/CDIAC-105b, Carbon Dioxide Information Analysis Center, Oak Ridge National
- 1921 Laboratory, Oak Ridge, TN, USA, 2011.
- 1922 van Hooidonk, R.: Modeled ocean acidification data in the Gulf of Mexico and wider Caribbean using satellites and
- 1923 climate model data for the Ocean Acidification Products for the Gulf of Mexico and East Coast project from 2014-
- 1924 01-01 to 2020-12-31 (NCEI Accession 0245950), NOAA National Centers for Environmental Information, Dataset,
- 1925 https://doi.org/10.25921/tt1c-dx53, 2022.
- 1926 Velo, A., Pérez, F. F., Tanhua, T., Gilcoto, M., Ríos, A. F., and Key, R. M.: Total alkalinity estimation using MLR
- and neural network techniques, J. Mar. Syst., 111–112, 11–18, https://doi.org/10.1016/j.jmarsys.2012.09.002, 2013.
- 1928 Wanninkhof, R., Pierrot, D., Sullivan, K., Barbero, L., and Triñanes, J.: Gridded surface water fugacity of CO₂
- observations, and calculated pH, aragonite saturation state and air-sea CO₂ fluxes in the northern Caribbean Sea
- 1930 from 2002 through 2019 (NCEI Accession 0207749), NOAA National Centers for Environmental Information,
- 1931 Dataset, https://doi.org/10.25921/2swk-9w56, 2019.
- 1932 Wanninkhof, R., Pierrot, D., Sullivan, K., Barbero, L., and Triñanes, J.: A 17-year dataset of surface water fugacity
- 1933 of CO₂ along with calculated pH, aragonite saturation state and air-sea CO₂ fluxes in the northern Caribbean Sea,
- 1934 Earth Syst. Sci. Data, 12, 1489–1509, https://doi.org/10.5194/essd-12-1489-2020, 2020.
- 1935 Wanninkhof, R., Triñanes, J., Pierrot, D., Munro, D. R., Sweeney, C., and Fay, A. R.: AOML ET: Partial pressure
- 1936 of CO₂ (pCO₂) and sea-air CO₂ fluxes for the global ocean, along with the predictor variables from 1998-01-01 to
- 1937 2023-12-30, using an Extra Trees (extremely randomized trees) machine learning (NCEI Accession 0298989),
- 1938 NOAA National Centers for Environmental Information, Dataset, https://doi.org/10.25921/0s8y-q287, 2024.
- Wanninkhof, R., Triñanes, J., Pierrot, D., Munro, D. R., Sweeney, C., and Fay, A. R.: Trends in sea-air CO₂ fluxes
- 1940 and sensitivities to atmospheric forcing using an extremely randomized trees machine learning approach, Global
- 1941 Biogeochemical Cycles, 39, https://doi.org/10.1029/2024GB008315, 2025.
- 1942 Watson, A. J., Schuster, U., Shutler, J. D., Holding, T., Ashton, I. G., Landschützer, P., Woolf, D., and Goddijn-
- 1943 Murphy, L.: Revised estimates of ocean-atmosphere CO₂ flux are consistent with ocean carbon inventory, Nature
- 1944 Communications, 11(1), 1–6, https://doi.org/10.1038/s41467-020-18203-3, 2020.
- Watson, A. J., Schuster, U., Shutler, J. D., Holding, T., Ashton, I. G., Landschützer, P., Woolf, D., and Goddijn-
- 1946 Murphy, L.: Revised estimates of ocean-atmosphere CO₂ flux accounting for near-surface temperature and salinity
- 1947 deviations from 1985-01-01 to 2019-12-31 (NCEI Accession 0301544), NOAA National Centers for Environmental
- 1948 Information, Dataset, https://doi.org/10.25921/2dp5-xm29, 2025.





- 1949 Wilkinson, M. D., Dumontier, M., Aalbersberg, I. J., Appleton, G., Axton, M., Baak, A., Blomberg, N., Boiten, J.-
- 1950 W., da Silva Santos, L. B., Bourne, P. E., Bouwman, J., Brookes, A. J., Clark, T., Crosas, M., Dillo, I., Dumon, O.,
- Edmunds, S., Evelo, C. T., Finkers, R., Gonzalez-Beltran, A., Gray, A. J. G., Groth, P., Goble, C., Grethe, J. S.,
- 1952 Heringa, J., Hoen, P., Hooft, R., Kuhn, T., Kok, R., Kok, J., Scott J. Lusher, S. J., Martone, M. E., Mons, A., Packer,
- 1953 A. L., Persson, B., Rocca-Serra, P., Roos, M., van Schaik, R., Sansone, S.-A., Schultes, E., Sengstag, T., Slater, T.,
- 1954 Strawn, G., Swertz, M. A., Thompson, M., van der Lei, J., van Mulligen, E., Velterop, J., Waagmeester, A.,
- 1955 Wittenburg, P., Wolstencroft, K., Zhao, J., Mons, B.: The Fair Guiding Principles for Scientific Data Management
- and Stewardship, Scientific Data, 3(1), https://doi.org/10.1038/sdata.2016.18, 2016.
- 1957 Winn, C. D., MacKenzie, F. T., Carrillo, C. J., Sabine, C. L., and Karl, D. M.: Air-sea carbon dioxide exchange in
- 1958 the North Pacific Subtropical Gyre: Implications for the global carbon budget, Global Biogeochem Cycles, 8, 157-
- 1959 163, https://doi.org/10.1029/94GB00387, 1994.
- 1960 Winn, C. D., Li, Y.-H., Mackenzie, F. T., and Karl, D. M.: Rising surface ocean dissolved inorganic carbon at the
- Hawaii Ocean Time-series site, Mar. Chem., 60, 33-47, https://doi.org/10.1016/S0304-4203(97)00085-6, 1998.
- 1962 Wu, Z., Lu, W., Roobaert, A., Song, L., Yan, X.-H., and Cai, W.-J.: A machine-learning reconstruction of sea
- 1963 surface pCO₂ in the North American Atlantic Coastal Ocean Margin from 1993 to 2021, Earth Syst. Sci. Data.
- 1964 https://doi.org/10.5194/essd-17-43-2025, 2025.
- 1965 Zeng, J., Iida, Y., Matsunaga, T., Shirai, T.: Surface ocean CO₂ concentration and air-sea flux estimate by machine
- learning with modelled variable trends, Front. Mar. Sci., 9, 989233, https://doi.org/10.3389/fmars.2022.989233,
- 1967 2022.
- 1968 Zeng, J.: NIES-ML3 ensemble product of surface ocean CO₂ concentrations and air-sea CO₂ fluxes reconstructed by
- using three machine learning models with new CO₂ trends, National Institute for Environmental Studies (NIES),
- 1970 Japan, https://doi.org/10.17595/20220311.001, 2022.
- 1971 Zhang, H., Menemenlis, D., and Fenty, I. G.: ECCO LLC270 ocean-ice state estimate (Tech. Rep.), Jet Propulsion
- 1972 Laboratory, California Institute of Technology, http://hdl.handle.net/1721.1/119821, 2018.
- 1973 Zweng, M. M, Reagan, J. R., Antonov, J. I., Locarnini, R. A., Mis-honov, A. V., Boyer, T. P., Garcia, H. E.,
- 1974 Baranova, O. K., John-son, D. R., Seidov, D., and Biddle, M. M.: World Ocean Atlas 2013, Volume 2: Salinity,
- edited by: Levitus, S. and Mishonov, A., NOAA Atlas NESDIS 74, 39 pp., 2013.
- 1976 Zweng, M. M, Reagan, J. R., Seidov, D., Boyer, T. P., Locarnini, R. A., Garcia, H. E., Mishonov, A. V., Baranova,
- 1977 O. K., Weathers, K. W., Paver, C. R., Smolyar, I. V.: World Ocean Atlas 2018, Volume 2: Salinity, edited by
- 1978 Mishonov, A., NOAA Atlas NESDIS 82, 2019.